REACTOR MATERIALS

A Quarterly Technical Progress Review

Prepared for DIVISION OF TECHNICAL INFORMATION, USAEC, by
R. W. DAYTON, E. M. SIMONS, and ASSOCIATES, BATTELLE MEMORIAL INSTITUTE

4 - JUN 19
Copy 4 1962

May 1962

● VOLUME 5

● NUMBER 2

TECHNICAL PROGRESS REVIEWS

To meet the needs of industry for concise summaries of current atomic developments, the Atomic Energy Commission is publishing this series, Technical Progress Reviews. Issued quarterly, each of the reviews digests and evaluates the latest findings in a specific area of nuclear technology and science.

The four journals published in this series are:

Nuclear Safety, Wm. B. Cottrell, W. H. Jordan, and associates, Oak Ridge National Laboratory

Power Reactor Technology, W. H. Zinn and J. R. Dietrich, General Nuclear Engineering Corporation

Reactor Materials, R. W. Dayton, E. M. Simons, and associates, Battelle Memorial Institute

Reactor Fuel Processing, Stephen Lawroski and associates, Chemical Engineering Division, Argonne National Laboratory

Each journal may be purchased ($2.00 per year for subscription and individual issues $0.55) from the Superintendent of Documents, U. S. Government Printing Office, Washington 25, D. C. See back cover for remittance instructions and foreign postage requirements.

The views expressed in this publication do not necessarily represent those of the United States Atomic Energy Commission, its divisions or offices, or of any Commission advisory committee or contractor.

Availability of Reports Cited in This Review

Unclassified AEC reports are available for inspection at AEC depository libraries and are sold by the Office of Technical Services, Department of Commerce, Washington 25, D. C. Some of the reports cited are not available owing to their preliminary nature; however, the information contained in them will eventually be made available in formal progress or topical reports.

Unclassified reports issued by other Government agencies or private organizations should be requested from the originator.

Unclassified British and Canadian reports may be inspected at AEC depository libraries. British reports are sold by the British Information Service, 45 Rockefeller Plaza, New York, N. Y.; Canadian reports (AECL series) are sold by the Scientific Document Distribution Office, Atomic Energy of Canada, Ltd., Chalk River, Ontario, Canada.

Classified U. S. and foreign reports identified in this journal as Classified may be purchased by properly cleared Access Permit Holders from the Division of Technical Information Extension, U. S. Atomic Energy Commission, P. O. Box 1001, Oak Ridge, Tenn. Such reports may be inspected at classified AEC depository libraries.

REACTOR MATERIALS

A REVIEW OF RECENT DEVELOPMENTS

Prepared for DIVISION OF TECHNICAL INFORMATION, USAEC,
by R. W. DAYTON, E. M. SIMONS, and ASSOCIATES,
BATTELLE MEMORIAL INSTITUTE

● MAY 1962
● VOLUME 5
● NUMBER 2

Foreword

Reactor Materials is one of a series of four quarterly technical progress reviews broadly covering the field of nuclear science and technology. Under the auspices of the USAEC Division of Technical Information, *Reactor Materials* is prepared by Battelle personnel from world-wide literature. It covers properties, behavior, and fabrication processes of materials applicable to nuclear reactor components and associated equipment.

The reader will recognize that the scope of this Review is too broad to permit detailed coverage of every topic. Rather, the authors and editors attempt to combine the highlights of significant new developments into an informative summary of current research for both management and the technical specialist. As a rule, enough of the results are presented to define the research and summarize the findings. For readers desiring more information on any particular topic, a complete set of references is provided at the end of each section.

Each quarter, a number of bibliographies, monographs, and books appear on subjects within the scope of *Reactor Materials*. Although the main purpose of this Review is to call attention to findings that are new and significant, such publications are noted in the text because they often represent excellent compilations of available information on important materials topics.

R. W. DAYTON
E. M. SIMONS
R. W. ENDEBROCK
Battelle Memorial Institute

Contents

Foreword

I FUEL AND FERTILE MATERIALS . . 1

Uranium Metal and Alloys 1
Plutonium 5
Thorium 11
Dispersion Fuels 11
Coated-Particle Fuel Materials 12
Refractory Fuel and Fertile Materials . . 17
Basic Studies of Irradiation Effects in Fuel Materials 23
References 24

II MODERATOR MATERIALS 28

Beryllium Metal and Alloys 28
Beryllium Compounds 34
Solid Hydrides 35
Graphite 36
References 37

III NUCLEAR POISONS 40

Dispersion Control Materials 40
Metallic Poison Materials 40
References 41

IV CLADDING AND STRUCTURAL MATERIALS 42

Corrosion 42
Metal-Water Reactions 47
Radiation Effects in Nonfuel Materials . . 47
Selected Mechanical Properties of Cladding and Structural Materials . . . 52
Selected Metallurgical Aspects of Cladding and Structural Materials . . . 55
References 61

V SPECIAL FABRICATION TECHNIQUES 65

Melting, Casting, Working, Heat-Treatment 65
Cladding 66
Welding and Brazing 69
Explosive Forming 70
Ceramic Technology 74
Nondestructive Testing 75
References 76

Issued quarterly by the U. S. Atomic Energy Commission. Use of funds for printing this publication approved by the Director of the Bureau of the Budget on November 1, 1960.

Section

I

Reactor Materials

Fuel and Fertile Materials

Uranium Metal and Alloys

Unalloyed Uranium

Investigators at National Lead[1] have determined the mechanical properties of normal-production-grade uranium having various fabricating histories at temperatures covering the hot-working range of uranium (473 to 668°C). The mechanical properties determined are presented in Table I-1.

All the materials tested exhibited a uniform decrease in ultimate tensile strength with increasing temperature. All the beta heat-treated materials have higher ultimate tensile strength than the as-fabricated materials, except at the highest testing temperatures.

Both elongation and reduction in area increased with increasing temperature. Furthermore, the materials that had received the greatest amount of reduction during fabrication were the most ductile. All materials tested showed a uniform decrease in yield strength with increasing temperature. The beta heat-treated materials exhibited higher yield strengths than the as-fabricated materials.

Argonne[2] has reported on an investigation performed to determine the effect of rolling temperature, roll-pass design, amount of reduction, and heat-treatment before and after rolling on the growth rate of uranium under irradiation. The growth rate, G_i,* was found to increase with decreasing rolling temperature and with increasing reduction of area at 300°C. The rate of elongation was proportional to the amount of (0 1 0) component present or, where shortening occurred, to the amount of (1 0 0) component. Oval-edge-oval roll passes resulted in somewhat higher irradiation growth rates than did round roll passes. Recrystallization after rolling effectively reduced the irradiation growth rate of uranium rolled at temperatures of 500°C and lower. Irradiation caused length decrease in uranium which was beta quenched after being round rolled at temperatures of 400°C and above and which was beta quenched after being oval rolled at temperatures of 300°C and above.

Argonne[3] has reported on the irradiation stability of the fuel elements used in the first core loading of the Experimental Breeder Reactor No. 1 (EBR-I). These elements are fully enriched uranium rods 0.365 to 0.385 in. in diameter and 60 to 80 in. long. Preirradiation heat-treatment consisted of a beta quench followed by an alpha anneal.

The major variables responsible for the changes in the fuel elements were burnup and temperature. Other variables examined, with the possible exception of slug diameter, either had no effect or their effects were overshadowed by the two major variables or by errors in the measurements.

Length Changes. Under the conditions of irradiation which existed in the EBR-I, the slugs initially increased in length with increasing burnup up to about 0.05 at.%. A maximum (of indefinite value) length increase was evident from about 0.05 to 0.2 at.% burnup. With continued increase in burnup from about 0.2 to 0.3 at.%, the slugs tended to shorten and ultimately to become shorter than their original length. Initially, temperature does not seem to have been a factor in the change in length of the slugs, but as burnup increases beyond about 0.05 at.%, the ratio of length change to at.%

*$G_i = \frac{\%\text{ length change}}{\text{at.}\%\text{ burnup}}$ for small elongations.

burnup decreases and finally becomes negative when plotted against increasing temperatures in the range from 285 to 395°C. It is possible that two different and opposing rates of length change are acting. Compressive creep, particularly at the high temperatures and for long periods of time, would tend to cause the specimens to shorten, whereas elongation with increasing irradiation would be the other factor. If this is the case, the slugs from the fuel rods wherein the fuel column lengthened more than 0.25 in. must have had over-all heat-transfer characteristics that resulted in lower temperatures.

Table I-1 TENSILE PROPERTIES OF URANIUM METAL AT ELEVATED TEMPERATURES[1]

(Average of Two Results at Each Temperature)

Temp., °F	Fracture, 10^3 lb	Ultimate tensile strength, 1000 psi	Elongation in 2 in., %	Reduction of area, %	Yield strength (0.2% offset), 1000 psi
		Alpha-Rolled Rod			
885	8.5	43.2	28	54	21.7
955	7.1	36.2	28	59	17.6
1025	5.2	26.6	28	62	15.8
1095	3.6	18.2	30	72	11.6
1165	2.5	12.8	34	82	9.0
1235	1.6	8.6	39	88	5.6
		Alpha-Rolled, Beta Heat-Treated Rod			
885	12.2	62.0	25	40	26.4
955	8.7	44.3	24	48	21.5
1025	8.0	40.7	23	50	21.4
1095	5.2	26.8	24	60	14.6
1165	3.5	17.8	27	74	12.9
1235	2.2	11.2	33	86	9.2
		Alpha-Extruded Billet			
885	8.0	40.6	24	44	20.8
955	6.8	34.9	23	52	18.0
1025	5.6	28.7	22	56	16.2
1095	3.9	20.0	23	60	11.8
1165	3.2	15.0	26	65	9.4
1235	2.2	11.4	32	80	6.6
		Alpha-Extruded, Beta Heat-Treated Billet			
885	12.1	62.4	24	40	27.5
955	10.6	54.0	23	46	21.6
1025	7.9	40.2	22	47	14.4
1095	6.8	24.9	23	55	13.8
1165	4.0	20.4	26	73	8.0
1235	2.1	10.4	32	88	7.6
		As-Cast Billet			
885	7.3	37.0	16	36	20.1
955	6.1	30.9	20	39	15.4
1025	5.7	29.0	22	42	16.2
1095	4.3	21.8	23	46	11.2
1165	2.9	14.6	25	63	7.3
1235	1.8	8.8	30	71	5.2
		As-Cast, Beta Heat-Treated Billet			
885	9.7	49.1	15	27	22.7
955	8.6	43.6	14	41	19.2
1025	6.4	32.5	18	44	20.3
1095	4.9	24.8	18	58	15.5
1165	3.4	17.2	24	68	10.6
1235	2.4	11.9	31	79	7.1

Diameter Changes. Diameters tended to become smaller as the lengths increased in the early stages of irradiation. With increasing burnups the diameters passed through a region of minimum values and finally tended to have diameters greater than the original unirradiated values. Temperature does not seem to have been a factor at low burnup levels, but at higher burnups the ratio of diameter change to burnup increased when plotted against temperature in the range from 285 to 395°C, but at a reducing rate. In general, the changes that took place in the diameters are the inverse of the changes in length.

Diameter Change/Length Change. This ratio is essentially constant at low burnup levels at about −0.30; but, with increasing burnup, bumping, warping, and swelling contribute to a large scatter in the data points. Temperatures in the range from 285 to 395°C do not seem to have been an important factor except that, at the higher temperatures, more scatter occurs.

Density Change. Density decreases almost linearly with increasing burnup over the range from 0 to 0.3 at.% burnup. The ratio of density change to at.% burnup seems to be relatively unaffected by temperature in the range 285 to 395°C.

Hardness Change. Hardness increases with burnup at a rate that decreases with increasing burnup. Rate of hardness increase with burnup decreases with increasing temperature in the range 285 to 395°C.

Shape Changes. Forty-five per cent of the "badly warped" slugs were associated with the lowest position in the fuel column. Eighty-two per cent of the slugs with elongations of 5 per cent or greater had also been in the bottom position of the fuel column. These slugs had both low temperature and low burnup with respect to other slugs in the rods. A preponderance of the negative length changes was associated with the

slug position just above the midplane of the reactor. This was a position of both high burnup and high temperature.

Work at Hanford[4] has yielded an empirical expression to describe fuel swelling. The derived expression is as follows: per cent volume increase = 2.5 (at.% burnup) + 0.0105 $[(T_m - 350°C)(\text{at.\% burnup})]^{1.68}$.

The term 2.5 (at.% burnup) in the expression is the theoretical component of swelling that may be attributed to the loss of fuel atoms and the gain of fission-product atoms by fuel fission. The term 0.0105 $[(T_m - 350°C)(\text{at.\% burnup})]^{1.68}$ is that component of swelling produced by the agglomeration of fission products, mainly gas atoms, to produce swelling by the generation of pores in the uranium.

The Russians[5] have published a compilation of data on uranium taken from 170 references. Chapters on uranium include: Structure and Physical Properties, Metallography, Mechanical Properties, Plastic Deformation and Texture, The Effect of Irradiation on Size Stability and Physicomechanical Properties, The Effect of Heating Cycles on the Size and Structure Stability, Heat-Treatment, Thermochemical Treatment, and Alloys.

Information on work done by the French[6] on the effect of heat-treatment of uranium and uranium-chromium alloys at alpha, beta, and gamma temperatures on the final structure of alpha uranium and on the distribution of certain impurities, especially hydrogen, has been translated.

The diffusion coefficient for hydrogen in uranium at 800°C was determined[7] as 14.2×10^{-5} cm^2/sec. (M. S. Farkas)

Alpha-Phase Uranium Alloys

Investigation at Mallinckrodt[8] has shown that the addition of small amounts of iron (100 to 500 ppm) and silicon (100 to 300 ppm) to dingot uranium produces a very pronounced change in the beta-treated grain size from that observed in dingot uranium. The greater the iron and silicon additions, within the above ranges, the smaller is the beta-treated grain size. It is believed that the iron and silicon additions form an unknown uranium-iron-silicon compound. By varying the heat-treatment, this compound can be made to grow in size or dissolve in solid solution. Accompanying the change in size and number of undissolved particles is a very pronounced change in the uranium grain size. It is possible that this very fine precipitate acts either as nucleating sites from which grains grow or as particles that block the way for expanding grains.

Grain refinement of uranium by alloying has been studied recently by Nuclear Metals.[9] Alloys of uranium containing 0.08 wt.% silicon, 0.1 wt.% chromium, 0.04 wt.% chromium–0.02 wt.% zirconium, and 0.05 wt.% chromium–0.08 wt.% molybdenum were found to have grain sizes that were one-third to one-quarter of the grain size found in unalloyed uranium after beta treatment and oil quenching. In addition, the uranium–0.05 wt.% chromium–0.08 wt.% molybdenum alloy showed the same degree of grain refinement by air cooling after beta treatment. In general, texture measurements indicated that the preferred orientations of these alloys are no greater than in unalloyed uranium. Compression tests on the heat-treated-alloy core blanks showed differences in structure that may be more indicative of surface deformation under irradiation than is metallographically determined grain size.

The English[10] have studied the oxidation resistance of uranium alloys containing up to 7.3 wt.% silicon, 10 wt.% titanium, 5 wt.% vanadium, 10 wt.% zirconium, 15 wt.% molybdenum, 10 wt.% niobium, and 1 wt.% copper in CO_2 at 500 to 1000°C and in air at 500°C. Additions of titanium, molybdenum, niobium, and copper reduced the attack by CO_2 at 680 to 1000°C by factors of up to 500. None of the elements were markedly beneficial in CO_2 at 500°C, and the silicon alloys showed a high rate of attack in CO_2 at most temperatures. Additions of molybdenum, titanium, and niobium reduced the attack in air at 500°C by factors up to 500.

The results of study on the uranium-cadmium phase diagram[11] indicate the presence of a single intermetallic phase, UCd_{11}, which melts peritectically at 473°C to form alpha uranium and a melt containing 2.5 wt.% uranium. The cadmium-rich eutectic (0.07 wt.% uranium) freezes at 320.6°C. Solid solubilities in uranium and cadmium appear to be negligible. Between 473 and 600°C the liquidus line is retrograde.

A review of diffusion studies that were performed on uranium, its alloys, and compounds has been published by Argonne.[12] Included are results and analysis of studies on diffusion in single-phase and multiphase uranium alloys, as well as diffusion of gases in uranium and in UO_2.

Recent articles on alpha-uranium alloys appearing in the *Journal of Nuclear Materials* include "Metastable Phases in the Uranium-Molybdenum System and Their Origin,"[13] "Monoclinic Phases in Uranium-Molybdenum Alloys,"[14] "Finely Dispersed Phases in Uranium-Molybdenum Ternary Alloys,"[15] and "Conservation of Nuclei of the Alpha Phase in the Beta Phase of Low Alloyed Uranium."[16]

(M. S. Farkas)

Gamma-Phase Uranium Alloys

On the basis of the results of irradiation tests performed by Atomics International[17] on a series of uranium-molybdenum alloys, it is concluded that the gamma phase is more resistant to radiation damage than the alpha phase. The swelling resistance of uranium-molybdenum alloys was found to increase markedly with increasing molybdenum content from 3 to about 10 wt.%. For burnups below about 0.3 at.%, swelling of the uranium–10 wt.% molybdenum alloy is reported to increase approximately linearly with temperature to about 1500°F. Above this temperature, swelling appears to be proportional to the cube of the burnup.

The retained and metastable gamma phase in gammatized (72 hr at 900°C, ice-water quenched) uranium–14 wt.% molybdenum, treated isothermally at 550°C, began to transform to the alpha plus gamma prime phase[18] after 20 hr. The gamma phase in similarly treated uranium–16 wt.% molybdenum samples began to transform to the gamma prime phase after 16 hr at 550°C. These times are shorter than for the uranium–10 wt.% molybdenum alloy, which is the most gamma-stable composition in the range from 5 to 16 wt.% molybdenum. However, the amount of alpha phase in the transformed structure decreases progressively with increasing molybdenum content. On the basis of metallographic observations, a transition phase is believed to form after short times at temperature in the two alloys studied, although no evidence of a transition structure was obtained by X-ray diffraction techniques.

(A. A. Bauer)

Epsilon-Phase Uranium Alloys

Measurements of electrical resistivity and magnetic susceptibility performed in England[19] are reported for uranium–70 and 74 at.% zirconium (approximately 50 wt.% zirconium) alloys in both the gamma- and epsilon-phase conditions. Both phases exhibit negative temperature coefficients of resistivity and paramagnetism which increase with temperature. It is concluded that the anomalous resistivity behavior may be a consequence of the alloy band structure and also that the structure of the epislon phase is primitive hexagonal and not an ordered form of the cubic gamma phase. In drawing the latter conclusion, the author was apparently not aware of limited Hall coefficient measurements which have been made and which would indicate the opposite conclusion.

(A. A. Bauer)

Aluminum-Uranium Alloys

Petzoq et al.[20] have developed the constitutional diagram for the psuedobinary system $ZrAl_2$-UAl_2. It is a simple eutectic system with the eutectic point at 10 at.% uranium and 1440 ± 10°C. $ZrAl_2$ does not take uranium into solid solution; however, UAl_2 can dissolve up to 22.5 at.% zirconium. When this occurs, the unit cell of UAl_2 is contracted.

Work by Boucher[21] on the solid-state diffusion of aluminum through UAl_3 during transformation provides more information on the stabilizing effect of silicon on UAl_3. Since the transformation of UAl_3 should take place by diffusion of aluminum through the compound, kinetic studies should be indicative of aluminum diffusion rates. When UAl_3 crystals are heated at 600°C, transformation to UAl_4 is complete within 1 hr. If 0.1 wt.% silicon is added, the transformation takes about 10 times longer. The addition of 0.6 wt.% silicon practically stops any transformation. After 100 hr only a slight change is noted, and there is no further effect after 1000 hr.

(R. F. Dickerson)

Zirconium-Uranium Alloys

Corrosion studies being performed at Bettis[22] on zirconium-base alloys should be of interest when the data have been completely accumulated and evaluated. Such things as oxygen and hydrogen overpressures, continuous change of water to reduce corrosion-associated hydrogen in solution, and low oxygen and hydrogen pressures are being studied.

(R. F. Dickerson)

Yttrium-Uranium Alloys

Sylcor[23] has in process the irradiation of two yttrium-uranium alloys. These contain 25 and 50 wt.% uranium. The test is designed to determine the increase in swelling temperature which might be brought about by the yttrium. With this in mind, one of the two capsules is operating between 500 and 700°C and the other between 700 and 900°C. A burnup of 4×10^{20} fissions/cm^3 is desired. Although the properties of yttrium-uranium alloys have been discussed in detail in earlier issues of this Review, a brief summary might be in order. Alloys were studied which contained from 5 to 95 wt.% uranium. All compositions were compatible with sodium at elevated temperatures and were dimensionally stable at those temperatures. Alloys containing up to 65 wt.% uranium held up well during thermal cycling through the beta-transformation temperature.

(R. F. Dickerson)

Mechanism of Corrosion of Uranium Alloys

The role of corrosion-product hydrogen in the mechanism of the aqueous corrosion of uranium and uranium alloys is being studied at the Imperial College of Science and Technology, England.[24] The program is concerned with the properties of the corrosion film. Included in the study are measurements of (1) film thickness by optical means, (2) capacity and conductivity of the film over a range of potentials, (3) hydrogen overvoltage, and (4) type of semiconductivity in the film by thermoelectric means.

On the basis of results obtained, British workers suggest that hydrogen diffusing through the oxide film on a corroding metal would be expected to change the electronic conductivity of the oxide and thus change the corrosion rate. The change would be dependent on the type of solution of hydrogen in the oxide (substitutional or interstitial) and the type of original conductivity in the oxide (n or p type). They further suggest that the amount of hydrogen in the oxide would depend on the activity of hydrogen at the oxide-metal interface and at the oxide-liquid interface. An increase in activity at either or both interfaces would be expected to increase the amount of hydrogen in the oxide. Evolution of corrosion-product hydrogen as gas would remove it from the reaction site.

(W. E. Berry)

Plutonium

In late 1961 the University of Chicago Press published a book, *The Metal Plutonium*, edited by A. S. Coffinberry and W. N. Miner ($9.50).

(V. W. Storhok)

Plutonium Metal and Alloys

Impact properties of notched and unnotched plutonium have been determined by Hanford[25] at temperatures ranging from −45 to 330°C. Results are presented in Table I-2. Brittle failures of the unnotched specimens were observed in the alpha and beta phases, whereas in the gamma phase extremely ductile behavior was observed. In the alpha phase, fracture grain size increased as test temperatures were increased from −45 to 100°C. Also tested was the effect of small iron additions on the unnotched impact properties of plutonium at 30 and 100°C. Results are shown in Table I-3. The higher impact strength of the higher iron specimen is attributed to the inhibiting effect of the Pu-Pu_6Fe

Table I-2 IMPACT TEST RESULTS ON PLUTONIUM[25]

Test temp., °C	Unnotched specimens: Impact energy, ft-lb: Average	Range	No. tested	Notched specimens: Impact energy, ft-lb: Average	Range	No. tested
−45	4.6	4.2–5.0	5	1.8	1.7–1.8	2
30	6.5	4.5–8.8	9	1.9		2
70	5.6	5.5–5.7	2			
100	6.9	5.1–10.0	10	3.1	2.7–3.5	3
130	9.9	8.2–12.9	3	1.9	1.8–2.0	2
175	7.7	6.5–9.0	3	1.8	1.7–2.0	4
230	*		1	11.1	9.9–13.5	5
300				11.0	9.0–13.8	4
330				(1)		1

*Specimen bent in U-shape and did not break during testing.

Table I-3 UNNOTCHED IMPACT TEST DATA SEGREGATED ON BASIS OF IRON CONTENT IN PLUTONIUM[25]

Test temp., °C	High iron, 1142 ppm: Eutectic present: Impact energy, ft-lb: Average	Range	No. tested	Low iron, 100 ppm: Eutectic absent: Impact energy, ft-lb: Average	Range	No. tested
30	7.5	5.3–8.8	4	5.7	4.5–7.8	5
100	7.7	5.7–10.0	6	5.8	5.1–6.2	4

Table I-4 EFFECT OF TEMPERATURE ON HARDNESS OF PLUTONIUM[25]

Test temp., °C	DPH (10-kg load)
100	190
23	286
0	310
−30	352
−65	380

eutectic on the formation of microcracks in cast plutonium.

Hardnesses of as-cast plutonium from −65 to 100°C are presented in Table I-4.

The effect of heat-treatment and cooling rate in the various phases on the microstructure and hardness of plutonium has been investigated, employing a Jominy end-quenching technique.[26] Plutonium bars containing 165 and 678 ppm iron were end quenched from the beta, gamma, delta, delta-prime, and epsilon phases. Alpha grain size was found to decrease with increasing cooling rate during cooling from all phases. The size of the Pu-Pu_6Fe eutectic network in the higher iron alloy decreased with increasing cooling rates when cooled from the epsilon phase. Cooling the high-iron plutonium from temperatures between 413 and 460°C produced a wide variety of Pu-Pu_6Fe configurations in the microstructures. The size of the Pu-Pu_6Fe eutectic network was found to be roughly double the alpha grain size. No apparent effect of cooling rates on hardness was noted. A density decrease noted near the quenched end of the bars reflects the promotion of microcracking by faster cooling rates. This tendency was less pronounced in the high-iron specimens.

In a compression test at room temperature, two plutonium−2.15 wt.% iron alloys exhibited brittle failures and had ultimate compressive strengths of 111,700 and 114,200 psi with plastic decreases in length at fracture of 6.7 and 7.4 per cent.[27] Average ultimate compressive strength of unalloyed plutonium at room temperature is 175,000 psi with a plastic decrease in length at fracture of 22.8 per cent. Tensile properties of plutonium−1.7 and 2.15 wt.% iron alloys are shown in Table I-5.

Oxidation of Plutonium Metal. The oxidation behavior of molten plutonium held at 900°C in an air atmosphere has been reported by Hanford.[28] Two 800-g pieces, contained in a magnesium oxide crucible, oxidized slowly, resembling burning charcoal. In contrast, plutonium turnings burn brightly. A plutonium oxide coating formed over the molten metal, protecting the metal from further oxidation. Even with intermittent stirring, it was not possible to oxidize completely the massive plutonium. It was necessary to cool, remove the oxide, and reheat the metal twice before oxidation was complete.

Beta Plutonium Alloys. The effect of a number of alloying additions on stabilization of beta plutonium has been investigated by Hanford.[25,28] Results are tabulated in Table I-6. None of the additions are as effective beta stabilizers as zirconium. A plutonium−3 at.% zirconium alloy, oil quenched from 200°C, exhibited a single-phase beta structure. A second phase (probably a plutonium-zirconium compound) appears after aging at room temperature. The effects of aging time on the room-temperature tensile properties of the alloy are shown in Table I-7. Strength was observed to increase with increasing aging time. Tensile and compression properties of the

Table I-5 TENSILE PROPERTIES* OF PLUTONIUM-IRON ALLOYS[27]

Alloy composition (balance Pu), wt.%	Ultimate strength, psi	Yield strength (0.01% offset), psi	Modulus of elasticity, 10^6 psi	Elongation, %	Reduction in area, %	Test temp., °C	Density, g/cm³
Unalloyed	50,900	32,100	14.3	0.068	0	30	19.55
1.7 Fe	54,500	26,700	7.1	0.23	0	30	17.54
1.7 Fe	29,700					125	17.54
1.7 Fe	24,500	8,720	3.8	0.59	0	127	17.54
2.15 Fe	35,900	25,700	6.7	0.044	0	30	17.07
2.15 Fe	34,100	10,750	5.0	0.43	0	127	17.07
2.15 Fe	14,150			1.0	0	220	17.07
2.15 Fe	4,260			12.5	5.9	318	17.07

*Testing speed, 0.015 in./min.

alloy at various temperatures and after various heat-treatments are presented in Tables I-8 to I-10. For comparison, the properties of unalloyed plutonium are shown in Tables I-11 and I-12. At low temperatures the strength of the beta-stabilizing alloy is comparable to that of unalloyed alpha plutonium. At elevated temperatures, however, the strength of the beta-stabilized alloy is greater than that of unalloyed beta plutonium.

Table I-6 DENSITIES AND RELATED DATA OF SOME PLUTONIUM-RICH ALLOYS[28]

Alloy composition (balance Pu)	Density, g/cm³	Phases present
2 at.% Sn	18.92	
3 at.% Mg	18.97	
1 at.% Hf	19.11	Alpha plus delta
2 at.% Hf	17.25	Alpha plus delta
1 at.% Si	16.35	Delta plus alpha
1 at.% Ti–500 ppm Si	18.39	Alpha plus delta
1 at.% Ti–1000 ppm Si	16.98	Delta plus alpha
1 at.% Ti–1 wt.% U	19.38	Alpha
1 at.% Ti–2 wt.% U	19.35	Alpha
1 at.% Ti–3 wt.% U	19.42	Alpha
1 at.% Ti–5 wt.% U	19.33	Alpha
3 at.% Cd	18.85	Alpha plus delta
3 at.% Tl	17.50	Alpha plus delta

Table I-13 shows[27] the transformation temperatures of plutonium–1, 2, and 3 wt.% titanium alloys.

Plutonium-Aluminum Alloys. Hardness and recrystallization properties of a plutonium–1 wt.% aluminum alloy have been investigated at Hanford.[28] The change in hardness as a function of per cent reduction is shown in Fig. I-1. The decrease in hardness measured for reductions of greater than 80 per cent is probably the result of a self-annealing effect caused by heat formed during working or by the leakage of dislocations at discontinuities or grain boundaries. Also, the hardness-measuring technique em-

Table I-7 STUDY OF THE EFFECT OF AGING TIME ON THE TENSILE PROPERTIES OF A BETA-STABILIZED PLUTONIUM–3 AT.% ZIRCONIUM ALLOY*[25]

Aging time after quench†	Ultimate strength, psi		Yield strength (0.01% offset), psi (test 2)	Elongation in 1 in., %	Reduction in area, %	Modulus of elasticity, 10^6 psi	Test temp., °C
	Test 1	Test 2					
20 min	40,872	41,500	22,200	0.076	0	6.24	25
7 hr	45,084	52,000	28,400	0.28	0	5.68	25
24 hr	40,272	45,700	24,400	0.112	0	6.34	25
48 hr	59,135	49,600	30,500	0.105	0	6.15	25

*All specimens were 0.250 in. in diameter. Testing speed: 0.015 in./(in.)(min).
†All tensile specimens were heat-treated at 220°C for 24 hr and then quenched in oil at room temperature. Average density after quenching was 17.40 g/cm³.

Table I-8 EFFECT OF HEAT-TREATMENT ON THE TENSILE PROPERTIES OF BETA-STABILIZED PLUTONIUM–3 AT.% ZIRCONIUM[28]

(Tensile Specimens, 0.250 in. in Diameter; Gauge Length, 1 in.; Testing Speed, 0.015 in./min; Density, Average 17.47 g/cm³)

Ultimate strength, psi	Yield strength, psi	Elongation, %	Reduction of area, %	Test temp., °C	Heat-treatment and remarks
16,300	15,480	6.25	25.0	200	Specimen held at 220°C for 5 hr; cooled to 200°C and held for 30 min and then tested
23,835		0	0	180	Specimen held at 220°C for 5 hr; cooled to 180°C and held for 30 min and then tested
28,748		0	0	160	Held at 220°C for 5 hr; cooled to 160°C and held for 20 min and then tested
36,842		0	0	130	Held at 220°C for 5 hr; cooled to 130°C and held for 20 min and then tested
45,546		0	0	70	Held at 220°C for 5 hr; cooled to 70°C and held for 20 min and then tested

ployed at these reductions may have had some effect on the hardness readings.

Changes in hardness of a 50 per cent cold-reduced plutonium–1 wt.% aluminum alloy with varying annealing times and temperatures are tabulated in Table I-14.

power of 25 kw/ft and an associated heat flux of 588,000 Btu/(hr)(sq ft). Dimensional changes of the $^{9}/_{16}$-in.-diameter $3^{1}/_{2}$-in.-long specimens were less than 0.45 per cent on the diameter and less than 0.55 per cent on the length. Metallographic examination showed a slight amount

Table I-9 TENSILE PROPERTIES OF BETA-STABILIZED PLUTONIUM–3 AT.% ZIRCONIUM ALLOY[28]

(Tensile Specimens, 0.250 in. in Diameter; Gauge Length, 1 in.; Testing Speed, 0.015 in./min; Density, Average 17.45 g/cm^3)

Ultimate strength, psi	Yield strength, psi	Elongation, %	Reduction of area, %	Test temp., °C	Length of time held at test temperature
12,552	9,971	0.05	4.4	200	20 min and tested
18,100		0	4.2	180	20 min
21,500		0	0	160	20 min
28,940		0	0	130	30 min
14,666		0	0	70	30 min

Plutonium-Ruthenium. A British[29] version of the plutonium-rich end of the plutonium-ruthenium system as determined by thermal analysis and dilatometry is shown in Fig. I-2.* Perhaps the most significant observation was the apparent existence of the zeta phase over a composition range, rather than at a single composition, as previously reported. Also, the eutectic composition appears to be at 12 at.% ruthenium, instead of at 10 at.% ruthenium as shown in previous phase diagrams. The observation that the delta-plus-zeta/delta-plus-eta boundary is not continuous with the zeta-plus-eta/delta-plus-eta boundary can probably be attributed to nonequilibrium conditions.

Plutonium-Gold Alloys. Mound Laboratory[30] reports that the one compound, AuPu, found in the gold-plutonium system appears to decompose eutectoidally to two phases. Eutectic reactions were found between AuPu and plutonium, apparently at a very low gold content, and between AuPu and plutonium at about 90 at.% gold.

Aluminum-Plutonium Alloys. Hanford[31] reports that two Zircaloy-2-clad aluminum–2.1 wt.% plutonium–2.0 wt.% nickel alloys, fabricated by injection casting, have been irradiated to 22 per cent burnup of the plutonium atoms. The capsules were operated with a specific

of segregation in the two-phase fuel core structure. Hardness from core outside diameter to center decreased from 78 to 65 KHN (Knoop hardness number).

Thorium-Plutonium and Niobium-Plutonium Alloys. In a study[32] of potential plutonium fuel alloys at Battelle, 90 per cent cold-reduced thorium–5 and 10 wt.% plutonium alloys were found to exhibit recrystallization characteristics similar to those of unalloyed thorium. A niobium–25.6 wt.% plutonium–6.1 wt.% silicon alloy, prepared using prealloyed $PuSi_2$ was found to have a microstructure consisting of niobium and approximately 30 vol.% $PuSi_2$. The $PuSi_2$ was present as a semicontinuous phase surrounding the niobium, suggesting that the melting temperature of $PuSi_2$ is lower than the melting temperature of niobium.

(V. W. Storhok)

Plutonium Compounds

A literature survey of the unclassified information on plutonium compounds was presented in *Nukleonika*[33] along with tabulations of important physical properties.

Russian investigators[34] have determined the heat of formation of $PuBe_{13}$ by microcalorimetric techniques to be: $\Delta H_{298} = 35.7 \pm 3.4$ kcal/mole. The material has a reported microhardness of 1045 kg/mm^2 and a lattice constant of 10.259 ± 0.001 *kX*.

*Figure I-2 is reprinted here by permission from the United Kingdom Atomic Energy Authority.[29]

Table I-10 COMPRESSION PROPERTIES OF BETA-STABILIZED PLUTONIUM–3 AT.% ZIRCONIUM ALLOY[28]

(Testing Speed, 0.015 in./min; Total Plastic Decrease in Length Was Determined from Load-Platen Displacement Curve at Point of Failure)

Ultimate strength, psi	Yield strength, psi	Plastic decrease in length, %	Test temp., °C	Heat-treatment, °C	Density, g/cm³ Before	Density, g/cm³ After
67,000	59,800	4.6	60	30 min at 60	17.36	17.77
64,600	57,900	5.3	80	30 min at 80	17.38	17.65
53,500	48,700	5.3	130	30 min at 130	17.37	17.40
45,600	41,000	6.0	160	30 min at 160	17.35	17.40
46,800	43,000	5.0	180	20 min at 180	17.40	17.44
32,800	27,700	5.0	200	20 min at 200	17.38	17.46

Table I-11 EFFECT OF TEMPERATURE ON TENSILE PROPERTIES OF ALPHA AND BETA PHASES OF PLUTONIUM*[28]

(Testing Speed, 0.015 in./min; Gauge Length, 1 in.)

Test temp., °C	Ultimate strength, psi	Yield strength (0.01% offset), psi	Modulus of elasticity, 10^6 psi	Elongation, %	Reduction of area, %	Phase
30	50,900	32,100	14.3	0.068		Alpha
70	43,800	15,200	12.6	0.43		Alpha
100	35,100	13,300	9.0			Alpha
110	33,100	12,300	10.0			Alpha
130	12,100	10,400	3.0	294.0	100.0	Beta
160	5,620	3,950		570.4	100.0	Beta
180	3,580	2,620		503.2	100.0	Beta
200	2,940	2,190		121.0	82.1	Beta

*From H. R. Gardner and I. B. Mann, Mechanical Property and Formability Studies on Unalloyed Plutonium, Paper 36 presented at Second International Conference on Plutonium, Grenoble, France, April 1960. Also available as USAEC Report HW-65019.

Table I-12 COMPRESSION STRENGTH AND RELATED DATA FOR HIGH-DENSITY PLUTONIUM[28]

Test temp., °C	Ultimate strength, psi	Yield strength, psi	Increase in area, %	Plastic decrease in length, %	Density,* g/cm³	Phase
70	118,400	80,200			19.53	Alpha
110	77,200	64,800		18.3†	19.53	Alpha
130		17,700	436	81.6‡	19.56	Beta
176		8,770	625	85.5‡	19.59	Beta
190		7,130	658	86.3‡	19.59	Beta

*Densities before testing.

†Total plastic decrease in length was determined from load-platen displacement curve at point of failure.

‡After exceeding the yield strength, the load was increased at a rapid rate to 100,000 lb. The increase in area and decrease in length data were taken after unloading and cooling to room temperature.

Table I-13 PHASE TRANSFORMATION TEMPERATURES IN PLUTONIUM-TITANIUM ALLOYS[27]

Composition (balance Pu), at.%	Probable transformation	Temp., °C
1 Ti	Alpha to beta	125
	Beta to gamma	235
	Gamma to delta	318
2 Ti	Alpha to beta	122
	Beta to gamma	255
	Gamma to delta	315
3 Ti	Beta to gamma	260
	Gamma to delta	310

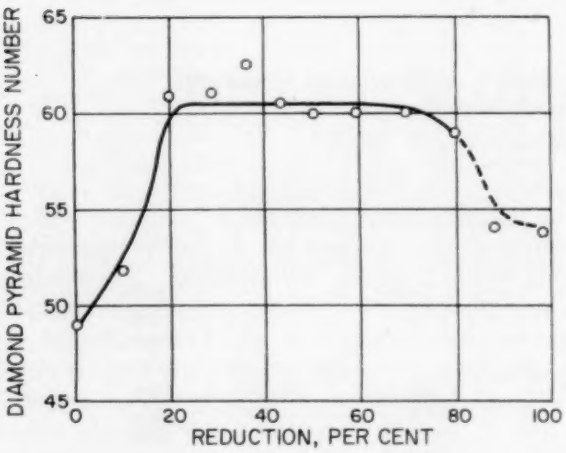

Fig. I-1 Diamond pyramid hardness number (DPHN) versus per cent reduction by rolling for a plutonium–1 wt.% aluminum alloy.[28]

In the work on plutonium-bearing glass at Mound Laboratory,[35,36] new compositions of increased strength are being investigated. One glass containing 69.42 SiO_2, 2.56 Al_2O_3, 5.58 CaO, 16.73 Na_2O, 5.58 K_2O, and 0.12 Fe_2O_3 (composition in wt.%) easily dissolves 15 to 20 wt.% of PuO_2. Such glasses lost only 0.2 per cent of the dissolved PuO_2 after leaching 2903 hr in room-temperature water. Heating a 12.66-μ-diameter fiber for 16 days at 100°C increased the tensile strength from 129,700 to 170,000 psi.

United Nuclear[37] has attempted the production of PuC by reaction of carbon and PuO_2, using 3:1 mole ratios. Argonne[38] mixes the oxide with pitch, decarbonizes the pitch, and reacts at 1450°C. Both laboratories obtain traces of Pu_2C_3 along with PuC, and some oxide exists in solid solution. Sintering of cold-pressed pellets at 1700°C resulted in compacts of only 80 to 85 per cent of theoretical density. As a result, United Nuclear is investigating liquid-phase sintering with a 0.1 wt.% nickel additive.

Battelle[39] is determining the vapor pressure of PuO_2 in various atmospheres and reports values from 1.41×10^{-9} atm to 2.03×10^{-8} atm in the temperature range 1450 to 1700°C.

No binder has been found to be more effective than water in producing good green strength in pressed pellets of PuC by Nuclear Materials and Equipment Corp.[40] This laboratory is also investigating the cause of weight losses during the early stages of sintering. A eutectoid structure has been detected by metallographic examination of sintered pellets, and Pu_2O_3 is present.[41]

Workers at Vallecitos[42] have prepared pellets of $(Pu,U)O_2$ by cold pressing and sintering or swaging. Swaging was found to be economical from a process-time standpoint but resulted in bodies of only 75 per cent of theoretical density. AERE, Harwell,[43] reports that PuO_2 is the diffusing species in the UO_2-PuO_2 system and that the solid-solution formation is more rapid in CO_2 than in argon or hydrogen atmospheres. The degree of solid-solution formation is most extensive at 1650°C, but higher densities are obtained at sintering temperatures of approximately 1500°C. The liquidus of the FeO-PuO_2 system was found[44] to exist in the range 1450 to 1550°C between 10 and 90 wt.% PuO_2, whereas that of the UC-PuC system varied linearly between PuC (1740°C ± 10°C) and UC (2390°C ± 10°C).

In studies[28] at Hanford on plutonium compounds, $PuSi_2$ was prepared by reacting mixtures of PuO_2 and SiC in vacuum at 1400°C or by arc melting plutonium and silicon metals under argon. The PuC peritectic at 1650°C was

Table I-14 CHANGE IN HARDNESS (DPHN) OF PLUTONIUM–1 WT.% ALUMINUM REDUCED 50 PER CENT BY ROLLING, FOR VARIOUS ANNEALING TIMES AND TEMPERATURES[28]

Annealing temp., °C	Hardness change for indicated annealing time							
	5 min	10 min	20 min	40 min	1 hr	2 hr	4 hr	7 hr
100	59	58	59	59	58	59	58	59
150	59	57	60	60	60	59	58	59
200	59	58	57	59	60	59	60	59
250	59	59	60	59	60	59	59	58
300	59	59	58	54	53	53	51	50

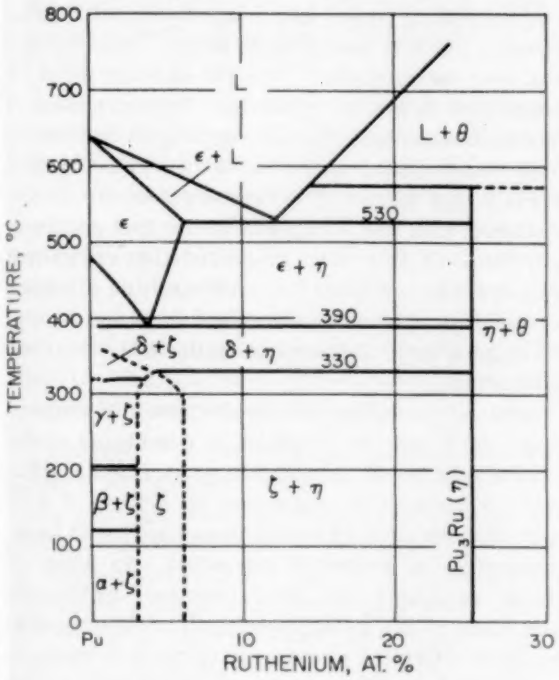

Fig. I-2 Plutonium-rich portion of the plutonium-ruthenium phase diagram.[29]

completely suppressed in a 50 wt.% UC solid solution.

The production of 70 per cent alpha Pu_2O_3 in PuO_2 pellets was reported after a 1500°C sinter in dry hydrogen. Greater sintered densities are obtained when using PuO_2 that is calcined below 400°C. This effect is attributed to surface-area considerations.[25] (W. M. Pardue)

Thorium

The solid-solution hardening of alpha thorium by zirconium has been demonstrated,[45] but the increase in hardness during the aging of the supersaturated alpha solid solution is very slight. Microscopic observations indicate that discontinuous precipitation usually occurred.

The most promising alloys investigated are those of compositions corresponding to the thorium-rich end of the beta solid solution, which exists above 1000°C, after subjection to heat-treatment. The beta solid solution transformed on quenching; tempering the quenched alloys produced a more stable structure with very useful mechanical properties. A study of the isothermal transformation of the beta solid solution was also carried out, and a time-temperature-transformation relation was obtained for a 39 at.% zirconium alloy. The transformation product is mainly lamellar and is shown to hold promise of high tensile strength.

Battelle reports[46] that dry-air oxidation data obtained for $(Th_9U)C_2$ and $(Th_9U)C$ at 900, 1100, and 1300°F, when averaged, are amenable to an Arrhenius plot. The rate equations are:

For $(Th_9U)C_2$,

$$W\,[\mathrm{mg/(cm^2)(hr)}] = 15{,}500 \exp\left(\frac{-13{,}600}{1.987T^\circ\mathrm{K}}\right)$$

For $(Th_9U)C$,

$$W\,[\mathrm{mg/(cm^2)(hr)}] = 19{,}000 \exp\left(\frac{-13{,}000}{1.987T^\circ\mathrm{K}}\right)$$

The activation energies for both compounds are similar, suggesting that the mechanism of oxidation may be the same for both compounds. The low absolute values of these activation energies indicate that the process is not very temperature sensitive. (V. W. Storhok)

Dispersion Fuels

The Clevite Corporation is developing, for the AEC, an aluminum-base fuel element which contains a large volume of U_3O_8-bearing glass fibers in the core. A recent report[47] describes some mechanical properties of this material clad with either an Alclad 5154 alloy or an Alclad Fiberglas-reinforced aluminum alloy. Figure I-3 shows, for example, the effect that temperature has on the ultimate strength of the two types of clad fuel plates. It should be noted that the plates had a different amount of cold work, varying between 5 and 15 per cent. It is reported, also, that cold-rolled or annealed Alclad 5154 fuel plates could be formed to a 5½-in. radius (MTR plate curvature) without cracking; however, the cold-rolled Alclad Fiberglas-reinforced plates must be annealed at 1000°F for 1 hr before forming. At Battelle[32] a study is under way to determine the effects of reactor irradiation on the properties and structural integrity of this fuel material.

Several reports that were published during the past quarter are concerned with stainless steel–UO_2 dispersion fuel elements. At Martin,[48] where a tubular element is being developed for

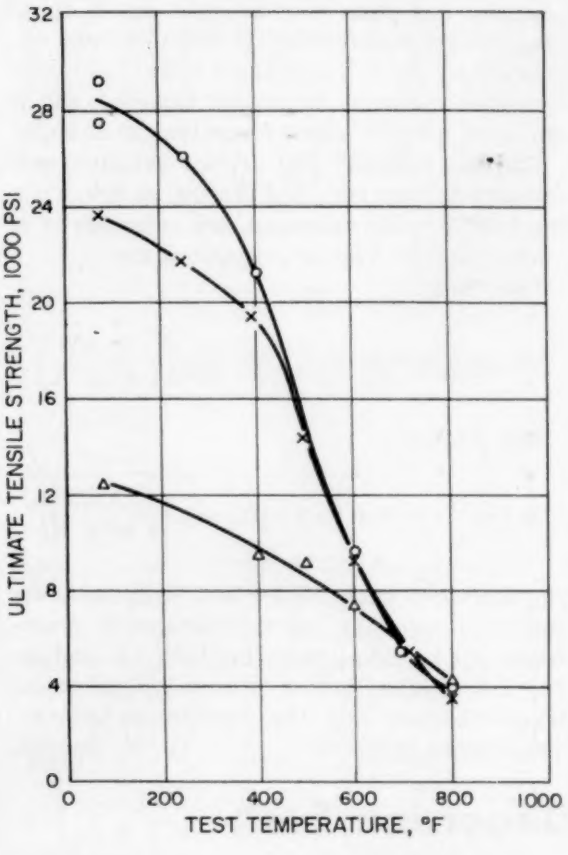

Fig. I-3 Effect of temperature on the ultimate tensile strength of U_3O_8-bearing Fiberglas plates clad with Alclad 5154 or Alclad Fiberglas-reinforced aluminum.[47] ○, Alclad 5154 cold rolled from 0.060 to 0.050 in. ×, Alclad 5154 cold rolled from 0.053 to 0.049 in. △, Alclad Fiberglas-reinforced aluminum cold rolled from 0.053 to 0.050 in.

mobile Army reactors, attention is directed at eliminating the permeability of the core to prevent waterlogging during operation. It has been shown that a powder-rolled core strip that is subjected to either 36 or 68 per cent reduction at 1175°C is not penetrated by a low-viscosity dye penetrant under pressure. However, after being cold formed into a tube, the core with a light hot reduction is penetrated, whereas the other is not. Furthermore, it is reported that hot-isostatic pressing at 2100°F will also provide a tubular core that is not penetrated by the dye.

At Phillips Petroleum Company,[49] damage to plate type fuel elements of stainless steel–UO_2 was observed in three nuclear cores at SPERT. Both blistering and rippling of the plates occurred during power excursion tests with initial reactor periods less than 20 msec. Little burnup had been accumulated; thus the damage must be attributed to causes other than fission gases. It has been assumed that the rippling is caused by high-temperature differences between the fuel surface and center. The blisters seem to be associated with UO_2 stringers at the fuel-cladding interface. It was also observed that corrosive damage had apparently penetrated the cladding in several places. (This might have led to waterlogging type failures, causing the observed blistering.)

The complexities of the structure of dispersion fuels and of irradiation conditions make interpretation of irradiation experiments difficult. A method is suggested by Keller et al.[50] for consideration of irradiation conditions independently of material variables, so long as these variables are held constant. Estimates are made of the relative severity of experiments made on identical specimens under different experimental conditions. A numerical application of the analysis was made to specimens of 18-8 stainless steel with 25 and 30 wt.% UO_2. Approximate failure limits for both specimen compositions are obtained, although both sets of data are very limited. Further experimentation is needed to establish more fully the limits of the application of the proposed model.

Coated-Particle Fuel Materials

Preparation and Testing

Both Nuclear Materials and Equipment Corporation (NUMEC)[51,52] and Hanford[27] have reported that they are investigating electroless processes for the deposition of metals on fuel particles. Hanford coated low-surface-area, normal UO_2 and obtained total alpha shielding with thicknesses of about 75 μ. The major obstacle to preparing thinner coatings has been the fact that the induction period prior to nickel deposition varies from run to run and definite plating times cannot be accurately measured. Similar techniques are being studied at NUMEC[51,52] to precoat spherical PuO_2 and PuO_2-UO_2 particles with nickel and to evaluate the products for use in reactor applications. Copper is electrolytically deposited on the nickel-coated particles. Once the processing variables

have been satisfactorily developed for copper coatings, other electrolytic coatings are to be studied.

Several review articles and papers have been presented on ceramic and metallic coatings on fuel particles.[27,53–55] In addition, a Polish report[56] on carbon coating of uranium dioxide powders was recently received. This report indicated that compact carbon coatings with a metallic luster were obtained on UO_2 particles by the pyrolysis of naphthalene in a fluidized-bed apparatus at temperatures between 1100 and 1300°C. The UO_2 particles were prepared from powder by cementing with pitch and cooking.

Battelle[32,39,58] has reported rather extensive results on ceramic-coated fuel particles. Alumina coatings have been deposited at temperatures from 700 to 1400°C by hydrolysis of $AlCl_3$. At temperatures below 1000°C the coatings are relatively porous; at temperatures above 1000°C the coatings are essentially of theoretical density. The grain size of the alumina coatings increases with increasing temperature but shows no sharp change at a particular temperature, as occurs in the case of coating porosity. Both porous and dense UO_2 particles are being coated, and the porous substrate permits more severe subsequent heat-treatments than does a dense substrate. The porous UO_2 evidently yields when stresses are set up due to differential thermal expansion. Alumina coatings deposited at 1400°C have, in the past, been somewhat inferior to coatings deposited at temperatures between 1000 and 1300°C. However, on the basis of heat-treatment in hydrogen at 1400°C for 48 hr, oxidation in oxygen at 1100°C for 24 hr, and a final acid leach, the 1400°C alumina coatings appear to be satisfactory if the small percentage of coated particles with irregular protrusions on their surface are removed before testing.

Heat-treatment of various types of Al_2O_3-coated particles is being carried out in an attempt to minimize irradiation damage in subsequent use. Heat-treatment of 1000°C alumina coatings on dense UO_2 particles is feasible at 1250°C, but similar treatments at 1500°C of coatings deposited at 1225°C were not satisfactory. Attempts to support 53-μ Al_2O_3 coatings on 127-μ UO_2 particles with a 127-μ overcoating of pyrolytic carbon (PyC) were negative in that the Al_2O_3 coatings had failed after heating to 1800°C. However, it was demonstrated that a 1500°C anneal of porous UO_2 particles coated at 1000°C was effective in significantly reducing coating damage in a later thermal cycle to 1760°C, although appreciable damage still occurred.

Additional studies of the behavior of Al_2O_3-coated UO_2 particles in an oxygen or air atmosphere have shown that the temperature at which rapid oxidation occurs is also dependent on the original temperature of application of the coating. Particles coated at 1400°C appear to have failed as a result of oxygen diffusion at 1500°C and by thermal stress at 1700°C, whereas particles coated at 1000°C failed as a consequence of thermal stress at about 1350°C. These results were obtained on dense UO_2 particles approximately 127 μ in diameter and coated with 40 to 50 μ of alumina. Oxygen permeability values for the coatings are summarized in Table I-15.

Beryllia and magnesia coatings are also being deposited, but the coatings have not yet proved to be as protective as alumina coatings.[32,39,58] However, a considerably more concentrated ef-

Table I-15 PERMEABILITY OF OXYGEN THROUGH Al_2O_3 COATINGS AT A PRESSURE OF 1 ATM OXYGEN[39]

Specimen	Test temp., °C	Test time, hr	UO_2 particle diameter, μ	Coating thickness, μ	Permeability, g/(cm²)(sec)	Oxidized and quenched structure
OXT-13	1300	120	68	65	1.09×10^{-9}	UO_{2+x}, U_4O_9
OXT-30*	1300	96	62	38	9×10^{-10}	
OXT-14	1200	96	68	65	5.38×10^{-10}	U_3O_8
OXT-15†	1200	96	260	158	4.23×10^{-10}	UO_2, U_3O_8
OXT-16	1200	1000	63	40	3.08×10^{-10}	UO_{2+x}, U_4O_9, U_3O_8
OXT-27*	1200	139	62	38	2.08×10^{-10}	UO_2
OXT-30*	1100	100	62	38	1.24×10^{-10}	

*Coatings were deposited at 1400°C. All other specimens were coated at 1000°C.
†Porous UO_2.

fort has been placed on the development of alumina coatings during the past several years. Recent efforts to deposit BeO coatings by the decomposition of beryllium basic acetate at 1400°C using water vapor as a midly oxidizing medium to prevent carbon deposition were unsuccessful because of equipment difficulties. The use of indirect or direct hydrolysis of $BeCl_2$ at 1400°C to deposit BeO has resulted in porous coatings. Impurities in the $BeCl_2$ feed are believed to be one source of difficulty.

Magnesia coatings are being deposited on porous UO_2 substrates by direct hydrolysis of MgI_2. Because MgO contracts to a greater extent than UO_2 in cooling from deposition to room temperature, the use of a porous substrate to prevent coating failure upon cooling is being investigated. Recent examinations of whole particles indicated that the coatings were relatively transparent and essentially free of cracks. After exposure to oxygen at 1100°C for 20 hr, about 1 per cent of the particles were found to be cracked. When the MgO-coated particles were first treated in hydrogen at 1250°C for 48 hr before the oxidation test, approximately 5 per cent of the particles were found to be cracked. These relatively favorable results are inconsistent with the results of microscopic examinations of mounted and sectioned MgO-coated particles. Further attempts to find a suitable selective reagent for dissolving the exposed UO_2 in the presence of MgO are being made to provide further information on the quality of the coatings and to resolve this apparent inconsistency.

Oak Ridge[59] is studying the compatibility of Al_2O_3-coated UO_2 in pressurized hydrogenated water at 360°C. After 100 hr the Battelle-prepared material had decreased 0.8 per cent in weight. Other corrosion studies are under way at Oak Ridge on oxide-coated particles in Santowax R and molten fluoride salts, and Battelle[32,39,58] is studying the MgO-H_2O reaction at high temperatures.

Battelle[32,39,58] is also investigating the advantages of using coated particles in metal-clad tubular elements under mildly oxidizing conditions. BeO-coated UO_2 particles exhibited somewhat better oxidation resistance than did initially porous coatings of Al_2O_3 on UO_2 after pressure bonding, although there was some loading variation between samples which was a complicating factor. Other studies with defected stainless-steel claddings containing various types of compacted fuel materials revealed that UO_2 particles coated with 5 to 10 μ of dense Al_2O_3 were considerably more resistant to failure in air at 815°C than uncoated UO_2 particles and that chromium-powder additions to the coated particles before compaction enhanced their oxidation resistance.

Carbide-Base Fuel. General Atomic reported[60] on its recent progress in the development of fuel compacts continuing PyC-coated $(Th,U)C_2$ particles. These studies were concentrated on improving General Atomic's process for the preparation of the carbide particles, designing equipment for scaling up the coating process to 1.3 kg/run, and improving the fabrication operation. A summary of the general design philosophy of the High-Temperature Gas-Cooled Reactor (HTGR) regarding the use of coated particles was recently reported,[61] and a review of General Atomic's procedures for the preparation of graphite fuel compacts containing carbon-coated dicarbide fuel particles is now available.[62]

Studies have also been carried out at Harwell[63] on the manufacture of UC particles and on coating of the particles with a layer of PyC as an aid to fission-product retention. These studies were carried out on 50- to 100-μ particles in a rotating furnace at 775°C using a 17 per cent mixture of propane in argon as the reactant feed. Particles coated with 20 μ of PyC were incorporated into graphite compacts, and xenon-release tests were carried out after neutron activation in BEPO. Release factors were found to be about 10 times less than those obtained for conventional uranium-carbon fuel compacts at 800°C. It should be pointed out that the xenon-release values reported by Harwell are not on the same basis as those used in the United States. The 0.07×10^{-7} to 3.40×10^{-7} values reported[24] are the rates at which xenon is lost divided by the total contained xenon, but in the United States the ratio of the total xenon released to total contained is employed. The units of the British data are believed to be sec^{-1}.

National Carbon[64–66] is coating dicarbide particles with PyC and fabricating them into graphite elements. Uranium dicarbide spheroids of 200-μ average diameter, coated with 60 μ of PyC, together with the matrix materials, are added to a sigma-blade mixer. On the basis of

the time of mixing versus coefficient of variation, a mixing time of 1 hr was chosen. The resulting mix was extruded into $^3/_4$-in.-diameter by 6-in.-long rods and baked at 2200°C. Other studies revealed that high forming pressures (6 to 15 tsi) damaged the coatings on the particles, and severe uranium and fission-product migration was found to have occurred in post-irradiation examination of two capsules irradiated at Oak Ridge. Parenthetically it might be added that the 2350°C final baking temperature for these elements is probably the primary cause of the difficulty.

In compatibility studies of PyC-coated UC_2 particles, Oak Ridge[67] has leached lots of 400- to 500-μ-diameter UC_2 particles coated with 80 to 100 μ of PyC (3M-D), and 250- to 300-μ-diameter particles with 40 to 50 μ of PyC (3M-F) in 8*M* HNO_3 for 8 hr at 90°C. The uranium removed, expressed in terms of UC_2, was 0.45 and 0.09 per cent, respectively. Two-gram samples of each of the leached particles were exposed to 100 cm^3/min of flowing helium containing 2.5 vol.% water vapor for 100 hr at 900°C. The losses in weight were 3.9 and 1.0 per cent, respectively, for lots 3M-D and 3M-F. Leaching of the coated particles with HNO_3 after heating at 900°C gave 0.08 and 1.8 per cent losses of the UC_2. Microscopic examination after exposure at 900°C showed that the coatings had been pitted and had a much duller appearance. Additional studies of the compatibility of PyC-coated UC_2 particles with Santowax R at 260°C and with molten fluoride salts are planned.

Battelle[32] has reported that the density of PyC coatings on particles decreases from 1.91 g/cm^3 at 950°C to a minimum value of approximately 1.50 g/cm^3 at 1500°C and then increases to a density of 1.94 g/cm^3 at a temperature of 1800°C. In addition, the density of the coatings appeared to increase linearly with deposition rate over the range of conditions studied at a coating temperature of 1400°C. This was surprising in that prior published work on extended surfaces indicated an increase in density with decreased reactant partial pressure, and hence lower rates of deposition. The density of the coating on the particles increased from 1.47 g/cm^3 at a deposition rate of 28 μ/hr to 1.58 g/cm^3 at a rate of 60 μ/hr. At an 1100°C particle-coating temperature, coating densities ranged from 1.81 to 1.91 g/cm^3 at deposition rates of 18 and 43 μ/hr, respectively.

A study of the kinetics of carbon deposition from methane and acetylene in a fluidized bed, as well as some limited evaluation on the protection afforded thorium and uranium dicarbides, uranium monocarbide, and uranium dioxide by the carbon coating, was published.[68] Other studies at Battelle[32,39] on the codeposition of silicon-PyC coatings indicated no improvement in strength was obtained by 1.5 at.% silicon additions to PyC.

Pelletizing techniques are being studied at Battelle[32,39,58] to prepare improved graphite-matrix as well as oxide-matrix elements containing coated particles. The pelletizing technique for graphite-matrix elements consists of spraying a slip containing −325-mesh (< 44 μ) graphite powder and the binder onto coated-particle fuels in a rotating drum. This technique is expected to result in improved support by the matrix material and is an alternative to chemical fabrication of equidistant fuel dispersions. Examples of the uniformity of the dispersions are shown in Figs. I-4 and I-5. Exploratory studies on explosive compaction techniques are also being carried out.

Irradiation and Evaluation

Oxide-Base Fuel. A final report on the SP-5 experiment has been issued by Battelle.[69] The fission-gas-release behavior of 100- to 140-μ-diameter UO_2 particles coated with 42 μ of vapor-deposited alumina was analyzed in detail. The fission-gas retention of this material was very good at low burnups when the particle coatings were intact. Deterioration was first noted at 1 at.% burnup and became relatively more severe between 3 and 5 at.% burnup. Cracking of the coating was the primary cause of fission-gas release, as differentiated, for example, from diffusion through undamaged coatings. Fission-gas-release rates initially were 10^{-7} of the generation rates but, after 6 at.% burnup, had deteriorated to 10^{-2} for long-lived fission gases and 10^{-4} for the shorter lived ones. It was not clear what actually caused this cracking, but two possibilities were suggested: (1) buildup of fission-gas pressure and (2) annealing effects, since the coatings are deposited in a strained condition and, upon annealing as a result of elevated temperature or radiation-induced effects, may crack. Other studies on Al_2O_3-coated UO_2 particles are currently under way to resolve which of these

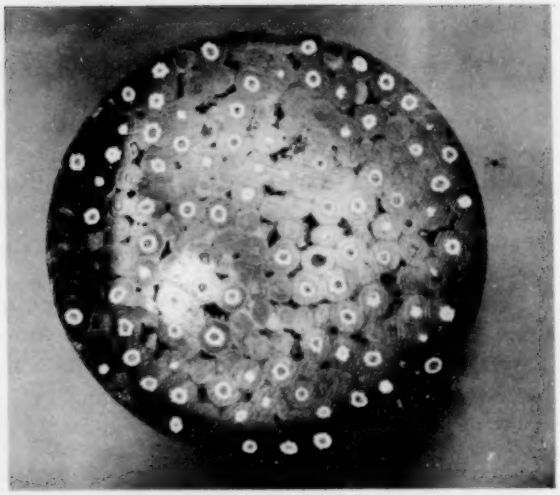

Fig. I-4 Sectioned surface of a cylindrical element (~1/4 in. in diameter) fabricated by chemical vapor-deposition techniques. Uranium dioxide particles, approximately 127 μ in diameter, were coated with about 53 μ of vapor-deposited Al_2O_3. The Al_2O_3-coated UO_2 particles were then overcoated with 120 μ of vapor-deposited PyC. These PyC-overcoated particles were then bonded together by passing methane gas slowly through a packed bed of the heated particles which resulted in carbon deposition throughout the interstices between the particles. (Unpublished data, courtesy of M. F. Browning.)

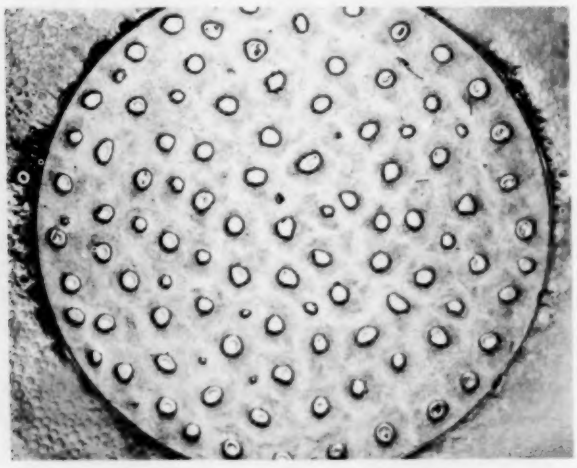

Fig. I-5 Sectioned surface of a cylindrical element (~1/4 in. in diameter) fabricated by pelletizing techniques. Al_2O_3-coated UO_2 particles were spray coated in a rotating drum using a suspension of finely divided graphite particles and pitch in a benzene solvent. The graphite-binder overcoated particles were then pressure baked using conventional fabrication techniques. (Unpublished data, courtesy of M. C. Brockway.)

causes or other possible effects may be responsible for the coating damage.

Fission-gas-release information on four types of unsupported coated 127-μ UO_2 particles has been reported by Battelle[32] and is shown in Table I-16. These preliminary data indicate that 42- to 54-μ alumina coatings which have a porous interlayer tend to retain fission gas better at low temperatures than an alumina coating which is dense throughout. The data also suggest that 45-μ PyC coatings on 127-μ UO_2 particles probably retain fission products about as well as 42- to 54-μ alumina coatings under the specified irradiation conditions. In another sweep-gas experiment, CFP-S-5, a specimen containing 4E material (dense-porous-dense Al_2O_3 coatings on UO_2) dispersed by National Carbon in a graphite matrix had R/B values (rate of release divided by rate of generation) for fission products between 10^{-5} and 10^{-6} for 200 hr of operation[32] at 1050°C. After 200 hr a leak developed between the capsule annulus and the sweep-gas system, and the experiment is now being continued as a static experiment. Static capsules attached to the sweep compartment contain 4E material dispersed in a graphite matrix and three types of unsupported PyC-coated fuel particles. Another sweep experiment, CFP-S-6, will have 127-μ UO_2 particles coated with 58 μ of dense Al_2O_3, the coating having been deposited at a temperature of 1225°C, dispersed in a graphite matrix.[58] This experiment will also be carried out in the 1000 to 1100°C temperature range, and additional materials will be irradiated in attached static capsules.

Carbide-Base Fuel. Oak Ridge[59,67] has reported that the capsule containing PyC-coated UC_2 particles (unsupported), which was irradiated in the Low-Intensity Test Reactor (LITR) to approximately 9 at.% burnup at a centerline temperature of about 1100°C, has been opened and that some damaged particles were observed. Krypton-release ratios were 100 and 1000 ppm for the two sections of the capsule. A sweep experiment in the MTR-48 facility has been carried to a burnup of 12 at.% at temperatures between 900 and 1450°C for 97 days. The specimen consists of a cylindrical graphite element fabricated by National Carbon and containing 250-μ UC_2 particles prepared and coated with 80 μ of laminar PyC by 3M (Minnesota Mining and Manufacturing Company). The R/B values

were in the range of 10^{-2} to 10^{-3} for this experiment. The next sweep experiment in the MTR-48 facility will involve a specimen fabricated by General Atomic containing PyC-coated $(Th,U)C_2$ particles. Four attached static capsules will contain unsupported PyC-coated particles from High Temperature Materials, 3M, National Carbon, and General Atomic. In another sweep experiment in the Oak Ridge Research Reactor (ORR) poolside facility, a specimen fabricated by 3M and containing 3M PyC-coated UC_2 particles had R/B values of 10^{-6} for one sample after 13 days of operation at approximately 1000°C, and 10^{-5} for another, until a helium purge stream was replaced with argon, thus causing the specimen temperature to rise to 1350°C. At this point the R/B values climbed to the 10^{-3} level.

General Atomic[60] purge capsules GA-309-4, -5, and -6, which contain PyC-coated $(Th,U)C_2$ particles in graphite matrices, were discharged from the General Electric Testing Reactor (GETR) after undergoing irradiation equivalent to the maximum expected in the HTGR core These capsules will provide the first opportunity to examine coated fuel particles after a high-burnup, high-temperature irradiation.

Battelle[32] data on two types of PyC-coated, 200-μ UC_2 particles are presented in Table I-17. The 55-μ laminar coatings, prepared at a coating rate of 37 μ/hr from acetylene at a deposition temperature of 1400°C, seem to retain fission products better than a 55-μ columnar coating prepared under identical conditions, except that the coating rate was reduced to 5 μ/hr. It is interesting to note, however, that 55-μ laminar PyC coatings on 200-μ UC_2 particles apparently behave more satisfactorily at low temperatures than similar 45-μ PyC coatings on 127-μ UO_2 particles. (J. H. Oxley)

Refractory Fuel and Fertile Materials

Properties and Behavior of Uranium Oxides

Measurements of the change of the melting point of UO_2 when irradiated to various ex-

Table I-16 BURNUP AND FISSION-GAS RELEASE FROM UNSUPPORTED COATED OXIDE PARTICLES IRRADIATED AT TEMPERATURES[32] OF APPROXIMATELY 90°C IN CAPSULE CFP-4

Specimen type	Specimen composition		Irradiation flux, 10^{13} nv	U^{235} fission burnup, at.%	Xe^{133} fractional release ratio,* ppm
	Fuel	Coating			
4E	UO_2	Dense-porous-dense Al_2O_3†	1.47	2.9	10
721C	UO_2	Dense-porous-dense Al_2O_3†	1.57	3.1	31
715A	UO_2	Dense Al_2O_3	1.50	3.0	130
920A	UO_2	Laminar PyC	1.72	3.4	290

*Ratio of number of atoms of Xe^{133} detected to number theoretically contained at the end of irradiation (saturation condition).

†Dense layer of Al_2O_3 next to UO_2 overcoated successively with a layer of porous Al_2O_3 and a layer of dense Al_2O_3.

Table I-17 BURNUP AND FISSION-GAS RELEASE FROM UNSUPPORTED COATED CARBIDE PARTICLES IRRADIATED AT TEMPERATURES[32] OF APPROXIMATELY 90°C IN CAPSULE CFP-4

Specimen type	Specimen composition		Irradiation flux, 10^{13} nv	U^{235} fission burnup, at.%	Xe^{133} fractional release ratio,* ppm
	Fuel	Coating			
919A	UC_2	Laminar PyC	1.64	3.2	18
918A	UC_2	Columnar PyC	1.60	3.1	250

*Ratio of number of atoms of Xe^{133} detected to number theoretically contained at the end of irradiation (saturation condition).

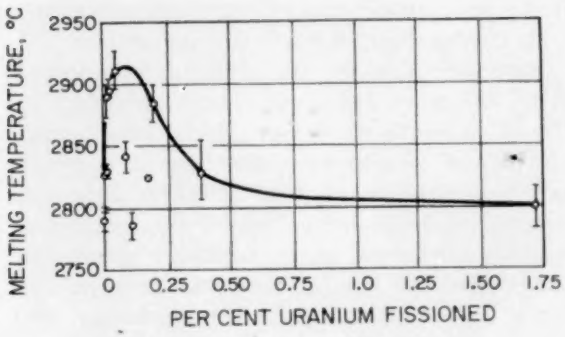

Fig. I-6 Melting point of UO_2 as a function of irradiation exposure.[70]

posures up to 15,000 Mwd/ton of uranium have been performed at Hanford[70,71] by high-temperature microscopy. The results of these measurements are summarized in Fig. I-6. The melting point increased from 2790°C for unirradiated UO_2 to a maximum of 2915°C at a burnup of 0.06 at.% and then decreased to about 2800°C at a burnup of about 1.75 at.%. Motion pictures of the UO_2 specimens taken during heating revealed that the volatility of the UO_2 varied inversely with the melting point. Both the irradiated and unirradiated UO_2 vaporized rapidly at temperatures near the melting point. Crystals grown by deposition of the vapor from irradiated UO_2 exhibited a higher melting point and lower vapor pressure than unirradiated vapor-deposited crystals. Thermal-conductivity and electrical-conductivity measurements performed on various types of irradiated and unirradiated UO_2 are presented in Figs. I-7 to I-10.

A recent paper[74] describes techniques employed in France for studying sintered UO_2 using optical and electron microscopy.

UO_3 was found by the Russians[75] to dissociate into U_3O_8 in the temperature range 450 to 650°C, with complete conversion attained above 550°C. At temperatures above 700°C, dissociation of the U_3O_8 was observed. Hoekstra et al.[76] studied the low-temperature oxidation of UO_2 to U_3O_7, which was found to be a diffusion-controlled diphasic reaction. Two tetragonal phases of U_3O_7 were identified: The one, α-U_3O_7, with lattice parameters of a = 5.46 A and c = 5.55 A,

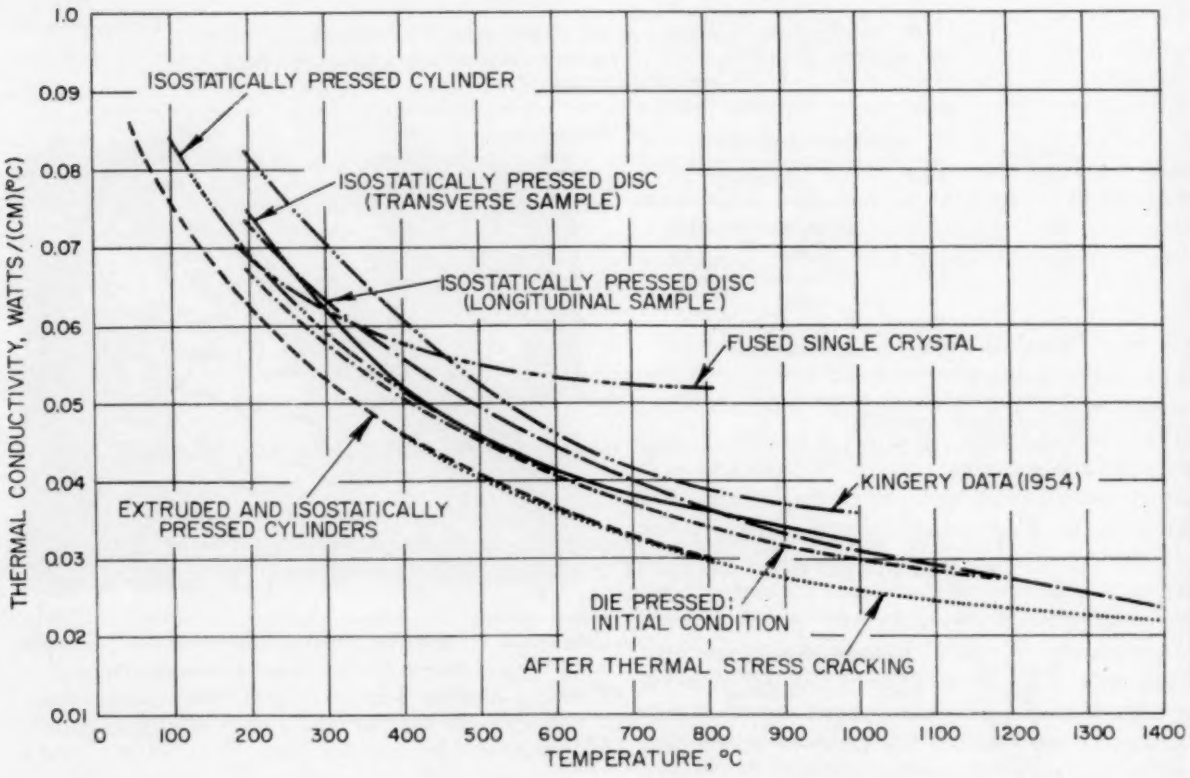

Fig. I-7 Thermal conductivity of unirradiated UO_2 (corrected to 100 per cent of theoretical density).[71] All samples except the single crystal were sintered polycrystalline material.

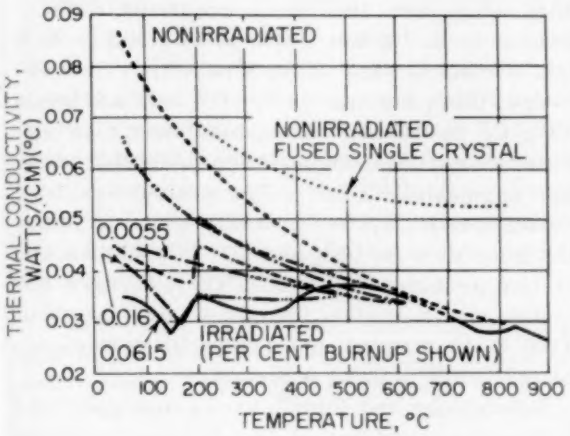

Fig. I-8 Effect of irradiation on thermal conductivity of UO_2 (corrected to 100 per cent of theoretical density).[71] All samples except the single crystal were extruded, isostatically pressed, and sintered polycrystalline material.

and the other phase, β-U_3O_7, with a = 5.38 A and c = 5.55 A. Annealing experiments with the β-U_3O_7 revealed a third tetragonal phase with an approximate composition corresponding to $UO_{2.3}$, which was found to be stable up to 500°C. Lattice parameters for the $UO_{2.3}$ were a = 5.41 A and c = 5.49 A. The oxidation of U_4O_9 was also found to be controlled by diffusion of oxygen through a second phase consisting of $UO_{2.3}$, which was in turn converted to β-U_3O_7. The oxidized surface layer which forms on UO_2 at 25°C was identified as amorphous UO_3. Properties of the UO_3 phases and $UO_{2.9}$ are discussed in a second paper by Hoekstra and coworkers.[77] The properties investigated include density, crystal structure, heat of solution, thermal stability, and infrared spectrum.

The British[78] have examined, by X-ray and metallographic methods, various BeO-UO_2-ThO_2 compositions following high-temperature heat-treatment. No interaction products other than a UO_2-ThO_2 solid solution were observed. Melting-point studies indicated that the BeO-UO_2-ThO_2 system can be considered a quasi-binary with a eutectic between 60 to 80 mole % BeO at about 2100°C. It was also noted that this system is sensitive to carbon contamination, and a phase of either UO or UO-UC appeared after prolonged heating in a carbon tube furnace. Attempts to hydrogen reduce ZrO_2 when in solid solution with UO_2 at 1050°C failed to produce any appreciable amount of substoichiometry or reduction.[40] Thermodynamic information on nonstoichiometric UO_2-ZrO_2 solid solutions at about 1000°C has been reported by Aronson and Clayton.[79] The solid-solution systems investigated can be represented by $U_yZr_{1-y}O_{2+x}$ with y values of 0.90, 0.80, and 0.70 and x values between 0.04 and 0.17.

A Canadian report[80] describes preliminary studies of glass formation in the systems Li_2O-B_2O_3, UO_2-B_2O_3, and UO_2-$NaPO_3$. Only one composition in the UO_2-B_2O_3 system was studied where there was considerable difficulty in dissolving the two compounds. The UO_2-$NaPO_3$ system appeared to be quite miscible, and glasses containing up to 40 per cent UO_2 were prepared. (R. H. Barnes)

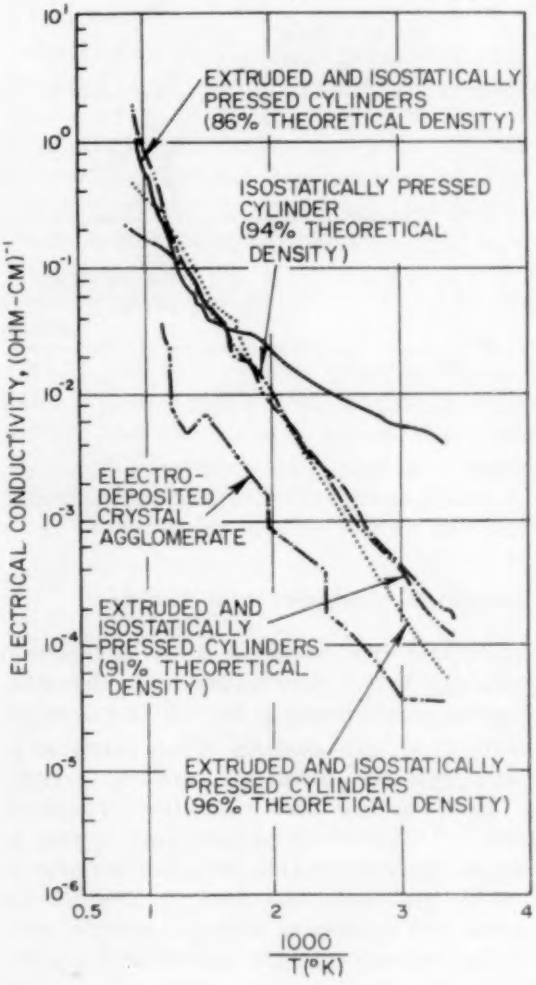

Fig. I-9 Electrical conductivity of unirradiated UO_2 (first heating cycle).[71] All cylindrical specimens were sintered polycrystalline material.

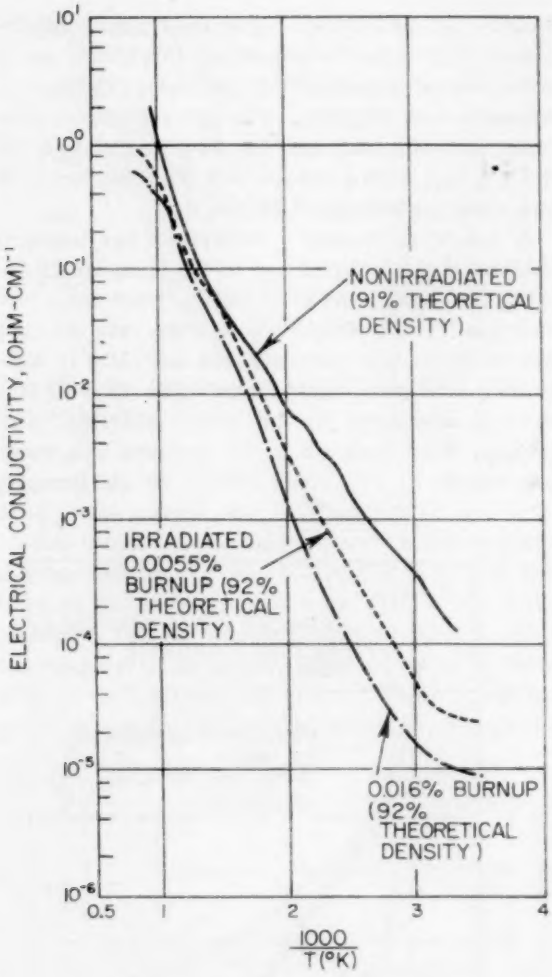

Fig. I-10 Electrical conductivity of irradiated UO_2 (first heating cycle).[71] All specimens were extruded, isostatically pressed, and sintered cylinders.

Properties of Carbides and Sulfides

Bloomfield has compiled a bibliography on uranium carbide.[81] Several hundred references are arranged according to the subjects covered.

Barta et al. are studying phase relations in ternary systems involving uranium, carbon, and some of the less refractory transition metals.[82,83] The UC-Cr pseudobinary system is a simple eutectic system, with the eutectic at 34 wt.% chromium and 1435°C. The UC-Cu pseudobinary system is a simple eutectic system. The eutectic contains over 95 wt.% copper. The UC-Fe pseudobinary system is a simple eutectic system, with the eutectic at 51.5 wt.% iron and 1170°C. The UC-UFe_2 system is a simple eutectic system. The eutectic is at 92 wt.% UFe_2 and 1040°C. A compound, $UFeC_2$, exists on a tie line between UC_2 and iron. It has a high melting point. A eutectic exists between $UFeC_2$ and iron at 61 wt.% iron and below 1360°C. A ternary compound exists in the uranium-carbon-cobalt system somewhere near the composition $UCoC_3$. The uranium-carbon-nickel ternary system probably contains binary tie lines between UNi_5 and UC, UC_2, and carbon at temperatures below 2000°C. A ternary eutectic exists in the UNi_5-Ni-C field at about 1100°C. No terminal solid solubilities were detected in any of these systems.

Benesovsky and Rudy[84] have investigated the high-carbon portions of the systems involving uranium, carbon, and each of the refractory metals hafnium, niobium, tantalum, and zirconium by means of lattice-parameter measurements. It was found that, at 1700 and 1800°C, the face-centered cubic solid solution, (U,M)C, can exist in equilibrium with graphite at high M contents; i.e., over 70 mole % ZrC, over 86 mole % HfC, over 72 mole % NbC, and over 77 mole % TaC. At these temperatures, U_2C_3 was not observed beyond 2 at.% M. The solubility of M in UC_2 is negligible in all cases. It was observed that UC and HfC are not completely soluble in one another at 1700°C; a gap exists between about 40 and 75 mole % HfC. This gap decreases with increasing temperature.

Chang[85] has obtained further evidence on the orientation relations between cubic and tetragonal UC_2. The data show this to involve a diffusionless transformation with a shear angle of 4 to 6°. He has also confirmed that cubic UC and UC_2 coexist near 2000°C.

Webb and Hayward have investigated the kinetics of diffusion of carbon from uranium-carbon alloys into type 304 stainless steel.[86] Uranium-carbon alloys containing 4.8 wt.% carbon or less will not carburize stainless steel through a sodium bond at temperatures up to 1600°F. Alloys containing more than 4.8 wt.% carbon in the form of UC_2 will lose carbon to stainless steel through a sodium bond at temperatures above 1000°F in amounts related to the total amount of UC_2. If the metastable UC_2 is transformed to U_2C_3, the rate of carbon transfer to the stainless steel is reduced by at least an order of magnitude. At 1200°F stainless steel was carburized by a uranium–5.0 wt.% carbon alloy to the extent of 0.12 per cent carbon in 800 hr and 0.40 per cent carbon in 12,800 hr.

Sheridan et al.[37] report that, after 2000 hr at 1500°F in contact with a uranium-carbon alloy of unspecified carbon content, no uranium was found in type 304 stainless steel. Likewise, no uranium was found in niobium or in a 2.25 Cr–1 Mo steel after 4000 hr under the same conditions. Beryllium converted entirely to UBe_{13}, Inconel X reacted to form a uranium-nickel-carbon eutectic melt, and Zircaloy-2 reacted to form ZrC and uranium metal.

Chubb et al.[86] have determined the rates of self-diffusion of carbon and uranium in uranium monocarbide. The rates of diffusion of C^{14} in uranium monocarbide are described by the equation, $D_C = 0.02 \exp(-50{,}000/RT)$, over the temperature range 1200 to 2000°C. The rates of diffusion of U^{235} in uranium monocarbide are described by the equation, $D_U = 0.0013 \exp(-64{,}000/RT)$, over the temperature range 1600 to 2100°C.

Rough and Chubb[87] have issued a report describing many of the elevated-temperature properties of uranium-carbon alloys. Hot-hardness data to 1500°C indicate that uranium–5, 7, and 9 wt.% carbon alloys begin to soften and show plastic behavior at 1000°C or below but that the alloys still have appreciable hardness at 1400°C. Microstructural data are presented which indicate a minimum in the uranium-carbon liquidus curve at about 6.2 wt.% carbon and a region of complete solid solution between UC and UC_2 above 2050°C and below 2350°C. The transformation of uranium–7 wt.% carbon alloys into U_2C_3 on reheating is described as being complete in ¼ hr at 1500°C but requires more than 1000 hr to go to completion at 1100°C. Dilation and resistivity data to 1600°C are presented in graphical form. The thermal-expansion coefficient of a uranium–4.8 wt.% carbon alloy is nearly linear to 1600°C and equal to 11.0×10^{-6}/°C.

Kalish et al.[88] obtained values from 10.9×10^{-6} to 12.6×10^{-6}/°C for the thermal-expansion coefficient of uranium–4.8 wt.% carbon alloys up to 1000°C.

Leitnaker and Witteman[89] report that between 2000 and 2550°K the vapor species over uranium-carbon alloys containing less than 52 at.% carbon contains more uranium than carbon; the vapor species over alloys containing more than 52 at.% carbon contains more carbon than uranium. The vapor pressure of uranium over uranium dicarbide in a graphite container from 1930 to 2365°K can be represented by the equation

$$\ln P_U \text{ (mm)} = -\frac{67.164}{T} - 0.111\left(\ln T + \frac{2000}{T}\right) + 12.140$$

However, Chang reports that, during electron-beam melting of uranium-carbon alloys, uranium was vaporized to cause the carbon content to increase from 4.5 to 5.0 wt.% in one case and from 7.3 to 7.4 wt.% in another case.[85]

Chang has studied the plastic deformation of uranium monocarbide at temperatures[85] from 1500 to 1860°C. The results of compression tests at strain rates of 2×10^{-5} to 2×10^{-3}/sec are summarized in Fig. I-11.

Webb and Hayward report that severe damage occurred to the fuel and cladding when a 12-in. column of ½-in.-diameter cast UC slugs was irradiated to 10,000 Mwd/metric ton of uranium at a maximum surface temperature[85] of 1450°F. The slugs were UC with carbon contents of 4.7 to 4.9 wt.%; the cladding was 10-mil-thick, type 304 stainless steel. It is suggested that the stainless steel was carburized during the irradiation.

AERE, Harwell, reports[44] that the rate of release of fission gases from sintered, irradiated uranium carbide during postirradiation annealing at 1400°C can be expressed by a diffusion coefficient of 5×10^{-16} cm²/sec.

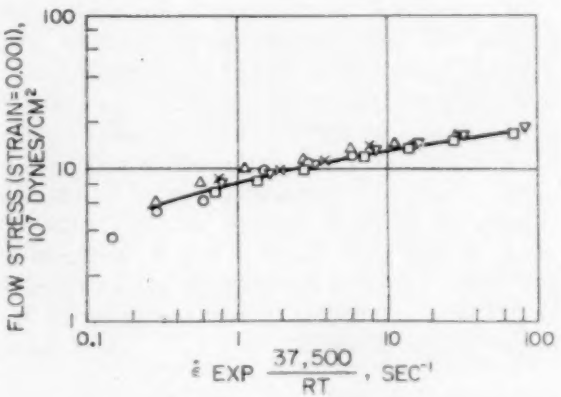

Fig. I-11 Summary of flow stress (strain = 0.001), strain rate ($\dot{\epsilon}$), and temperature (T) relations from compression-test data on uranium monocarbide.[85] ○, 1855°C. ×, 1803°C. △, 1714°C. □, 1833°C. ▽, 1513°C.

Resistivity and lattice strain of uranium monocarbide showed significant changes at a burnup of only 0.004 at.% of the uranium during reactor irradiation at 150°C, according to Rough and Chubb.[87] The damage apparently saturated at this burnup, and no further significant change occurred as a function of longer exposures. Specimens irradiated at 700°C showed significantly smaller increases in resistivity, and it is indicated that a portion of the damage was annealed out during irradiation at this temperature. Uranium sesquicarbide showed large increases in resistivity but no gross dimensional changes during irradiation to a burnup of 0.56 at.% of the uranium at 700°C. Metastable uranium dicarbide which had begun to precipitate graphite and uranium sesquicarbide disintegrated in NaK at 870°C.

Griffiths irradiated some UC having a bulk density of 92 per cent of the theoretical density and a resistivity of 62 μohm-cm to an integrated thermal-neutron flux of 6×10^{17} nvt in four steps.[30] A negligible change in resistivity was observed at 10^{16} nvt, a 2 per cent increase in resistivity was observed at 7×10^{16} nvt, and a 2.5 per cent increase in resistivity was observed at 6×10^{17} nvt. The material was then annealed for 1 hr at successively higher temperatures. In anneals between 100 and 130°C, about 30 per cent of the radiation-induced change in resistivity was annealed out. No further change occurred up to 700°C, but between 700 and 730°C the remaining radiation-induced change in resistivity was annealed out. This clearly indicates two types of radiation damage to UC affecting its resistivity.

At Argonne,[38] studies have shown a hardness of only 184 DPH for uranium monosulfide. The uranium monosulfide showed negligible reaction with NaK, stainless steel, vanadium, or niobium in two weeks at 800°C. Under the same conditions it showed a 0.7-mil reaction with zirconium. Uranium monosulfide begins to oxidize rapidly in dynamic oxygen at 375°C. US–50 mole % ThS solid solution has a hardness of 277 DPH. Thorium monosulfide has a hardness of 234 DPH and begins to oxidize rapidly in dynamic oxygen at 500°C. (W. Chubb)

Fabrication of Refractory Fuels Other Than Uranium Oxides

Argonne[91] is investigating the preparation of UC by precipitation from a liquid metal. A carbide was made at 800°C by adding carbon to liquid zinc containing 15 wt.% uranium and 12 wt.% magnesium. Good agitation, about 15 per cent excess carbon, a reaction time of about 5 hr, and a settling time exceeding 1 hr all appeared to be necessary conditions for satisfactory yields. Much more work is required to develop methods for separating the supernatant liquid metal and unreacted carbon from the UC product. The UC was ground to reduce the as-precipitated particle size from an average 25 to 30 μ (range 1 to 140 μ) down to an average 4 to 6 μ, but cold-pressed pellets "exploded" at about 400°C during sintering attempts both under argon and in vacuum.

A series of experiments at Atomics International[92] on the preparation of UC by the UO_2-carbon reaction indicates that the reaction follows a second-order rate equation of the form $x/(1-x) = Kt$, where x is the fraction of total CO evolved in time t. An activation energy of about 5 kcal/mole was obtained from experimental results above 1450°C. British workers, however, have accumulated further evidence[44] to support their contention that the measured equilibrium pressures of CO do not correspond to either of the reactions $UO_2 + 3C \rightarrow UC + 2CO$ or $UO_2 + 4C \rightarrow UC_2 + 2CO$. They remark that variations in the UO_2-carbon mixing as well as in the pressing procedure can have a deleterious effect on the rate and extent of reaction at 1400°C and that much more work is required before any positive conclusions can be made.

Argonne[38] is utilizing this UO_2-carbon reaction to produce UC powder in a plasma flame. The feed material is made from a slurry of UO_2 in a petroleum pitch-solvent solution. The solvent is evaporated at room temperature, the dry material is pulverized, and the powder is carbonized in an inert atmosphere. The carbonized material is crushed and sized to control the particle size and to produce a free-flowing powder. The best carbide that has been achieved in a 6-in.-long nitrogen flame contained 60 wt.% UC and 40 wt.% UO_2, with probable nitrogen contamination of the carbide. Recently acquired equipment producing a helium flame 12 to 15 in. long is expected to yield better results.

Argonne has developed[93] a laboratory fabrication process for preparing spherical particles of thorium oxides containing 10 wt.% uranium uniformly distributed throughout the thoria ma-

trix. The particle size of the fuel, which is designed for use in a boiling-water slurry, can be varied from 5 to 50 μ. The process seems adaptable to large-scale production and differs in detail from the Japanese technique for preparing spherical ThO_2, as described in the previous Review. The thorium, as its nitrate, is dissolved in water and reacted with ammonium hydroxide to give a nitrate-stabilized sol which is adjusted nearly to the gel point. Uranium as a crystalline uranyl nitrate is added to and dissolved in the thorium sol immediately prior to spraying. The resultant solution of colloidal thorium uniformly mixed with dissolved uranyl nitrate is then sprayed through a suitable nozzle so that droplets of the liquid can assume near-spherical shape in free fall. An ammonia-air mixture is used to cause the sol to gel, which simultaneously fixes the uranium as an insoluble compound uniformly distributed throughout the gel particle. The spherical particles so obtained are collected, washed, classified, dried at 300°C, and fired to 1500°C.

(E. O. Speidel)

Basic Studies of Irradiation Effects in Fuel Materials

Ceramic Fuels

The effects of neutron irradiation on the crystal structure of UC and UN samples are reported.[94] The neutron doses (n) range as high as 1.1×10^{18} nv, corresponding to burnup of the order of 3.5 Mwd/metric ton. The dosage is measured by the percentage increases in unit cell size in the crystals. It is found that the cell sizes vary as $[1 - \exp(-n\gamma)]$, where γ is a function of the material. The numbers of atoms in both UC and UN which are affected per fission event are calculated.

A review has been made at Chalk River[95] of the mechanisms causing migration of fission-product gases. Mechanisms leading to escape from the solid include concentration-gradient diffusion, gross plastic deformation (squeezing), grain growth, stoichiometric changes of oxygen bonding, vaporization (including that causing void migration), fission recoil, and knockout by fission-fragment impact. Effective trapping results from migration to closed pores; some experimental studies by subsequent grinding are reviewed. Re-entry of the gas into the solid oxide has also been established and is significant at pressures of tens of atmospheres. A remarkable disproportioning of the isotopes of natural xenon trapped in the oxide has been observed. It appears that the disproportioning occurs before the trapping. Possible mechanisms for the disproportioning and trapping are discussed. Experimental results on measured gas release are also given.

On the basis of neutron-activation studies, research at Battelle[96] indicates that the diffusion of Xe^{133} in UO_2 single crystals is about two orders of magnitude lower than in sintered UO_2 at 1400°C. It is believed that this low value for diffusion results because of fewer defects in the single-crystal material.

At Oak Ridge,[97] studies of in-pile release of krypton, xenon, and iodine from UO_2 have been monitored continuously at temperatures from 500 to 1000°C. At 600°C and below, releases were primarily recoil atoms, whereas a diffusion release occurred at 700°C and above, having the same temperature dependence for krypton, xenon, and iodine (30 kcal/mole activation energy).

(F. A. Rough)

Irradiation Effects in Metallic Fuels

Irradiation growth phenomena in uranium have been studied at Harwell[98] based on electron transmission microscopy of thin films. Dislocation loops formed during irradiation, principally on $\{1\,1\,0\}$ and $\{0\,2\,3\}$ planes. In the absence of stacking fault contrast in the loops, the most probable Burgers vectors are a $[1\,0\,0]$ or $\frac{1}{2}\sqrt{(a^2 + b^2)}$ $(1\,1\,0)$ for both the $\{1\,1\,0\}$ loops and the $\{0\,2\,3\}$ loops. These loops produce dimensional changes only in the directions of the macroscopic growth and contraction, $[0\,1\,0]$ and $[1\,0\,0]$, respectively. If it is assumed that the $\{0\,2\,3\}$ loops are formed by interstitials or vacancies, then the magnitude of the dimensional changes produced by the loops is in reasonable agreement with the macroscopic growth. It is concluded, therefore, that the formation of the loops is the mechanism of the growth phenomenon.

At National Lead Company of Ohio,[99] experimental preferred-orientation data were used to test the adequacy of a proposed elastic solution

for the prediction of dimensional changes in experimental uranium fuel elements during irradiation. The data were obtained by measurements of the intensity of X rays diffracted by samples from a hollow, cylindrical uranium fuel core that had been subjected to a rapid quench from the beta phase. For the irradiation conditions assumed, the stresses calculated for the elastic model are well in excess of those required for the initiation of creep and plastic flow. Thus the results indicate that the elastic model is inadequate and that a model is required in which strain rate depends on stress.

Phenomena thought to contribute to swelling in alpha uranium irradiated up to about ½ at.% burnup at 400 to 650°C are discussed in an article from Harwell.[100] Metallographic examination shows in all specimens an array of small bubbles 0.1 μ in diameter and ½ μ apart, presumably containing most of the fission gases. In about one of three specimens, grain-boundary cracks contribute 1 per cent to the volume increase and are probably due to irradiation embrittlement and internal stressing by thermal cycling. Acceleration of swelling leading to breakaway by coalescence of small bubbles is not expected below 1½ at.% burnup in alpha uranium, provided the gas bubbles are on a fine scale as observed so far, but breakaway could occur at ½ at.% burnup if internal cracking occurs. The mechanism of nucleation and growth of fission-gas bubbles in alpha uranium and the role of surface tension in controlling bubble size are discussed.

In a study at Bettis[101] on irradiation of two-phase fuel alloys, it has been found that the volume change is due to two mechanisms. At temperatures below 500°C, there is a small contribution from gas-bubble formation and expansion. Also, under proper conditions of temperature and burnup rate, extensive microcracking occurs, resulting in large volume changes. It is proposed that the cracking is caused by stresses resulting from neutron-induced phase reversions in the vicinity of the gas bubble acting with the stress field surrounding the bubble. It is predicted that the latter effects will not occur at high fission rates.

Another article (in Russian)[102] that may be of interest concerns Haziguti's and other theories of radiation growth of alpha uranium.

(F. A. Rough)

References

1. National Lead Co. of Ohio, Summary Technical Report for the Period July 1, 1961, to Sept. 30, 1961, USAEC Report NLCO-840, Oct. 20, 1961. (Classified)
2. J. H. Kittel, Effects of Rolling and Heat Treatment on Anisotropic Irradiation Growth of Uranium, USAEC Report ANL-6344, Argonne National Laboratory, November 1961.
3. W. F. Murphy et al., Examination of Uranium from the First Core of the EBR-I, USAEC Report ANL-6113, Argonne National Laboratory, September 1961.
4. Hanford Atomic Products Operation, Fuels Development Operation Quarterly Progress Report, July, August, September 1961, USAEC Report HW-71422, Oct. 13, 1961. (Classified)
5. G. Sergeyev et al., *The Metallography of Uranium and Certain Reactor Materials*, Atomizdat, Moscow, 1960 (in Russian).
6. A. Robillard, Influence of Heat Treatments in the Beta and Gamma Phases on the Micrographic Structure of Uranium, USAEC Translation HW-TR-28 (translation from French Report CEA-1057, 1959).
7. C. Oblinger and H. Dube, Determination and Application of the Diffusion Coefficient for Hydrogen in Uranium at 800°C, *Nuclear Sci. and Eng.*, 11(3): 263–266 (1961).
8. Mallinckrodt Chemical Works, Process Development Quarterly Progress Report, April–June 1961, USAEC Report MCW-1465, Aug. 1, 1961.
9. D. S. Kneppel, Grain Refinement of Uranium by Alloying and Heat Treatment, USAEC Report NMI-7011, Nuclear Metals, Inc., Oct. 11, 1961. (Classified)
10. J. E. Antill and K. A. Peakall, Oxidation of Uranium Alloys in Carbon Dioxide and Air, *J. Less-Common Metals*, 3: 239–246 (June 1961).
11. A. Martin et al., The Cadmium-Uranium Phase Diagram, *Trans. Met. Soc. AIME*, 221: 789–791 (August 1961).
12. S. J. Rothman, Diffusion in Uranium, Its Alloys, and Compounds, USAEC Report ANL-5700(Pt. C), Argonne National Laboratory, May 1961.
13. K. Tangri and G. Williams, Metastable Phases in the Uranium-Molybdenum System and Their Origin, *J. Nuclear Materials*, 4(2): 226–233 (July 11, 1961).
14. J. Lehmann, Monoclinic Phases in Uranium-Molybdenum Alloys, *J. Nuclear Materials*, 4(2): 218–225 (July 19, 1961).
15. D. Kramer, Finely Dispersed Phases in Uranium-Molybdenum Ternary Alloys, *J. Nuclear Materials*, 4(3): 281–286 (1961).
16. J. Beaudier et al., Conservation of Nuclei of the Alpha Phase in the Beta Phase of Low Alloyed Uranium (in French), *J. Nuclear Materials*, 4(3): 325–328 (1961).

17. W. A. Holland, Irradiation Properties of Uranium-Molybdenum Alloys, *Trans. Am. Nuclear Soc.*, 4(2): 337–338 (November 1961).
18. W. A. Holland, Isothermal Transformation of Uranium–14 and Uranium–16 Wt.% Molybdenum Alloys at 550°C. Interim Report, USAEC Report NAA-SR-6125, Atomics International, Dec. 1, 1961.
19. R. D. Barnard, Some Physical Properties of the Gamma and Delta Phases in the Uranium-Zirconium System, *Proc. Phys. Soc.*, 78: 722–727 (Nov. 1, 1961).
20. G. Petzoq et al., The System $ZrAl_2$-UAl_2, *J. Nuclear Materials*, 4(3): 316–321 (1961).
21. R. Boucher, Diffusion of Aluminum During the Transformation UAl_3-UAl_4 in the Solid State, paper presented at Symposium on Solid-State Diffusion, Saclay, France, July 3–5, 1958.
22. Westinghouse Electric Corp., Bettis Atomic Power Laboratory, Core Materials and Quality Engineering Technical Progress Report for the Period June 26 to September 25, 1961, USAEC Report WAPD-MRK-11, Oct. 6, 1961. (Classified)
23. S. D. Strauss and J. L. Zambrow, Irradiation of Uranium-Yttrium Alloys, USAEC Report SCNC-329, Sylvania Electric Products, Inc., August 1961.
24. J. S. L. Leach, Hydrogen and the Corrosion of Uranium and Other Oxide Covered Metals, British Report NP-10541, September 1960.
25. Hanford Atomic Products Operation, Plutonium Metallurgy Operation Quarterly Progress Report, January, February, March 1961, USAEC Report HW-68486, Apr. 15, 1961. (Classified)
26. H. R. Gardner, The Heat Treatment of Plutonium, USAEC Report HW-67938, Hanford Atomic Products Operation, February 1961.
27. Hanford Atomic Products Operation, Plutonium Metallurgy Operation Quarterly Progress Report, July, August, September 1960, USAEC Report HW-66985, Oct. 15, 1960. (Classified)
28. Hanford Atomic Products Operation, Plutonium Metallurgy Operation Quarterly Progress Report, October, November, December 1960, USAEC Report HW-67765, Jan. 15, 1961. (Classified)
29. R. G. Cope et al., Studies of Alloys of Plutonium with Transition Elements and Gold, British Report AWRE-0-36/61, August 1961.
30. J. F. Eichelberger, Mound Laboratory Monthly Progress Report for July 1961, USAEC Report MLM-1117, Mound Laboratory, July 15, 1961.
31. F. W. Albaugh, Reactor and Fuels Research and Development Operation Monthly Report, October 1961, USAEC Report HW-71535A, Hanford Atomic Products Operation, Nov. 15, 1961. (Classified)
32. R. W. Dayton and C. R. Tipton, Jr., Progress Relating to Civilian Applications During October 1961, USAEC Report BMI-1549(Del.), Battelle Memorial Institute, Nov. 1, 1961.
33. USAEC Translation AEC-tr-4142 [translated from *Nukleonika*, 2(3): 47–48, 50–52 (1957)].
34. V. V. Akbachinskiy and L. M. Kopytin, Heat of Formation of $PuBe_{13}$ (in Russian), *At. Energ.*, 9(6): 504–505 (1960).
35. J. F. Eichelberger, Mound Laboratory Monthly Progress Report for May 1961, USAEC Report MLM-1115, Mound Laboratory, May 30, 1961.
36. J. F. Eichelberger, Mound Laboratory Monthly Progress Report for June 1961, USAEC Report MLM-1116, Mound Laboratory, June 30, 1961.
37. A. Strasser, Carbide Fuel Development. Phase III Report, September 15, 1960–September 15, 1961, USAEC Report NDA-2162-5, United Nuclear Corp., Sept. 30, 1961.
38. Argonne National Laboratory, Reactor Development Program Progress Report, October 1961, USAEC Report ANL-6454, Nov. 15, 1961.
39. R. W. Dayton and C. R. Tipton, Jr., Progress Relating to Civilian Applications During November 1961, USAEC Report BMI-1557, Battelle Memorial Institute, Dec. 1, 1961. (Classified)
40. Nuclear Materials and Equipment Corp. (Unpublished)
41. K. H. Puechl, Development of Plutonium Bearing Fuel Materials. Monthly Progress Letter, October 1961, USAEC Report NUMEC-P-35, Nuclear Materials and Equipment Corp., Nov. 5, 1961.
42. J. M. Cleveland et al., Fast Oxide Breeder Project I—Fuel Fabrication, USAEC Report GEAP-3486, General Electric Co., Vallecitos Atomic Laboratory, Aug. 15, 1960.
43. J. D. L. Harrison et al., The Sintering Behavior of Mixed UO_2 and PuO_2 Powders, British Report AERE-R-3765, July 1961.
44. AERE Research Group, Harwell, June 1961. (Unpublished)
45. R. H. Johnson and R. W. K. Honeycombe, The Structure and Heat Treatment of Some Thorium-Zirconium Alloys, *J. Nuclear Materials*, 4(3): 295–310 (1961).
46. R. W. Dayton and C. R. Tipton, Jr., Progress Relating to Civilian Applications During June 1961, USAEC Report BMI-1524(Del.), Battelle Memorial Institute, July 1, 1961.
47. R. H. Baskey, Fuel-Bearing Fiberglass in Aluminum Base Fuel Elements, Eighth Quarterly Report, July 1 to September 30, 1961, USAEC Report ORO-506, Clevite Corp.
48. The Martin Co., PM-1 Nuclear Power Plant Program, 9th Quarterly Progress Report, March 1 to May 31, 1961, USAEC Report MND-M-1820, July 10, 1961.
49. R. E. Heffner, Damage to Stainless Steel Fuel in SPERT Reactors, USAEC Report IDO-16729, Phillips Petroleum Co., Nov. 22, 1961.
50. D. L. Keller et al., Irradiation Effects in Dispersions, *Nuclear Sci. and Eng.*, 11: 154–158 (October 1961).

51. Nuclear Materials and Equipment Corp., Development of Plutonium Bearing Fuel Materials. Progress Report for Period July–September 1961, USAEC Report NUMEC-P-80, Sept. 30, 1961.
52. K. H. Puechl, Development of Plutonium Bearing Fuel Materials. Monthly Progress Letter, November 1961, USAEC Report NUMEC-P-36, Nuclear Materials and Equipment Corp., Dec. 5, 1961.
53. L. D. Stoughton, Ceramic Coatings for PBR Fuel Elements, *Atomics*, 14: 16–20 (July 1961).
54. Coatings for Nuclear Fuels Explored, *Chem. Eng. News*, 39(44): 80 (Oct. 30, 1961).
55. F. Forscher et al., Coated Fuel Particles, in *Fuel Element Fabrication with Special Emphasis on Cladding Materials*, Vol. 2, pp. 253–266, Academic Press, London and New York, 1961.
56. T. Adamski and F. Mucha, Coating of Some Materials with Carbon by Pyrolysis of Hydrocarbons in a Fluidized Bed, Polish Report PAN-232/IV, May 1961.
57. Reference canceled.
58. R. W. Dayton and C. R. Tipton, Jr., Progress Relating to Civilian Applications During September 1961, USAEC Report BMI-1546(Del.), Battelle Memorial Institute, Oct. 1, 1961.
59. W. O. Harms, Oak Ridge National Laboratory, Nov. 27, 1961. (Unpublished)
60. General Atomic Div., General Dynamics Corp., 40-Mw(e) Prototype High-Temperature Gas-Cooled Reactor Research and Development Program, Quarterly Progress Report for the Period September 30, 1961, USAEC Report GA-2747, October 1961.
61. General Atomic Div., General Dynamics Corp., A Review of Fuel Element Research and Development for the High-Temperature Helium Gas-Cooled Reactors, USAEC Report GA-2283, Jan. 8, 1961.
62. W. V. Goeddel, General Atomic Div., General Dynamics Corp., Apr. 27, 1961. (Unpublished)
63. P. Marien (Ed.), Research and Development Division First Semiannual Report for Period July 1–December 31, 1960, British Report NP-10477 (DPR-34), June 1961.
64. National Carbon Co., USAEC Interim Status Report Phase III, Graphite-Matrix Nuclear Fuel Elements, June 30, 1961.
65. M. A. Bobal, USAEC Fuel Cycle Development Program Monthly Newsletter, July 1961, National Carbon Co., Aug. 29, 1961.
66. M. A. Bobal, USAEC Fuel Cycle Development Program Monthly Newsletter, August 1961, National Carbon Co., Sept. 20, 1961.
67. Oak Ridge National Laboratory, Nov. 7, 1961. (Unpublished)
68. J. H. Oxley et al., Kinetics of Carbon Deposition in a Fluidized Bed, *A.I.Ch.E. Journal*, 7(3): 498 (September 1961).
69. G. E. Raines and W. H. Goldthwaite, In-Pile Fission-Gas-Release Behavior of Alumina-Coated UO_2 Particles Irradiated to High Burnup, USAEC Report BMI-1552, Battelle Memorial Institute, Nov. 6, 1961.
70. Hanford Atomic Products Operation, Fuels Development Operation Quarterly Progress Report, July, August, September 1960, USAEC Report HW-69085, Oct. 15, 1960. (Classified)
71. Hanford Atomic Products Operation, Fuels Development Operation Quarterly Progress Report, April, May, June 1961, USAEC Report HW-70557, July 15, 1961. (Classified)
72. Reference canceled.
73. Reference canceled.
74. A. Porneut, Optical and Electronic Microscopy of Sintered Uranium Dioxide, *J. Nuclear Materials*, 4: 200–217 (July 1961).
75. V. G. Vlasov and A. G. Lebedyev, The Dissociation Kinetics of Uranium Oxides, *Zhur. Priklad. Khim.*, 34(8): 1739–1744 (1961).
76. H. R. Hoekstra et al., The Low Temperature Oxidation of UO_2 and U_4O_9, *J. Inorg. & Nuclear Chem.*, 18: 166–178 (March 1961).
77. H. R. Hoekstra and S. Siegel, The Uranium Oxygen System: U_3O_8-UO_3, *J. Inorg. & Nuclear Chem.*, 18: 154–165 (March 1961).
78. K. D. Reeve, An Exploratory Study of the BeO-UO_2-ThO_2 System, British Report AERE-M/R-2727, December 1958.
79. S. Aronson and J. C. Clayton, Thermodynamic Properties of Nonstoichiometric Urania-Zirconia Solid Solutions, *J. Chem. Phys.*, 35: 1055–1058 (September 1961).
80. J. Ceric and M. K. Murthy, Canadian Uranium Research Foundation, Fellowship Report No. 6101 for Period April 16, 1961–May 15, 1961, Canadian Report NP-10765, May 30, 1961.
81. M. Bloomfield, Uranium Carbide, A Bibliography, Report NAA-SR-Memo-6512, Atomics International, June 13, 1961.
82. J. Barta et al., Phase Diagrams of Uranium Monocarbide-Transition Metal Systems, *J. Nuclear Materials*, 4: 322–324 (1961).
83. Binary Carbide-Metal Systems, Progress Reports Nos. 4 and 5, British Report AERE-EMR-PR-1084, 1961.
84. F. Benesovsky and E. Rudy, Contribution to the Knowledge of the Ternary Systems of Uranium and Carbon with Zirconium, Hafnium, Niobium, and Tantalum, USAEC Translation AEC-tr-4834 [translated from *Planseeber. Pulvermet.*, 9: 65–75 (1961)].
85. Atomics International, Annual Technical Progress Report, AEC Unclassified Programs, Fiscal Year 1961, USAEC Report NAA-SR-6370, Aug. 15, 1961.
86. W. Chubb et al., Diffusion Coefficients of Uranium and Carbon in Uranium Monocarbide, USAEC Report BMI-1551, Battelle Memorial Institute, Nov. 6, 1961.

87. F. A. Rough and W. Chubb, Progress on the Development of Uranium Carbide Type Fuels. Final Report on the AEC Fuel-Cycle Program, USAEC Report BMI-1554, Battelle Memorial Institute, Nov. 17, 1961.
88. H. S. Kalish et al., Nuclear Fuel Research, Fuel Cycle Development Program, Quarterly Progress Report, July 1 to Sept. 30, 1961, USAEC Report NYO-2695, United Nuclear Corp., Nov. 22, 1961.
89. J. M. Leitnaker and W. G. Witteman, The Dissociation Pressure of Uranium Dicarbide, USAEC Report TID-13629, Los Alamos Scientific Laboratory, September 1961.
90. L. B. Griffiths, The Effect of Irradiation and Postirradiation Annealing on the Electrical Resistivity of Uranium Monocarbide, *J. Nuclear Materials*, 4: 336 (1961).
91. Argonne National Laboratory, Reactor Development Program Progress Report, November 1961, USAEC Report ANL-6473, Dec. 15, 1961.
92. Hanford Atomic Products Operation, Uranium Ceramic Fuels, US/UK Newsletter No. 12, November 1961.
93. C. E. Crouthamel et al., Preparation of High-Density Spherical Thorium Oxide Particles with Up to 10 At.% Uranium, USAEC Report ANL-6340, Argonne National Laboratory, June 1961.
94. J. Adam and M. D. Rogers, X-ray Diffraction Studies of Fission Fragment Damage in Uranium Carbide and Nitride, *J. Nuclear Energy*, 14: 51–53 (April 1961).
95. W. B. Lewis, Behavior of Fission Gases in UO_2 Fuel, Canadian Report DL-45, November 1961.
96. R. H. Barnes et al., Xenon Diffusion in Single Crystal and Sintered UO_2, USAEC Report BMI-1533, Battelle Memorial Institute, Aug. 1, 1961.
97. Oak Ridge National Laboratory, Solid State Division Annual Progress Report for Period Ending August 31, 1961, USAEC Report ORNL-3213, Dec. 29, 1961.
98. B. Hudson et al., Dislocation Loops and Irradiation Growth in Alpha Uranium, British Report AERE-R-3752, June 1961.
99. P. R. Morris and R. N. Thudium, Prediction of Dimensional Changes in Uranium Fuel Elements During Irradiation—Test of the Elastic Solution, USAEC Report NLCO-838, National Lead Co. of Ohio, Nov. 6, 1961. (Classified)
100. S. F. Pugh, Swelling in Alpha Uranium Due to Irradiation, *J. Nuclear Materials*, 4: 177–199 (July 1961); also British Report AERE-R-3458.
101. H. J. Levinstein and T. R. Padden, Mechanism of Swelling in Irradiated Two-Phase Alloys, USAEC Report WAPD-247, Westinghouse Electric Corp., Bettis Atomic Power Laboratory, December 1961. (Classified)
102. Yu. N. Sokurskiy, On the Haziguti's and Other Theories of Radiation Growth of Alpha Uranium, *At. Energ.*, 10(3): 274–278 (1961).

Section II

Reactor Materials

Moderator Materials

Beryllium Metal and Alloys

Beryllium Fabrication

A furnace and mold design that has been developed[1] permits casting relatively small beryllium ingots free of centerline shrinkage and with a reasonably fine grain size. The graphite mold has a water-cooled copper bottom. The top of the mold is heated by the same induction coils that heat the melting crucible.

The high volume shrinkage (48 per cent) and variations in density of compacted beryllium powder present difficulties in the production of pressureless sintered billets.[2a] However, tubes (a more difficult shape) could be produced in a thin graphite mold with a graphite core. Yields of 25 per cent for thin-walled tubes and up to 60 per cent for thicker walled tubes and solid cylinders were obtained. Grain sizes of ASTM 6 and 7 could be maintained for sintering temperatures up to 1240°C. Grain growth was rapid at 1250°C.

Finned beryllium tubing was produced by Sylcor[3] by isostatic pressing of beryllium powder in a shaped plastic mold at 400°F under oil pressures of up to 100,000 psi to make a compact having 85 per cent of the theoretical density. After the plastic mold was stripped, the compact was placed in a sealed and evacuated thin steel can which was then filled with fine fused MgO powder. This can was placed in a furnace under an argon pressure of 5000 psi and heated to 1100°C for 90 min. After stripping, the finned tube produced had properties similar to those of hot-pressed beryllium (45,000 to 50,000 psi ultimate tensile strength, 1 to 2 per cent elongation) and a fine-grained equiaxed structure of random orientation. The tubes that were produced were leaktight to helium.

Beryllium rods have been impact extruded[3] in a Dynapak machine from fully dense hot-pressed beryllium billets and from cold-pressed compacts approximately 85 per cent dense. All the billets were canned in mild steel. Extrusion was carried out at 900, 750, and 600°C, with an extrusion ratio of 10 : 1 and an extrusion rate of approximately 500 in./sec. The best extrusions were obtained from the hot-pressed billets that were extruded at 900°C; these showed an ultimate strength of about 100,000 psi and 10 per cent elongation. The texture was highly oriented.

The work of Yans (USAEC Report NMI-1212) on controlling the texture of hot upset sheet by making use of upset-forging techniques for sheet production was repeated in a British laboratory[2b] and extended to include sheet from vacuum-melted billets. The texture of sheets from all the materials used was similar, but the grain size of that from cast billets was large. Subsequent open press forging at 600°C of the cross-grain sheet followed by annealing 12 hr at 750°C caused recrystallization and grain refinement to a grain size of the same order of magnitude as that of the powder-metallurgy sheet, without essentially altering the structure.

Preliminary attempts[4] to extrude short lengths of a beryllium channel section using a composite lubricant were encouraging. The billet was turned to a 32-μin. (rms) finish and encapsulated in a 0.062-in.-thick carbon steel sheet. The sheet was electroplated with 0.020 in. of copper and coated with a liquid lubricant made with a mica base. The Beryllium Corporation reports[5,6] that angles, channels, and Z sections can be formed by bending sheet metal at about 1400°F. Beryllium sheet 0.060 in. thick requires a 3T to 4T radius for roll forming and a

7T radius for press-brake forming. Thicker sheet (0.188 in.) could be roll formed at 3T to 4T and press-brake formed at 4½T. The extrusion of preformed steel and beryllium composites followed by roll reduction without rejacketing has been investigated. This process, developed especially for T sections, has shown great promise for all structural shapes. Preliminary tests indicate that this process allows the production of beryllium with excellent mechanical properties and is relatively economical.

Beryllium sheet, 0.020 in. thick and containing 1.49 per cent BeO, was vacuum annealed by Brush Beryllium[7] at 1400°F for 8 hr and furnace cooled to 800°F, followed by air cooling. The prior reduction ratio was 17.8:1. This sheet was completely recrystallized, with an average basal-plane orientation in the plane of the sheet of only 1.2 times normal. The sheet appeared to be somewhat ductile at room temperature and withstood a 2.4T bend at 1400°F.

An experimental pressure-welded joint[8] in a tube prepared from Brush QMV hot-pressed block beryllium showed tensile yield and elongation values at the joint almost equal to those of the base metal and above those given in Brush Specification S-200-B. (W. Hodge)

Physical Metallurgy of Beryllium

The Institute of Metals (London) held a three-day conference[2] in October 1961 to discuss progress in the metallurgy of beryllium. In several papers[2c–2f] the authors reached the conclusion that beryllium is not a special brittle material but a normal metal. Commercial beryllium is a complex, unstable, age-hardenable alloy, highly susceptible to precipitation-aging phenomena which, in turn, are dependent on impurity levels and earlier mechanical and thermal treatment. It appears to obey the same precepts that have been applied to other metals which exhibit a ductile-brittle transition, but the effect is markedly orientation dependent. The purity, grain size, and orientation affect the mechanical properties of the metal both at temperatures in the ductile-brittle transition range and at temperatures above 400°C. Perlmutter,[2e] after summarizing the available knowledge about beryllium gained from U. S. Air Force contracts and other sources, showed the very real advantages that can accrue from the application of correctly designed beryllium structures in missiles that must return intact to the atmosphere from outer space. He noted that, although beryllium is characterized as "brittle," the degree of brittleness is far from that of a ceramic, since even highly oriented sheet can accommodate thickness strains of 0.1 to 0.2 per cent (at a width-to-thickness ratio of 90). It was further stressed[2f] that, with more research in all areas, beryllium should become a most promising structural material during the next six years. However, every effort must be expended toward lowering the cost of the raw material and improving quality control.

Gasc[2g] reviewed some of the aspects of brittleness of beryllium at room temperature. These helped to explain the phenomenon, but not enough is known to suggest methods of obtaining sheets in which the grain size is fine, uniform, and homogeneous, or heat-treatments that would bring about a redistribution of impurities and so lead to adequate plastic deformation.

Bennett[2h] found that there is a significant difference between the mechanical properties of beryllium water quenched after 24 hr at 900°C and metal that is slow cooled. The former contains a widely dispersed precipitate, whereas the latter is characterized by a coarsening of the grain boundaries.* His experiments suggest that these effects are due to an impurity that dissolves in beryllium at temperatures above 850°C.

Meredith and Sawkill[2i] obtained a series of microstructures after heat-treatment of hot-extruded cast ingot beryllium which are indicative of a precipitation reaction. This precipitation occurs in the range 550 to 750°C, initially at grain boundaries and around inclusions. This is followed by general precipitation within the grains and overaging at the boundaries. The factor that limits ductility above 400°C is the amount of iron in solution.

Wolff et al.[2j] reported that the room-temperature tensile properties of commercial beryllium can be altered by an aging treatment. Samples of extruded rod, solution treated at 1100°C for 1 hr and aged at 400°C for eight days, showed an ultimate strength of 52,000 psi but reached 95,000 psi after one week at 700°C,

*In a previous Review this work was described, and the words "slow cooled" and "quenched" were inadvertently interchanged. The present statement is correct.

with corresponding elongations of 1 and 14 per cent, respectively. These treatments had little effect on Young's modulus or the yield strength.

Studies[2j] with the electron microbeam analyzer indicated that iron segregated to the grain boundaries during aging. Strain-aging studies showed that a yield point which was induced by aging and eliminated by straining could be recovered by subsequent aging. The yield point, absent in the solution-treated material, could be observed in some samples after aging at 400°C but not in others. The rods which did not develop a yield point had a somewhat larger grain size than those which did.

Bunce and Evans[2k] prepared beryllium ingots by melting and casting electrolytic flake and subsequently rolled or extruded the ingots. A considerable concentration of impurities was found at the grain boundaries in the extruded condition, and after heat-treatment (200 hr at 700°C), there was intense precipitation within the grains. Grain size had an important effect on ductility. Heat-treatments of a worked matrix which did not increase the grain size increased the ductility. Sheet produced by direct rolling of ingot stock had considerable ductility and a low degree of texture after recrystallization. The authors believe that this type of sheet has greater possibilities for successful forming than sheet produced by powder-metallurgy methods.

Olds et al.[2l] also found that the ductility of cross-rolled beryllium sheet depended on both strain rate and impurity content. Figure II-1 shows the effect of aluminum on elongation.* At a strain rate of 10%/min, the elongation varied from 20 to 40 per cent between 200 and 400°C and decreased at higher temperatures. At a strain rate of 0.1%/hr, the ductility was in general lower, with a rather sharp maximum at approximately 200°C and a minimum at 600°C (Fig. II-2).

Moore et al.[2m] showed that the normal minimum ductility found in hot-worked beryllium at 600°C is associated with an aged condition that can be remedied by overaging. They found that iron was involved in the aging reaction and drew a solid-solution boundary in the beryllium-iron phase diagram on the basis of their tensile-test results. X-ray diffraction data suggested

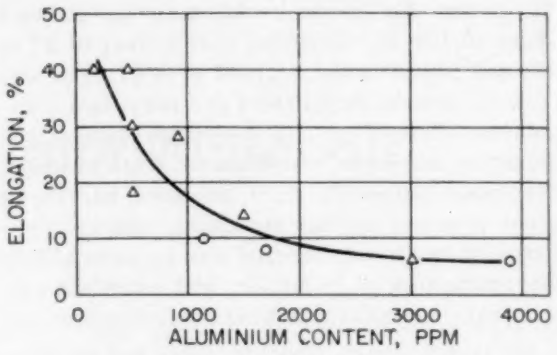

Fig. II-1 Curve relating ductility of beryllium to aluminum content at 600°C in high-strain-rate tests.[2l] ○, by chemical analysis. △, by spark-gap mass-spectrometric analysis.

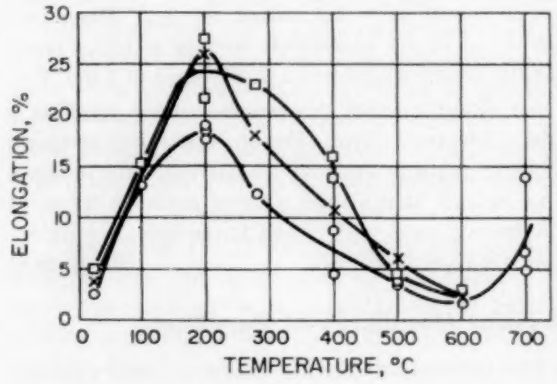

Fig. II-2 Ductility versus temperature curves for beryllium sheets at a low strain rate of 0.1%/hr.[2l] □, batch 1. ○, batch 2. ×, batch 3.

that beryllium contains two types of impurity precipitates at equilibrium temperatures above this boundary and a third (only) below it. These phases are believed to be complex, not simple beryllium binaries. The maximum ductility at 600°C was obtained in overaged beryllium containing 0.15 per cent iron.

Allen and Moore[2n] made calculations based on the Stroh analysis which indicated that the ductile-brittle transition in beryllium could be reduced to 20°C with a grain size of about 1 μ in rolled and recrystallized metal. They also indicated that the same result may be possible in extruded and recrystallized beryllium with a grain size of 16.5 μ.

Gelles et al.[2o] reported that the beta phase in a beryllium–8 at.% nickel alloy, very rapidly quenched, showed a transformation temperature

*Figures II-1 and II-2 are reprinted here by permission from the Institute of Metals, London.

as low as 242°C. Preliminary measurements of the tensile properties of the beta-phase beryllium-nickel alloy at 1070°C indicated that this phase is more ductile than alpha beryllium at this temperature or than alpha-plus-gamma beryllium-nickel at 1060°C.

Cottrell et al.[2p] reported that the solubility of hydrogen in solid beryllium is negligibly low, the hydrogen evolved during vacuum-fusion analysis being directly attributable to a surface absorption effect. The room-temperature brittleness of beryllium was shown to be due to an orthodox ductile-brittle transition effect which occurs in the range 100 to 200°C and which is uninfluenced by any attempt at hydrogenation.

Spangler et al.[9] determined the critical resolved shear stress (CRSS) for basal glide of three single crystals with varying levels of purity. A value of 400 psi for vacuum-distilled zone-melted bar* after seven zone-melting passes was the lowest CRSS observed, whereas a value of 800 psi for Pechiney SR-grade material after three passes is the lowest observed for what is essentially a starting material. These tests demonstrate a strong relation between the expected purity level and the CRSS for basal glide.

The preliminary observations[9] by electron-transmission microscopy have shown that dislocations in beryllium do not move as they have been observed to do in other metals. When a specimen was heated to 200°C, however, and cycled over a narrow range of temperature, a slow movement of the dislocations could be observed.

Greetham and Martin[2q] prepared single crystals of beryllium by the floating-zone zone-refining technique and determined the CRSS for slip on the (0 0 0 1) and (1 0 $\bar{1}$ 0) planes. No clear relation between CRSS and purity of beryllium became apparent. The CRSS for (1 0 $\bar{1}$ 0) slip decreased rapidly with increase in testing temperature from −196 to 200°C, and more slowly thereafter. The CRSS for basal slip appeared to fall with increasing testing temperature up to 25°C, in contradistinction to previous investigations which showed an increase in CRSS for basal slip with increase in testing temperature. The authors believe that this difference was due to the increased purity of the samples under test.

Wilsdorf and Wilhelm[2r] examined dislocation patterns in single-crystalline and polycrystalline beryllium. They found that glide dislocations are strongly hindered in their movements and often pinned by small precipitates in commercially pure beryllium; in Pechiney flake beryllium, in which obstacles are comparatively rare, the dislocations have a pronounced tendency to align themselves along crystallographic directions. Dislocation arrays of very high density were found to lie in the (1 $\bar{2}$ 1 0) plane. (W. Hodge)

Properties of Beryllium

Beryllium and molybdenum have been shown[10] to have low thermal conductivity at low temperatures, thus indicating strong electron-imperfection scattering of the predominant electronic component of thermal conductivity. Figures II-3 to II-7 show,* respectively, total thermal conductivity, lattice thermal conductivity, electrical resistivity, Lorenz ratios, and thermoelectric power with respect to pure copper. In these curves, Be-I indicates properties determined in the direction parallel and Be-II those determined in a direction perpendicular to the pressing axis.

In a report[11] on the thermal expansion of SNAP materials, the thermal coefficient of expansion of beryllium for the temperature range 77 to 1200°F is given as 9.07/°F.

It was reported that heat-treatment of extruded beryllium tubing at approximately 750°C for relatively short times increased its ductility above 300°C but had little effect at room temperature. Slow cooling at 3 to 5°C/hr from 750, 850, and 900°C to room temperature resulted in the best improvement on transverse specimens.[2s]

Irradiation of Brush QMV beryllium to a dose of about 2.75×10^{21} fission neutrons/cm^2 at temperatures up to 480°C produces little volume change but markedly embrittles beryllium. Helium bubbles impede the flow of dislocation lines; thus slip and twinning become more difficult.[12]

Protective films formed on beryllium sheets in dry CO_2 at 1 atm and temperatures[13] up to

*The vacuum-distilled material was produced by Nuclear Metals, Inc.

*Figures II-3 to II-7 are reprinted here by permission from the *Journal of Applied Physics*.[10]

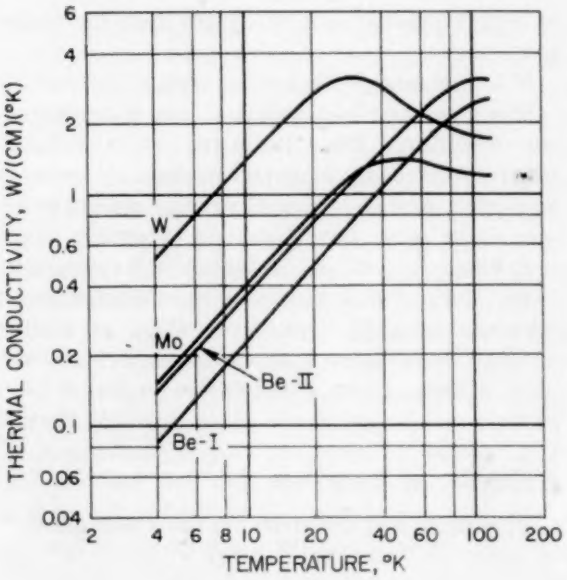

Fig. II-3 Total thermal conductivity of several reactor metals.[10]

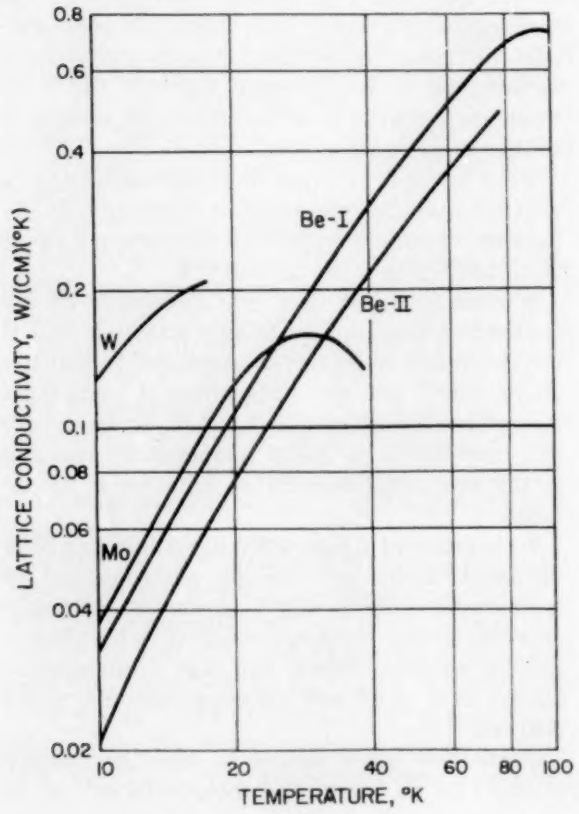

Fig. II-4 Lattice thermal conductivity of several reactor metals.[10]

850°C. At 1000°C, breakaway was obtained after 1500 hr, but the presence of 3 vol.% water vapor at 1 atm normally resulted in breakaway at temperatures of 700°C or above. Increasing the pressure to 20 atm had little effect in dry gas at 700°C but caused severe attack on some specimens when ~0.7 vol.% water vapor was present.

Exposed to CO_2 containing 4 vol.% H_2O as vapor, high-purity Pechiney flake beryllium exhibited a breakaway reaction after 60 to 70 hr at 725°C. At 650°C the reaction rate was similar to that observed in dry CO_2. Analyses of the specimens after testing showed an increase in the carbon content of 0.031 per cent in the 650°C and 0.1 per cent in the 700°C test. Indications were obtained that the breakaway phenomena observed in wet CO_2 may have been caused by reaction of the Be_2C with hydrogen formed in the reaction of beryllium with water.[14,15]

A British patent claims that improved resistance of beryllium to corrosion by CO_2 at high temperatures is obtained by melting the beryllium under an electric arc in a vacuum or an inert gas at low pressure.[16]

Evidence is presented[17] of the formation of a second reaction product apart from BeO at the metal-oxide interface in a metallographic, X-ray, and electron-diffraction investigation of the breakaway phenomenon in beryllium exposed to CO_2 containing 2 vol.% H_2O at 700°C.

Further experiments[18] indicate that hydrogen will agglomerate in beryllium at temperatures below 400°C, preferably at grain boundaries. Both the diffusivity and the permeability of hydrogen in and through beryllium are significantly higher than those for helium in this metal.

An extensive investigation[19] of the corrosion of beryllium in air and in nitrogen demonstrated that the reaction in air approaches a linear rate (i.e., $n = 1$ in the rate-law equation, fluctuating from $n = 0.9$ to $n = 1.2$ under isothermal conditions). An induction period was always observed. The mechanism is temperature dependent with an activation energy of 30 kcal/mole. The high-temperature corrosion product appeared by X-ray and metallographic analyses to be quite different from normal beryllium oxide or beryllium nitride. In air the rate of reaction with nitrogen increases more rapidly with temperature than does the rate with oxygen.

(W. Hodge)

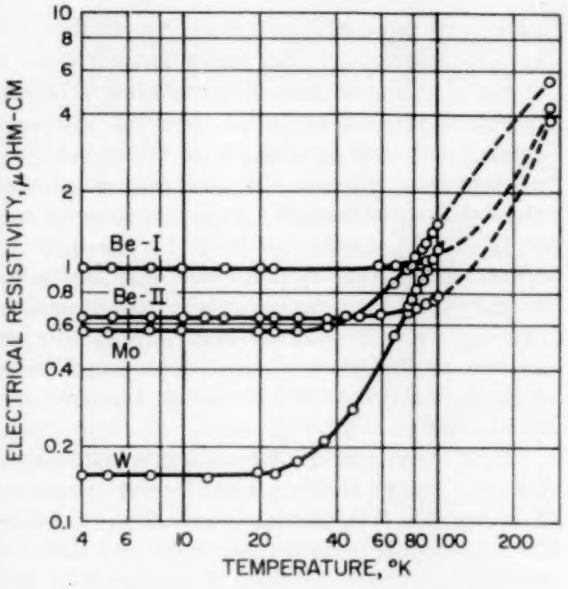

Fig. II-5 Electrical resistivity of several reactor metals.[10] The dotted curves indicate interpolated values.

Miscellaneous Beryllium Studies

The construction and operation of a point-projection X-ray microscope for use with beryllium has been described.[21] With this instrument a radiomicrograph formed by variations in the thickness and composition of a specimen is recorded at the same time as the divergent-beam diffraction pattern. The information obtained from these combined records has included the determination of orientation, lattice parameters, and the degree of perfection in single crystals and some aspects of deformation, fracture, and recrystallization in polycrystalline specimens.

Contaminated beryllium chips can be upgraded[20] with a loss of less than 0.5 per cent beryllium. The chips are cleaned in a liquid-phase degreaser, followed by centrifuging and then a continuous sink-float process to remove high- and low-density trash. Afterward, the cleaned chips are reduced to −200-mesh powder in an attrition mill without contamination except for an increase in BeO content of approximately 0.49 per cent.

The Kettering Laboratory of the University of Cincinnati published a collection of 18 papers[21] by various people who have long been concerned with the detection, cure, and prevention of beryllium disease, together with a consensus of opinions by the three groups participating: (1) Clinical and Diagnostic; (2) Analytical, Experimental, and Environmental; and (3) Epidemiological.

O'Boyle[22] discusses the coatings currently being used on beryllium where corrosion or wear is a problem. He notes their relative merits and how the coatings are specified.

A German magazine[23] presented a comprehensive review of the present state of beryllium research in relation to the problem of brittleness. Lockheed published an annotated bibliography[24] consisting of publications released during the first quarter of 1961. It showed good coverage of foreign as well as domestic literature (215 entries, 99 pages). The AEC published a list[25] of approximately 568 refer-

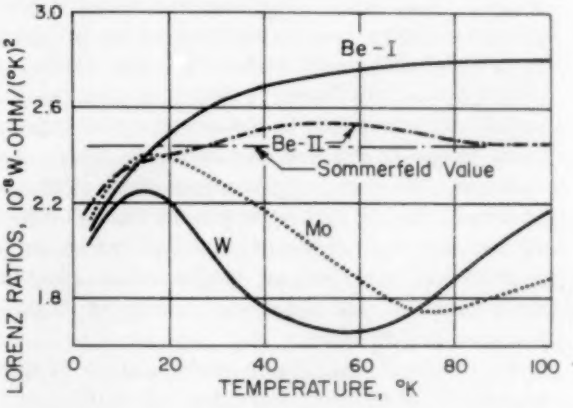

Fig. II-6 Lorenz ratios of several reactor metals.[10] The Sommerfeld value for the electronic components is 2.44×10^{-8}.

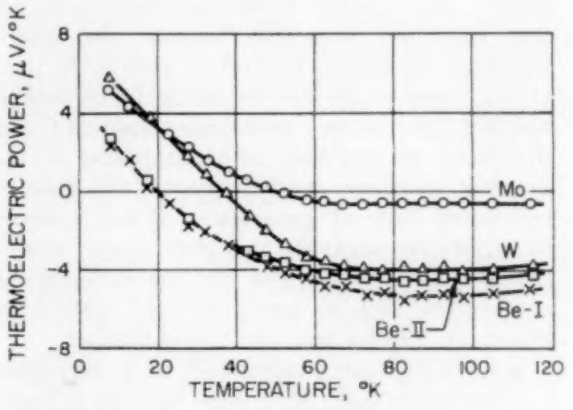

Fig. II-7 Thermoelectric power of several reactor metals with respect to pure copper.[10]

ences to selected books, articles, and unclassified reports that have appeared in abstracts and indexes between August 1959 and December 1960 (55 pages, not annotated).

(W. Hodge)

Beryllium Compounds

Beryllium Oxide

Investigators at Atomics International continue to report various aspects of the high-temperature behavior of BeO. Chang and Graham[26] have observed transient creep effects in hot-pressed BeO loaded in compression at temperatures up to 1900°C. These effects were evidenced as a series of discontinuities, or steps, in the stress-strain curve. The authors suggest that each step resulted from limited grain-boundary motion and that creep proceeds by a mechanism somewhat different from that proposed in the Nabarro-Herring theory. The mechanism ascribed to the creep in this experiment is one of grain-boundary slide, shear, and rotation. The rate of grain-boundary motion is governed by the rate at which stress relaxation at corners and edges of crystals can occur by a diffusion mechanism. Mathematical derivations lead to rate equations similar to those of Nabarro and Herring.

Austerman[27] described decrepitation of BeO ceramics when they were heated at temperatures exceeding 2050°C. A very sharp temperature dependence for the onset of the phenomenon was observed. It is characterized by crystal growth followed by fragmentation of large crystals. Specimens heated at 2050 to 2300°C experienced 15 per cent bulk expansion and contained numerous cracks. An order-disorder transition in BeO at 2050°C is proposed. Apparently the transition is caused by thermal excitation. Austerman suggests that the onset of disorder is accompanied by increased mobility of dislocations and also an increased rate of generation of dislocations. Intergranular stresses probably result in dislocation movement. The moving dislocations accumulate against some barrier within the structure, and tilt boundaries are formed.

McClelland and associates[28] have developed a translucent BeO. Both pure BeO hot pressed at 1750°C and 4000 psi for 4 hr and BeO–1 wt.% MgO hot pressed at 1600°C and 1500 psi for 4 hr yielded translucent bodies having densities that were 99.5 to 100 per cent of the theoretical density. Crystal sizes ranged from 10 to 200 μ, and examination showed that all grain-boundary porosity had been removed. Thermal-conductivity measurements on translucent and conventional, opaque, 99 per cent dense BeO showed the conductivity of the translucent material to be higher by about 13 per cent. Infrared absorption by transluent BeO is similar to but somewhat higher than that of single-crystal BeO. No steady-state creep was observed in translucent BeO specimens loaded compressively at 10,000 psi at temperatures up to 1600°C.

Work continues at Atomics International on growing single BeO crystals.[29] Austerman and Hopkins are investigating crystal growth from the reversible reaction of BeO and water at high temperature. $Be(OH)_2$ is formed from BeO by reaction with water in a carrier gas at 1300 to 1650°C. $Be(OH)_2$ is volatilized at these temperatures. Further downstream in the furnace, where the temperature is several hundred degrees lower, $Be(OH)_2$ is decomposed on seed crystals. Two crystal habits have been observed in this process: platelets measuring 5 mm in diameter by 1 mm thick and rods measuring 20 mm long by 2 mm in diameter. The size of crystals grown by this process is apparently limited by the impurities present in the system, and rigorous attempts are being made to assure maximum cleanliness. Oak Ridge investigators[30] also are attempting to grow single BeO crystals and also are experiencing contamination problems. In this work the crystals are precipitated from an LiF–25 mole % BeF_2 melt at 800°C by introducing water vapor. Both helium and hydrogen have been used as a carrier gas for the water, although the contamination problem is lessened by the use of hydrogen.

In other work at Oak Ridge, a process for purifying $Be(OH)_2$ is being developed. This process involves dissolving the hydroxide in aqueous HNO_3 + EDTA (ethylenediamine tetraacetic acid) and extracting with a solution of acetylacetone in CCl_4. Impurities in the aqueous phase are complexed by the EDTA, and the Be^{2+} ion reacts with acetylacetone to yield beryllium acetylacetonate. This organic solution is then back extracted with strong acid, and $Be(OH)_2$ is recovered by precipitation with NH_3. The impurity levels of cations attained in $Be(OH)_2$ treated by this process are as follows:

<20 ppm: Ti
<10 ppm: Al, Ba, Ca, Cr, Fe, K, Na, Ni
<15 ppm: Co, Cu, Li, Mg, Mn, Mo, Pb, Sn
<1 ppm: B

Investigators at General Electric are exploring foamed BeO ceramics.[31] A foamed slurry is produced by reacting beryllium metal powder with H_3PO_4 within a dilute acid slurry of powdered BeO. An example of the practice of this process is as follows: 50 g of UOX-grade BeO in 100 ml of 30 per cent H_3PO_4 is treated with 0.2 g of −325-mesh beryllium powder, whereupon hydrogen is evolved. The resulting stable foam is dried and cured at 300°C for 72 hr and then fired at 1370°C for 6 hr. The fired ceramic had a bulk density of 0.97 g/cm^3, with pore diameters ranging from 0.005 to 0.1 in. A flame-impingement test of a $\frac{5}{16}$-in.-thick panel showed ΔT's of 350 to 550°C for hot-face temperatures of 800 to 1540°C. Flame impingement seemed to have no harmful effects on the specimen.

Irradiation effects in BeO are being studied at Oak Ridge.[30] Specimens were right cylinders measuring 0.428 to 0.8 in. in diameter by 1 in. long. They were fabricated either by hot pressing to densities of 2.75 to 2.87 g/cm^3 or by cold pressing and sintering to densities of about 2.68 g/cm^3. The purity of the specimens was not given. Irradiation was done in the ETR to total exposures ranging from 1.1×10^{20} to 2.8×10^{21} nvt (fast). Specimen temperatures ranged from 110 to 1025°C.

The BeO pieces experienced varying degrees of damage during these irradiations as evidenced by cracking and spalling. However, specimens receiving moderate exposure at medium-to-high temperatures were intact. Grain growth was detected in specimens irradiated to medium-to-high exposures at both high and low temperatures. Asymmetrical line broadening was observed by X-ray diffraction in specimens receiving high exposure at low temperature. Specimens irradiated to a similar high dose at high temperature exhibited symmetrical line broadening. Lattice expansions for high-exposure specimens were as follows:

$$\Delta c/c_0 = 7 \times 10^{-3} \text{ at } 110°C$$

$$\Delta c/c_0 = 1 \text{ to } 2 \times 10^{-3} \text{ at } 444 \text{ to } 1025°C$$

This effect seemed to saturate at a dose of about 3×10^{20} nvt. Dimensional changes were more dependent on total exposure than on any other factor, being proportional to integrated flux raised to some power between 1 and 2. Also, dimensional changes were inversely proportional to irradiation temperature. The helium content of the irradiated BeO specimens varied linearly with flux up to 1.6×10^{21} nvt, the slope of the line being approximately 205 standard μl of helium/g of BeO/10^{21} nvt. This value is considerably lower than some reported in the recent literature. Tritium content was proportional to exposure squared up to 2.1×10^{21} nvt, reaching 6.4 ppm at that point.

(A. K. Smalley)

Other Beryllium Compounds

Brush Beryllium is studying Ta_2Be_{17} having compositions from 29.5 to 30.5 wt.% beryllium (stoichiometric Ta_2Be_{17} is 29.8 wt.% beryllium).[32] This compound is reported to have good strength up to 2750°F with no minimum in strength in the range from room temperature to 2750°F. In tests at 2300°F a maximum strength of 82,000 psi and an average strength of 77,000 psi were recorded. At temperatures from 800 to 2300°F in 100-hr tests, no spalling of any kind was observed for specimens in this composition range. Ta_2Be_{17} has been cycled from 1600°F to below red heat 50 times with excellent results, but the cooling and heating rates were not reported. This is quite an improvement over the results for zirconium beryllides.

The University of California Lawrence Radiation Laboratory has been studying the beryllium-boron system, and three compounds were reported:[33] BeB_2, BeB_6, and one having a beryllium-to-boron ratio between 6:1 and 2:1. A eutectic was reported between beryllium and the unknown phase at 972 ± 15°C.

(R. W. Getz)

Solid Hydrides

A discussion of the properties of zirconium hydride and yttrium hydride has been included in a publication of the American Institute of Mining, Metallurgical, and Petroleum Engineers.[34] The phase diagram of the zirconium-hydrogen system is discussed, and the mechanical properties of zirconium hydride are given. Cladding techniques for zirconium hydride are

included. Physical properties are given for yttrium hydride.

Zirconium Hydride

Studies of the zirconium-hydrogen system at Atomics International[35] have shown evidence for the delta-plus-epsilon two-phase region at elevated temperatures. It was found at 550°C for H/Zr = 1.72 to 1.73 and at 600°C for H/Zr = 1.74.

The electrical resistivity of $ZrD_{1.84}$ was also measured.[35] Values ranged from 24.8 μohm-cm at 4.2°K to 51.2 μohm-cm at 300°K. The Debye temperature was calculated to be 210°K.

Lithium Hydride

Tensile tests of Inconel containers filled with lithium hydride were conducted by Union Carbide.[36] The Inconel was unaffected by 3000 hr of thermal cycling between 200 and 900°F, including a 4-hr dwell time at the maximum temperature during each cycle.

Calcium Hydride

The density of cold-pressed calcium hydride was measured by Union Carbide.[36] Results varied from 1.46 g/cm^3, when a pressure of 15,000 psi was used, to 1.63 g/cm^3, when a pressure of 50,000 psi was used. The theoretical density calculated from X-ray diffraction measurements was found to be 1.92 g/cm^3.

The creep rate of calcium hydride was also measured.[36] There was no creep at 850°F after 150 hr under a load of 350 psi, but it amounted to 10 per cent after 100 hr at 1000°F under the same load.

Alloy Hydrides

The hydriding characteristics of 161 intermetallic phases have been investigated[37] at Denver Research Institute; 51 were shown to react directly with hydrogen, and 15 of these formed ternary hydride compounds. Indirect evidence was obtained for the reaction of 31 additional compounds. Partial analysis of the data indicates that a quantitative relation could be developed which would predict the possibility of hydride formation. This relation would be based on the size of available interstitial sites, metallic valence, coordination of metal-metal and metal-hydrogen atoms, and elastic lattice strain. Evidence is presented which indicates that the greatest thermal stability is exhibited by hydrogen atoms that are bonded in the smallest sites. Also, the maximum hydrogen absorption in a ternary hydride is not limited to that attainable by the individual components of the compound. (H. H. Krause)

Graphite

The effects of elevated-temperature irradiation on many types of graphite are being investigated. A current radiation study being conducted by General Atomic[38] will provide information on strength, thermal conductivity, permeability, and dimensional stability of graphites and control-rod materials over the range 370 to 1430°C as a function of radiation dosage, up to and including that which would be obtained in a full core lifetime of the HTGR. Preliminary data on specimens irradiated with 2×10^{21} (>0.1 Mev) neutrons/cm^2 in the 1400°C range are given in Table II-1. Within experimental error, no changes in helium permeability were noted for five of the graphite types, whereas two types indicated an increase. The dimensional contraction observed was attributed to the relatively large amount of nongraphitizing carbon added during manufacture, and the extent of contraction may be a function of regraphitization temperatures (following impregnation steps).

Table II-1 IRRADIATION EFFECTS ON GRAPHITE SAMPLES[38]

(Irradiation Conditions: Integrated Neutrons >0.1 Mev, 2×10^{21} nvt; Maximum Temperature, >1400°C)

Type of sample	Helium permeability change*	Contraction, % change
General Atomic (Morgan base stock)	1x	0.6–0.8
General Atomic (Speer brush grade carbon)†	14x	1.5–1.9
Great Lakes†‡	−0.5x	0.1–0.4
Great Lakes†‡		1.2–1.5
Great Lakes†‡		0.7–1.1
Hawker Siddeley	0.5x	1.0–1.95
National Carbon	1.4x	0.5–0.8
National Carbon	7x–36x	0.6–0.9
General Electric Co. of England	−0.25x	0.5–0.7

*Factor of 2x increase is within experimental error.
†With carbon black added during manufacture.
‡Base stock only.

Table II-2 IRRADIATION EFFECTS ON FUEL-MATRIX GRAPHITES[40]

Graphite	Radiation dose, 10^{20} nvt ($E > 1$ Mev)	Length contraction, %
ARF-2-4	10.4	0.098
	11.94	0.309
ARF-3-2	10.4	0.126
	11.94	0.295
HX-10	12.93	0.730
HX-10	8.62	0.182
HX-12	12.93	0.942
HX-12	8.62	0.429
EY-X-60	12.92	1.271
EY-X-60	8.62	0.711

Other studies at Hanford[39] have shown a strong dependence of irradiation-induced change upon manufacturing heat-treatment. For example, lampblack-base graphite, heat-treated to only 1400°C before irradiation to 1200 Mwd/adjacent ton, contracted 0.6 per cent. In contrast, similar graphite heat-treated to 3000°C before the same radiation dosage contracted 0.2 per cent.

Preliminary irradiation data have been reported by Hanford[40] for special graphites developed for fuel matrices. Dragon Project and Armour Research Foundation graphites, irradiated in the temperature range 500 to 700°C, had relatively high contraction rates compared with nuclear-grade graphites. Data are shown in Table II-2. These graphites will undergo additional irradiation.

The effects on graphite from fission-product damage have not been studied extensively; until a recent study by the French,[41] Wigner energy storage in fueled graphite had not been measured. In this study an impregnated graphite, which contained 0.0332 g of U^{235} per cubic centimeter of graphite, received an exposure of 1.33×10^{18} nvt (thermal). The measured Wigner energy storage was 31.2 ± 3.1 cal/g (using a 200°C calorimeter temperature). Unfueled graphite irradiated to 1.33×10^{18} nvt at 32°C would be expected to contain only 2.7 cal of stored energy per gram, or only 9 per cent of the energy storage obtained in this test.

An innovation in graphite-impregnation techniques at Aeroprojects[42] may offer significant advantages. In preliminary experiments, ultrasonic activation of grade ATJ-82 graphite specimens led to more rapid and effective impregnation with furfuryl alcohol resin. After carbonization, the permeability of this graphite was lower (by a factor of 4) after three ultrasonic impregnation cycles than after five mechanically agitated cycles. This work is of particular interest, since, at present, the low-permeability large graphite elements needed for gas-cooled reactors are manufactured by multiple-impregnation methods.

(M. C. Brockway)

References

1. B. H. Hessler and J. P. Denny, Beryllium Casting, Report NP-11072, Beryllium Corp., July 5, 1961–Nov. 10, 1961.
2. Papers presented at Institute of Metals Conference on the Metallurgy of Beryllium, London, Oct. 16–18, 1961.
   a. G. L. Reeves and R. L. Keeley, The Pressureless Sintering of Beryllium Powder to Billets for Hot Extrusion.
   b. D. A. Barrow and R. L. Craik, Fabrication of Beryllium Sheet by Upset Forging.
   c. R. F. Bunshaw, A French Look at the Problems in Beryllium.
   d. A. J. Martin and G. C. Ellis, The Ductility Problem in Beryllium.
   e. I. Perlmutter, Metallurgical Considerations in the Application of Beryllium to Airborne Structures.
   f. L. A. Riedinger, Beryllium as a Structural Material for Aircraft, Missiles, and Spacecraft.
   g. C. Gasc, A Study of Mechanical Anisotropy and Heterogeneity in Beryllium Sheets.
   h. W. D. Bennett, Recent Beryllium Research in Canada.
   i. J. E. Meredith and J. Sawkill, A Precipitation Reaction in Commercially Pure Beryllium.
   j. A. K. Wolff et al., Impurity Effects in Commercially Pure Beryllium.
   k. J. E. Bunce and R. E. Evans, A Study of Effect of Grain Size, Texture, and Annealing Treatment on the Properties of Wrought Beryllium Ingot.
   l. G. C. Olds et al., High-Temperature Ductility of Powder-Fabricated Beryllium at High and Low Strain Rates.
   m. A. Moore et al., Precipitation Aging and Improved Mechanical Properties in Commercially Pure Beryllium.
   n. B. Allen and A. Moore, The Tough-Brittle Transition in Beryllium.
   o. S. H. Gelles et al., The Stability of the High-Temperature Phase in Beryllium and Beryllium Alloys.
   p. P. Cottrell, An Evaluation of the Hydrogen Content of Commercially Pure Beryllium and

Its Effect upon the Ductile-to-Brittle Transition Temperature.

q. G. Greetham and A. J. Martin, The Effect of Purity and Orientation on the Deformation of Beryllium Single Crystals.

r. H. G. F. Wilsdorf and F. Wilhelm, On the Behavior of Dislocations in Beryllium.

s. J. C. Guest and M. J. Hudson, Tensile Properties of Extruded Beryllium Rod and Tubing.

t. K. J. H. Mackay et al., Divergent-Beam X-Ray Microscopy of Beryllium.

3. I. Scheinhartz, The Fabrication of Beryllium by Hot Isostatic Pressing and by Impact Extrusion, USAEC Report SCNC-332, Sylvania Electric Products, Inc., September 1961.
4. Northrop Corp., Norair Division, Program for the Development of Extruded Beryllium Shapes, Interim Engineering Report No. 12, Mar. 1 to May 31, 1961, Report NOR-61-163.
5. K. C. Taber and E. E. Weismantel, Development of Techniques for Producing Beryllium Structural Shapes, Third Interim Technical Report, Jan. 29 to Apr. 28, 1961, Report NP-10346, Beryllium Corp.
6. E. E. Weismantel and K. C. Taber, Development of Techniques for Producing Beryllium Structural Shapes, Fourth Interim Technical Report, May 19 to Nov. 13, 1961, Report NP-11184, Beryllium Corp.
7. E. M. Grala et al., Rolling Improved Beryllium Sheet, Technical Report No. 231-234, Brush Beryllium Co., July 5–Oct. 4, 1961.
8. S. S. Smith, Jr., Pressure Welding of Beryllium, Report RD-118, Menasco Mfg. Co., Aug. 25, 1961.
9. G. E. Spangler et al., Preparation and Evaluation of High-Purity Beryllium, Bimonthly Progress Report, Nov. 2, 1960–Jan. 1, 1961, Report NP-9819, Franklin Institute.
10. R. L. Powell et al., Low Temperature Transport Properties of Commercial Metals and Alloys. IV. Reactor Grade Be, Mo, and W, *J. Appl. Phys.*, 31(7): 1221–1224 (1960).
11. J. D. Watrous, Thermal Expansion of SNAP Materials, USAEC Report NAA-SR-6047, Atomics International, July 30, 1961.
12. J. B. Rich et al., The Mechanical Properties of Some Highly Irradiated Beryllium, *J. Nuclear Materials*, 4(3): 287–294 (1961).
13. AERE Research Group, Harwell, England, April 1961. (Unpublished)
14. Oak Ridge National Laboratory, Gas-Cooled Reactor Program, Quarterly Progress Report for Period Ending June 30, 1961, USAEC Report ORNL-3166, Aug. 28, 1961.
15. M. T. Simnad (Ed.), Proceedings of the 10th Annual AEC Corrosion Symposium Held at General Atomic Division, General Dynamics Corp., San Diego, California, May 9 Through 11, 1961.
16. T. Raine and J. A. Robinson, Production of Improved Beryllium, British Patent 875,539 (to Associated Electrical Industries, Ltd.), Aug. 23, 1961.
17. R. Smith, Metallographic Observations on the Oxidation of Beryllium in Wet Carbon Dioxide, in *Fuel Element Fabrication with Special Emphasis on Cladding Materials*, Vol. 2, pp. 147–156, Academic Press, London and New York, 1961.
18. C. E. Ells and W. Evans, The Behavior of Hydrogen in Beryllium, Canadian Report CRGM-1041 (AECL-1347), August 1961.
19. W. Bradshaw and E. S. Wright, High Temperature Corrosion of Beryllium in Air, Report LMSD-895073, Lockheed Aircraft Corp., January 1961.
20. Z. L. Ardary et al., Beryllium Chip Processing, USAEC Report Y-1328, Union Carbide Nuclear Co., Y-12 Plant, Dec. 15, 1960.
21. The Kettering Laboratory, University of Cincinnati Workshop on Beryllium, Jan. 5 and 6, 1961.
22. D. O'Boyle, Surface Coatings for Beryllium Parts, *Machine Design*, 33(26): 147–150 (Dec. 21, 1961).
23. H. Weik, The Plastic Deformation of Beryllium (in German), *Metall.*, 15: 686–694 (July 1961).
24. J. B. Goldman (Comp.), Beryllium, A Survey of the Literature, Report NP-10640, Lockheed Aircraft Corp., June 1961.
25. Z. D. Lane, Current Beryllium Literature: A Selected Bibliography, August 1959–December 1960, USAEC Report UCRL-5705(Suppl. 1), University of California Lawrence Radiation Laboratory, May 1, 1961.
26. R. Chang and L. J. Graham, Transient Creep and Associated Grain-Boundary Phenomena in Polycrystalline Alumina and Beryllia, USAEC Report NAA-SR-6483, Atomics International, Sept. 30, 1961.
27. S. B. Austerman, Decrepitation of Beryllium Oxide at High Temperature, USAEC Report NAA-SR-6428, Atomics International, Sept. 30, 1961.
28. J. D. McClelland et al., Fabrication and Properties of Translucent Beryllium Oxide, USAEC Report NAA-SR-6454, Atomics International, Oct. 30, 1961.
29. S. B. Austerman and A. R. Hopkins, Beryllium Oxide Single Crystal Growth. II. Water Vapor Transport Method, USAEC Report NAA-SR-6420, Atomics International, Nov. 15, 1961.
30. Oak Ridge National Laboratory, Aircraft Nuclear Propulsion Program Progress Report, May 1–June 30, 1961, USAEC Report ORNL-3226, Dec. 13, 1961. (Classified)
31. General Electric Co., Flight Propulsion Laboratory Dept., High-Temperature Materials Program, Progress Report No. 5, Part A, August 15–October 15, 1961, USAEC Report GEMP-5A, Nov. 15, 1961.
32. J. Booker et al., Investigation of Refractory Metal Beryllides and Silicides as Very High Temperature Materials, Report NP-10692, Brush Beryllium Co., July 15, 1961.

33. C. L. Hoenig et al., Investigation of the System Beryllium-Boron, *J. Am. Ceram. Soc.*, 44: 385–389 (August 1961).
34. The Metallurgical Society, American Institute of Mining, Metallurgical, and Petroleum Engineers, A Symposium on Metallic Moderators and Cladding Materials, Held at Philadelphia, Pa., Oct. 19, 1960, *Nuclear Metallurgy (Volume VII), IMD Special Report Series No. 10.*
35. Atomics International, Annual Technical Progress Report, AEC Unclassified Programs, Fiscal Year 1961, USAEC Report NAA-SR-6370, Aug. 15, 1961.
36. C. W. Hamill et al., Metal Hydrides for Shielding Applications, USAEC Report Y-1366, Union Carbide Nuclear Co., Y-12 Plant, Oct. 6, 1961.
37. R. L. Beck, Investigation of Hydriding Characteristics of Intermetallic Compounds, USAEC Report LAR-54, Denver University, Denver Research Institute, August 1961.
38. General Atomic Div., General Dynamics Corp., 40-Mw(e) Prototype High-Temperature Gas-Cooled Reactor, Research and Development Program, USAEC Report GA-2204, September 1961.
39. F. W. Albaugh, Reactor and Fuels Research and Development Operation Monthly Report, October 1961, USAEC Report HW-71535A, Hanford Atomic Products Operation, Nov. 15, 1961. (Classified)
40. F. W. Albaugh, Reactor and Fuels Research and Development Operation Monthly Report, November 1961, USAEC Report HW-71921A, Hanford Atomic Products Operation, Dec. 15, 1961. (Classified)
41. A. H. Willis et al., Wigner Energy Storage In Fission Product Damaged Graphite, French Report BLG-62, June 28, 1961.
42. W. B. Tarpley and H. Kartluke, Ultrasonic Impregnation: Preparation of Low Permeability Graphite, USAEC Report NYO-10009, Aeroprojects, Inc., December 1961.

Section III

Reactor Materials

Nuclear Poisons

Dispersion Control Materials

Work at the Bureau of Mines[1] has shown that a ductile dispersion of 17 wt.% Gd_2O_3 in niobium can be produced by powder techniques. The mixture was hand blended, sintered, and forged to a reduction of 85 per cent. Attempts are also being made to determine the hafnium-carbon phase diagram. Homogeneous compounds will be produced by sintering techniques.

The Martin Company[2] has summarized its fabrication techniques for producing control rods of europium titanate dispersed in stainless steel. The control material is prepared by blending 68.8 wt.% Eu_2O_3 with 31.2 wt.% TiO_2 and firing in air at 1550 to 1600°C for 2 to 3 hr. The compacts are crushed to powder, which is then blended with 57.4 wt.% stainless-steel powder (−325 mesh). Compacts are pressed at 30 tsi and sintered at 1250°C for 1 hr in hydrogen. The sintered compacts are (1) coated with stainless steel by flame spraying, (2) roll clad at 1150 to 1200°C, and (3) then cold rolled to size.

Poisoned glasses representing high, intermediate, and low softening points have been prepared at Argonne[3] for evaluation as control materials. Fabrication techniques have been developed for B_4C glasses, and glasses containing Eu_2O_3, Gd_2O_3, Sm_2O_3, and Dy_2O_3 are being prepared.

In recent years considerable controversy has existed over the boron-carbon system. Armour[4] has recently completed a study in an attempt to clarify the system. In that study, only one carbide phase was found to exist over the range 9 to 20 at.% carbon. The terminal solubility of carbon in boron was found to be 0.1 to 0.2 at.%. A eutectic reaction was found at 29 at.% carbon and 2375°C. No allotropy of boron was observed. The freezing reaction between the carbide and boron was reported to be a degenerate peritectic-eutectic reaction at the composition and melting point of boron.

Colton[5] has reported on the boron silicides and has indicated that the oxidation resistance is good at temperatures to 1370°C. The B_6Si is reported to melt at about 1950°C. It contains 69.8 wt.% boron and has a density of 2.43 g/cm^3. Oxide-bonded B_6Si is reported to have excellent shock resistance and a bend strength of 13,000 psi at 25°C and 10,800 psi at 1095°C. It is an electrical insulator and has a thermal conductivity of 0.012 to 0.027 watt/(cm)(°C) at room temperature. (G. W. Cunningham)

Metallic Poison Materials

The properties of europium and its alloys were compared by Lesser and Erben[6] with those of boron, cadmium, hafnium, gadolinium, and samarium for reactor control. The alloy silver-cadmium-europium was found to fulfill to the greatest degree the requirements for a reactor control material. This alloy also possesses good corrosion resistance and machinability.

At Knolls, Dearing and Andrako[7] studied the corrosion rate of reactor-grade hafnium in 540°F water, 680°F water, and 750°F steam. Tests were continued for 96 days in steam and 196 days in water. They concluded that there was no linear correlation between steam and water corrosion in low-iron hafnium and, further, that the corrosion mechanism in steam is different from that in water.

Gadd and Evans[8] reported on the scaling behavior of hafnium in air in the temperature range 600 to 1200°C. The hafnium scaled ini-

tially at a rate between parabolic and cubic, followed by a transition to a much faster rate because of scale cracking. The scaling behavior of hafnium in air was almost identical with that of zirconium, except that zirconium exhibited growth whereas the hafnium was dimensionally stable. (W. E. Murr)

References

1. U. S. Bureau of Mines, Quarterly Metallurgical Progress Report No. 12, July 1 to Sept. 30, 1961, USAEC Report USBM-U-863.
2. Martin Co., Nuclear Div., Sixth Quarterly Progress Report, June 1 to August 31, 1960, USAEC Report MND-M-1817.
3. Argonne National Laboratory, Reactor Development Program Progress Report, November 1961, USAEC Report ANL-6473, Dec. 15, 1961.
4. R. P. Elliott, The Boron-Carbon System, USAEC Report ARF-2200-12, Armour Research Foundation, Illinois Institute of Technology, June 7, 1961.
5. E. Colton, Introducing Boron Silicide, *Nuclear Eng.*, 5: 324–325 (August 1961).
6. R. Lesser and E. Erben, Europium and Europium Alloys, *Metall.*, 15: 30–33 (January 1961).
7. B. E. Dearing and A. M. Andrako, The Corrosion Behavior of Hafnium in Aqueous Media as a Function of Temperature, USAEC Report KAPL-M-BED-3, Knolls Atomic Power Laboratory, Aug. 4, 1961.
8. J. D. Gadd and R. B. Evans, High Temperature Scaling of Hafnium in Air, *Corrosion*, 17(9): 109 (September 1961).

Section

IV

Reactor Materials

Cladding and Structural Materials

Corrosion

Zirconium Corrosion

Hydrogen absorption in zirconium alloys exposed to 400 to 600°C steam has been reported by Harwell.[1] Zircaloy-2 was found to absorb about 30 per cent of the hydrogen theoretically available from corrosion during initial exposure. Upon continued exposure, hydrogen absorption suddenly rose to 80 to 100 per cent of theoretical. Binary zirconium alloys containing chromium, cobalt, copper, nickel, silver, tungsten, and possibly tin exhibited a similar increase in hydrogen uptake. On the other hand, unalloyed zirconium, binary iron alloys, and ternary copper-tungsten alloys were found to absorb a constant percentage of theoretical hydrogen during the corrosion tests.

The results suggest that the high hydrogen pickup is associated with (1) the presence of certain foreign elements in the oxide film and (2) cracking of the oxide film next to the metal. The cracks apparently were too small to be detected by capacitance measurements that were made on the oxide film.

The Harwell workers suggest further that hydrogen enters the oxide film during the reaction by which water molecules are split up in reacting with oxygen anion vacancies in the oxide film. They also believe that activated diffusion of the water down into pores and the subsequent reaction with oxygen vacancies would increase the chances of hydrogen being absorbed in the oxide lattice. This mechanism was suggested as being associated with cracking in the oxide film and a sudden increase in hydrogen absorption.

Hydrogen ions were believed to migrate through the oxide film by loosely attaching themselves to oxygen ions to form a hydroxyl ion and then jumping from one to another of the oxygen ions. Less than 1 hydroxyl ion per 1000 oxygen ions was detected in the oxide film, suggesting that hydrogen diffusion was very rapid.

Nuclear Metals has recently summarized[2] research conducted on the mechanism of corrosion of zirconium alloys in high-temperature steam. By removing the steam corrodent and then introducing gaseous HCl, the researchers demonstrated that (1) cracking of the oxide film occurred during corrosion and cracks extended into the oxygen-rich zone beneath the oxide, (2) thermal cycling caused premature cracking of the oxide and accelerated corrosion, and (3) the critical film thickness for cracking to occur was 8 to 9 μ in steam at 700°C. Other experiments with zirconium intermetallic compounds demonstrated that unalloyed zirconium was a better getter for hydrogen and had a greater affinity for oxygen than any of the intermetallics studied. The compounds studied were those containing aluminum, beryllium, chromium, copper, iron, molybdenum, nickel, palladium, platinum, ruthenium, silicon, silver, tin, or tungsten.

Recent work by Hanford[3] has shown that weight gains of single specimens of Zircaloy-2, Zircaloy-3, or nickel-free Zircaloy-2 go through two or more repetitive cycles during corrosion in 360°C water and 400°C, 1500-psi steam. Metallographic sections of Zircaloy-2 specimens revealed a layered oxide structure with the number of layers corresponding to the apparent number of cycles in the weight-gain curve. On the basis of these observations, Hanford workers suggest that stresses in the film periodically cause it to crack at or near the oxide-metal interface. They further suggest that this effect might be masked when plotting the average weight gain of two or more speci-

mens—the resulting curve having only one transition in kinetics, as has generally been reported. (W. E. Berry)

Aluminum Corrosion

Oak Ridge has presented new results and summarized all the data that have been obtained on the effect of high heat flux on the corrosion of aluminum by water.[4] They conclude that, at heat fluxes of 1 to 2×10^6 Btu/(hr)(sq ft), temperatures to 250°F, and flow rates to 50 ft/sec, (1) penetration would be less than 1.5 mils in 15 days (lifetime of the fuel element) under hot-spot, hot-channel conditions if the water were adjusted to *p*H 5 (thus aluminum could be safely used), (2) 6061 alloy would be better than 1100 alloy because of its better strength, and (3) neither 1100 nor 6061 alloy would be suitable in neutral water because of the probability of getting complete penetration of the 10-mil-thick cladding within 15 days at hot spots on the fuel-element surface.

Hanford[5] and Argonne[6] have summarized the results of investigations on the corrosion resistance of aluminum alloys in high-temperature water. Reports from both laboratories gave details of specimen preparation and descaling methods. Hanford has summarized information obtained under static conditions. The results emphasized the beneficial effects of low silicon in the alloys and of iron-nickel additions over a wide range of composition. Argonne summarized information obtained under dynamic conditions in laboratory tests and in reactors. The results demonstrated that improved corrosion resistance of alloy X-8001 could be obtained by decreasing the water *p*H from 7 to 5, using H_3PO_4 to adjust the *p*H, and having a high ratio of corroding aluminum surface to volume of circulating water. Increased corrosion of aluminum was noted with surface boiling, on in-reactor fuel plates, and with galvanic couples at *p*H below 3.5. (W. E. Berry)

Steel Corrosion and Corrosion Products

Pitting of steel in concentrated caustics at 316°C has been investigated at the Naval Research Laboratory.[7] Pitting, which was obtained in 40 per cent NaOH, resembled that observed in conventional boilers at hot spots. No pitting was encountered when steel was exposed to 316°C 28 per cent LiOH. This suggested to the investigator that substitution of LiOH for NaOH as an alkalizing agent in the secondary side of nuclear reactors warrants a trial.

Chalk River has described[8] its experience in crud (Fe_3O_4 corrosion product) deposition problems in water-cooled reactors. Their experience was found to support the generally accepted belief that crud deposition on zirconium fuel elements was due to one factor, or perhaps a combination of factors, namely, (1) presence of a high ionizing-radiation flux, (2) presence of a high thermal flux, and (3) presence of higher temperatures at the fuel-element surface. The effect on crud deposition of water *p*H, neutron and thermal fluxes, length of irradiation, and prior crud inventory were among the variables studied. (W. E. Berry)

Corrosion of Iron- and Nickel-Base Alloys

Work at Bettis has been concerned with the utilization of carbon steels as structural components in water-cooled reactors. Observations on the performance of carbon steels and engineering problems associated with their use were comprehensively reviewed in a recent report.[9] Advantages of carbon-steel structures, compared with stainless-steel structures, are lower cost, improved thermal conductivity, and superior resistance to chloride-induced stress-corrosion cracking. The principal disadvantage is relatively poor resistance to general corrosion and to pitting corrosion. On the basis of considerable experience, Bettis workers concluded that carbon steels are suitable for use in thick-walled sections, but not in thin-walled components because of pitting. However, additional long-term studies are advisable to verify findings.

Susceptibility to stress-corrosion cracking in the presence of chloride ion remains as a major problem in water-cooled-reactor utilization of stainless steels. Russian investigators evaluated various iron-chromium, nickel-chromium, iron-chromium-nickel, and iron-chromium-nickel-molybdenum alloys in aqueous NaCl solutions.[10] They found that anodic polarization in these alloys generally increases with increasing chromium content. Additions of nickel, and particularly molybdenum, enhance the stability of the passive state of stainless steel in the presence of chlorides. Potential means for reducing the susceptibility of type 316 stainless steel to stress-corrosion cracking are being investigated at Alco Products. Kanigen

(electroless) nickel plating of type 316 was studied[11] but did not afford the required protection. On the basis of a literature survey,[12] Alco workers are now investigating Inconel cladding of type 316 stainless steel as a means of eliminating stress-corrosion cracking.

Although high-temperature oxidation kinetics and mechanisms in the case of nickel oxidation are well established, uncertainties concerning the oxidation process at low temperature exist. The British reported[13] the results of a study of the oxidation of nickel between 570 and 930°F under 7.6 cm oxygen pressure. For times up to 20 hr, the oxidation process followed cubic kinetics. An activation energy for the oxidation process in this temperature range was determined to be 41 kcal/mole. This suggests cation-vacancy diffusion as the rate-controlling process, in accordance with Gulbranson's findings. Preliminary results suggested that preirradiation of bare or preoxidized nickel foils reduces the subsequent oxidation rate by a factor of about 2.

Studies on the air oxidation of the Fe–25 Cr–4 Al–1 Y alloy at 2010 to 2600°F were continued to 1000 hr at General Electric.[14] Throughout these tests, parabolic behavior was observed, with rate constants as shown below:

Temp., °F	Time, hr	K_p, $(g/cm^2)^2/sec$
2012	0–160	8.7×10^{-13}
	160–1000	3.85×10^{-13}
2192	0–100	5.5×10^{-12}
	100–1000	2.26×10^{-12}
2400	0–200	2.2×10^{-11}
	200–1000	1.08×10^{-11}
2597	0–450	2.3×10^{-10}

On the basis of the initial rates at various temperatures, the activation energy for oxidation was calculated as 45 kcal/mole, suggesting diffusion of aluminum to the oxide-metal interface as the rate-controlling process. The calculated activation energy of the lower rates, 69.5 kcal/mole, suggests that diffusion of oxygen or aluminum through the scale determines the rate of oxidation. (E. S. Bartlett)

Niobium Corrosion

The sequence of reactions involved in the low-pressure oxidation of niobium has been described by Oak Ridge.[15] At 850 to 1200°C, under oxygen pressures of 3×10^{-5} to 5×10^{-3} mm, the initial reaction is linear and is associated with oxygen diffusion into the metal. As the metal becomes saturated, oxygen precipitates internally, giving a second linear reaction. These reactions are followed by parabolic formation of an adherent NbO_2 surface film and subsequent oxidation of the NbO_2 to porous Nb_2O_5, accompanied by a transition to linear behavior. The slower oxidation in low-pressure air as compared with that in an equivalent pressure of pure oxygen is attributed to adsorbed nitrogen, which reduces the number of sites available for adsorbing oxygen. Alloying is relatively ineffective in reducing the low-pressure oxidation rates.

Parabolic behavior is also observed in water vapor at 300°C, according to the British.[13] The oxides formed are NbO and NbO_2. The introduction of oxygen into the water vapor increases the oxidation rate and promotes formation of Nb_2O_5. A maximum in the niobium-water oxidation rate is observed at 550°C and a minimum between 575 and 600°C, similar to the behavior observed in oxygen and in air.

The suggestion that oxygen diffusion through the adherent scale is rate determining has been strengthened by results of a recent study at General Electric.[16] The activation energy for oxygen diffusion in Nb_2O_5 was determined as 28.2 kcal/mole. This value agrees fairly well with energies[17,18] of 27.4 and 22.8 previously determined for the parabolic oxidation of niobium in the temperature range 200 to 500°C.

Coatings based on zinc, aluminum, and silicon are under study for protecting niobium and niobium alloys from oxidation. The Naval Research Laboratory[19] has recently shown that the life and resistance to embrittlement of zinc-coated niobium are increased moderately by the addition of nickel-aluminum to the coating. Niobium, dip-coated with zinc–5 wt.% nickel–1 wt.% aluminum, was unhardened after 1000 hr at 1800°F, whereas the pure zinc coating prevents hardening for only 400 to 600 hr at 1800°F. At 2000°F the alloy coating was protective for 20 hr but allowed contamination of the substrate. Thus the zinc coating appears to be capable of minor improvement but does not appear suitable for long-time exposures above 1800°F.

Data from Armour[20] indicate that zinc coatings are protective to niobium-vanadium alloys.

Coatings of zinc, zinc–10 wt.% aluminum, and zinc–10 wt.% tin protected niobium–40 wt.% vanadium and niobium–75 wt.% vanadium–5 wt.% titanium for 28 hr at 1800°F, plus 4 hr at 2000°F, without failure.

Armour[21] has also observed rapid oxidation of $NbAl_3$ at 1000 to 1600°F, the highest rate occurring at 1380°F.

Silicide coatings are attractive for protecting niobium at higher temperatures. Tapco[22] has presented life data (98 per cent confidence) for its titanium-chromium-modified silicide coating on D-31 alloy (niobium–10 wt.% molybdenum–10 wt.% titanium) as follows:

1800°F	400+ hr	2600°F	15+ hr
2000°F	400+ hr	2700°F	5 hr
2300°F	250+ hr	2800°F	1 hr
2500°F	100+ hr		

Above 600°F this coating does not spall from the substrate on impact and remains protective.

Chance-Vought[23] is also engaged in the development of protective silicide coatings. A silicon-chromium-aluminum cementation coating appears attractive; it has protected niobium–1 wt.% zirconium for 10 hr at 2600°F without failure.

(W. D. Klopp)

Molybdenum Corrosion

The protective life of nickel-chromium electrodeposited coatings on molybdenum can be significantly increased by spraying with alumina, according to recent British information.[24] A 5-mil nickel-chromium coating is protective for 300 to 500 hr at 2000°F. Application of a 3-mil top coat of sprayed alumina increased the life to 1200 hr.

Chemical analysis of the Chromalloy W-2 silicide coating on molybdenum by British investigators[25] gave the following results, in at.%:

Molybdenum	62.1	Chromium	0.28
Silicon	34.6	Titanium	0.18
Aluminum	4.6	Copper	0.18
Iron	0.18	Nickel	0.08

The aluminum was present as a thin external alumina film and is apparently an unintentional contaminant. Chromalloy[26] describes W-2 as a chromium-stabilized silicide coating.

Chromalloy[26] has conducted a limited comparative study on the life of various silicide coatings on molybdenum. Data from this study, summarized below, indicated that the Durak B coating is exceptionally protective to molybdenum at 2700°F.

Coating	No. of samples tested	Average life to failure at 2700°F, hr
Pfaudler PFR-6	36	26.6
Chance-Vought	4	<2
Chromalloy W-2	38	46.4
Chromizing Durak B	17	246

The accelerated low-temperature oxidation behavior of $MoSi_2$ has been studied at Armour.[21] The maximum oxidation rate was observed at about 900°F.

(W. D. Klopp)

Tantalum and Tungsten Corrosion

Studies at Sylcor on aluminide and beryllide coatings for tantalum have been summarized recently.[27] The aluminum–50 wt.% tin coating appears to be superior and is capable of protecting tantalum and tantalum–10 wt.% tungsten for up to 100 hr at 2800°F. Beryllides offer good protection at 2500 to 2700°F but suffer from rapid interdiffusion with tantalum at these temperatures.

Ruthenium-modified tungsten "heavy metal" alloys are moderately more oxidation resistant than tungsten at 2000°F, according to Armour.[28] Tungsten-molybdenum-iron-nickel alloys containing 0.5 to 1 wt.% ruthenium exhibit a metal loss rate of 1.5 mils/hr in air at 2000°F, compared to 7 mils/hr for unalloyed tungsten.

Complex silicide coatings for protecting tungsten are under development at Tapco.[29] A coating that exhibits promise consists of titanium-yttrium-zirconium-silicon-oxygen. The coating elements are applied to tungsten by vapor plating individually in vacuum using an NaF carrier, followed by preoxidation at low temperatures. A 3.5-mil coating of this composition protected tungsten for 2.5 hr at 3200°F, compared with 0.5 hr for a 1-mil straight silicide coating.

Tungsten disilicide, like $MoSi_2$ and $NbAl_3$, has been shown by Armour[21] to exhibit accelerated low-temperature oxidation. The maximum rate is observed at 1800°F.

(W. D. Klopp)

Corrosion of Miscellaneous Metals

To investigate the chemical stability of uranyl sulfate fuel solutions at temperatures above those for which type 347 stainless steel is satisfactory (625°F), Oak Ridge constructed a titanium pump loop for operation at 3000 psia and 700°F. This system has been proof-tested, using 680°F, 2710-psia water, with satisfactory performance.[30]

The study of the oxidation resistance of the platinum-group metals (rhodium, palladium, platinum, Pt–30 Rh alloy, and iridium) at temperatures from 2192 to 2912°F was continued at General Electric.[14] Comparison of tests in air and argon indicated that palladium loses metal by evaporation of the metal, whereas the other metals studied lose metal (in air) by sublimation of the oxide. Thin, dense Al_2O_3 coatings over the noble metals provided some, but not complete, inhibition of metal loss.

Another material for which General Electric workers studied oxidation behavior was a series of Cr–0.5 Y alloys containing from 5 to 35 at.% rhenium. In 50 hr at 2552°F, all alloys lost weight because of volatilization of rhenium oxide. Alloys with higher rhenium contents exhibited the poorest oxidation behavior.

The British have tabulated[31] all known information relative to the compatibility of various materials that may be of use in CO_2-cooled reactors. Intermaterial compatibility, as well as material-CO_2 compatibility, is considered.

(E. S. Bartlett)

Corrosion by Liquid Metals

The Sodium Reactor Experiment (SRE) being operated by Atomics International is provided with a bypass loop where samples of various materials can be exposed to sodium coolant taken from the main flow circuit. Samples of type 304 stainless steel, zirconium, and beryllium were exposed in this facility over a two-year period and were then subjected to various examinations to ascertain corrosion and activity levels.[32] Exposure temperatures ranged from about 300 to about 850°F. Corrosion findings can be summarized as follows:

—Type 304 stainless steel: No alteration in microstructure or mechanical properties was found; some oxidative weight gains were observed for hot-leg specimens.

—Zirconium: Moderate hydriding occurred, but the degree was enough to indicate the possibility of severe localized hydriding of the zirconium-clad moderator cans present in the SRE; tabs with polished surfaces displayed low weight gains, whereas weight changes were erratic for tabs with unpolished surfaces.

—Beryllium: Distinct weight losses occurred, presumably owing to spalling of nonadherent oxide layers.

Table IV-1 presents sodium-corrosion data obtained at Atomics International[33] as an adjunct to a program of zirconium-alloy development. The data, which were obtained in natural-convection sodium systems with oxygen levels of 10 ppm or less, show virtually no difference between the alloy behavior and that of unalloyed zirconium control specimens.

Brookhaven National Laboratory, in an investigation[34] to find materials for the containment of the lead-bismuth eutectic, found no corrosion or mass transfer in carbon-steel thermal convection loops containing the eutectic inhibited with titanium or zirconium. Operating conditions included a 650°C peak temperature, a ΔT of 150°C, and an exposure time of approximately 5000 hr. After about 10,000 hr of operation, a $1\frac{1}{4}$ wt.% chromium–$\frac{1}{2}$ wt.% molybdenum steel loop containing uninhibited eutectic evinced no corrosion effects; the hot- and cold-zone temperatures were 400 and 200°C, respectively.

The Los Alamos Molten Plutonium Reactor Experiment (LAMPRE) is based on a plutonium-

Table IV-1 CORROSION[33] OF SELECTED ZIRCONIUM ALLOYS AND ZIRCONIUM IN SODIUM AT 1000 AND 1200°F

Material	Average weight gain, mg/cm², for indicated exposure time at 1000°F					
	75 hr	163 hr	300 hr	500 hr	1500 hr	2500 hr
Zirconium alloy (1.5 Al + 1.5 Sn + 1.5 Mo)	0.18	0.33	0.40	0.42	0.55	0.58
Unalloyed zirconium	0.14	0.23	0.33	0.30	0.50	0.56

Material	Average weight gain, mg/cm², for indicated exposure time at 1200°F				
	37.5 hr	130 hr	240 hr	1050 hr	2500 hr
Zirconium alloy (1.25 Al + 1 Sn + 1 Mo)	0.37	0.50	0.76	0.74	0.69
Unalloyed zirconium	0.41	0.53	0.73	0.68	0.69

iron eutectic fuel contained by tantalum. Some corrosion occurs in this system in the 600 to 800°C range of interest, and consequently a broad supporting compatibility study has been conducted. This study has included laboratory experiments and, in addition, as LAMPRE operates, selected fuel capsules can be charged and withdrawn to provide a means of exploring radiation-induced corrosion. One general finding[35] has been that tantalum subjected to a high annealing temperature (1300 to 1450°C) has distinctly better corrosion resistance than material subjected to lower temperature anneals. It has been observed also[36] that additions of carbon (500 ppm), silicon (0.4 to 1.5 wt.%), or aluminum (0.3 to 0.7 wt.%) to the fuel reduce the rate of intergranular attack of the tantalum at 750°C; it is interesting to note that at 625°C carbon may be ineffective or even detrimental. At present there is assurance for LAMPRE operation at temperatures up to about 650°C. Above this level, however, solution attack of tantalum can present a problem, but some control seems possible through carbon and silicon additions. Promise also exists for the use of tantalum alloyed with tungsten, thorium, yttrium, or hafnium. The 625°C corrosion behavior of such experimental alloys has been shown[37] to be equal to that of pure tantalum. Further experiments are planned to determine whether such materials have corrosion resistance superior to that of tantalum at higher temperatures.

The possibility that thermoelectric potentials encourage the dissolution process between a liquid metal and a corroding surface is being investigated at Brookhaven. Results of certain experiments were reported[38] at the Tenth Annual AEC Corrosion Symposium held in May 1961. With liquid bismuth as the corroding medium, it was found that "(1) iron migrates through bismuth toward the anode, chromium toward the cathode; (2) a 5 wt.% chromium steel, when immersed in liquid bismuth, is electropositive to all the other steels tested. This steel is the one selectively attacked: when two iron electrodes are immersed in liquid bismuth at different temperatures, the potential between them is a function of the iron dissolved in the bismuth, and the lower temperature electrode becomes more anodic as the temperature differential increases." These data, although limited in scope, are, as the author states, in the direction of indicating a definite thermoelectric-potential influence in the corrosion process. (J. H. Stang)

Metal-Water Reactions

Studies of metal-water reactions to determine rates of reaction of molten reactor fuel and cladding metals with water are continuing at Argonne.[39,40] The principal laboratory procedure uses a condenser discharge to provide almost instantaneous heating and melting of metal wire in water or steam. The energy input to the wire indicates reaction temperature; the transient pressure measures reaction rate; light emission indicates time-temperature; hydrogen generated gives extent of reaction; and particle size of the residue indicates the surface area exposed to reaction. A second method consists of heating the metal inductively and subjecting it to a steam pulse to induce a metal-steam reaction.

The series of condenser-discharge runs[39] with Zircaloy-3 wires in water was completed. A series of runs in heated water and a series in room-temperature water showed good agreement with previous results with pure-zirconium wires under similar conditions.

Data obtained on the reaction of molten aluminum with steam by the pressure-pulse method[39] were reexamined, and it was concluded that the reaction at 800, 1000, and 1200°C can be described by the cubic rate law. The reaction was found to have an activation energy of 21.7 kcal/mole.

Studies of the reaction of aluminum-uranium alloys with steam by the pressure-pulse method[40] are in progress. Preliminary results indicated that reaction rates of alloys of 5 wt.% uranium in aluminum were greater than those of pure aluminum at 800 and 1000°C but lower at 1200°C. An alloy of 20 wt.% uranium in aluminum showed a greater reaction rate than pure aluminum at 1200°C. (A. W. Lemmon, Jr.)

Radiation Effects in Nonfuel Materials

Defects: Structure and Properties

Metals. Threshold energies for atomic displacements have been measured[41] by fitting curves calculated with simple threshold models

to curves for the variation of cross section for atomic displacement with energy. Measurements were made as a function of bombarding electron energy from 0.5 to 1.3 Mev. The observed variations agree with previous measurements but not with the recent machine calculations made at Brookhaven.[42] For copper, nickel, and iron, using some previous data as well, the conclusion was made that basic damage processes are equivalent for both low- and high-energy recoils. Data on copper and silver verified that the threshold increases with increase in atomic number in the family copper, silver, and gold. Data for aluminum do not fit a simple threshold picture, which is explained as evidence for the production of multiple defects in aluminum in the range of bombarding energies used. The data are tabulated below:

	Threshold energy, ev	Resistivity per Frenkel pair, μohm-cm/at.%
Copper	22	1.3
Silver	28	1.4
Nickel	24	3.2
Iron	24	12.5

Other experimenters[43] have also reported a 22-ev displacement energy for copper.

Preliminary results of measurements of the range of D_2^+ ions in aluminum have been reported.[44] Thin films of aluminum were vacuum deposited on optical quartz substrates and bombarded with various energy D_2^+ ions. After bombardment, the aluminum films were removed with sodium hydroxide, and the amount of damage in the quartz was measured in terms of its optical properties. The ranges inferred were

D_2^+ ion energy, kev	Range, A
15.0	990
18.8	1270
24.6	1530
33.6	2020

The ion range here is defined as being equal to the aluminum thickness for which the relative damage in the quartz is 50 per cent of its maximum value.

Radiation-induced defects that have been studied contribute to the mechanical hardness of molybdenum but do not affect the electrical resistivity.[45] Molybdenum (99.92 per cent) was irradiated between 40 and 220°C up to doses of 1.9×10^{20} neutrons/cm^2 and annealed at various temperatures. Two types of defects that were isolated had activation energies of 4500 and 76,000 cal/mole, respectively. These defects cannot be of the Frenkel type since they do not affect the electrical properties.

Aluminum foils (thinned to 1000 A), irradiated in the Chalk River NRX reactor to a dose of 7×10^{19} neutrons/cm^2 ($E_n > 500$ ev), were observed by transmission electron microscopy.[46] From the observed dislocation positions, inferences were drawn that even foils this thin did retain vacancies (contrary to previous suggestions) which were capable of inhibiting dislocation motion. No defect clustering was observed with the microscope since no loops were seen.

Makin et al.,[47] in extending their studies[48] of dislocation loops formed by neutron irradiation in copper, report that about 50 point-defect pairs are formed per primary knock-on atom. They also conclude that the loops are formed by nucleation of defects where the nuclei for the interstitial loops are formed directly by the irradiation, as opposed to being formed by the chance encounter of isolated point defects.

In studying the effects of radiation damage on the mechanical properties of iron,[49] three recovery stages were observed between room temperature and 400°C in samples irradiated to 3×10^{18} nvt. These occurred at about 175, 250, and 350°C. Only a single zone at 375°C appeared in iron irradiated to 1×10^{20} nvt. This higher exposure is in the region where electrical resistance is decreasing as a function of dose. The recovery zones at 175 and 250°C are explained in terms of iron carbides precipitating from supersaturated solution. Isochronal annealing of neutron-irradiated iron, titanium, and zirconium has also been reported[50] up to 500°C.

No change was observed in the characteristic (Debye) temperature of Armco iron and electrolytic copper[51] after neutron irradiations up to a dose of 10^{19} neutrons/cm^2. Third-order distortions were observed and described as unordered static displacements of atoms. The formation of such displacements has been used to explain in part the observed increase in microhardness due to the irradiation.

Walker[52] has prepared a very extensive analysis of electron-produced damage in metals. The importance of using these techniques as a tool for studying basic mechanisms is discussed, as well as the most recent results of experiments. The report is divided into five sections which include a general analysis of the features of electron damage; a review of the studies of low-temperature bombardment of high-purity copper; recent work on the influence of lattice imperfection on damage and recovery processes; a report of some new results in aluminum, silver, gold, nickel, and iron; and, finally, discussion of current outstanding problems.

Further observations[53] have been reported that damage, similar to that caused by primary knock-ons, is produced by the beam of an electron microscope.[54] Small spots and loops have been observed in thin evaporated single-crystal gold films, introduced by bombardment from negative ions emitted from the tungsten filament. The ions have not been identified as yet but seem to depend on impurities in the tungsten. Coating a filament greatly increases the rate of damage. The spots anneal when the films are heated to 350°C. Above this temperature the damage consists of small tetrahedral stacking faults.

Defects in Metal Alloys. Annealing of the electrical resistivity due to neutron damage in high-purity copper and copper alloys has been studied[55] between −196 and 150°C. Doses up to 5×10^{17} nvt were obtained by week-long irradiations in the BEPO reactor. Annealing peaks were observed in all specimens at approximately −140, −60, and 0°C. The two lower peaks are superimposed at 0°C. About 0.02 per cent of silver or cadmium enhances the first peak considerably, whereas higher concentrations enhance the second peak at the expense of the first. These two peaks are explained in terms of the release and migration of interstitials from traps, which are identified as single and paired impurity atoms, respectively. The 0°C peak is due to vacancy migration to impurity atoms. The plateau annealing is explained in terms of annealing zones which consist of high vacancy concentrations surrounding the track of the primary knock-ons. The same annealing regions and interpretations have been observed in beryllium-copper alloys, but the details are different because the damage volume around a primary knock-on is considerably smaller. This reduction in size is due to the shorter distance of energy transfer along collision chains. One of the details that is significantly different is that the first annealing region, which occurs at about −120°C in beryllium-copper, is a trough, indicating that the release mechanism of this region produces an increase in resistivity.

Defects in Other Materials. Studies of uranium-doped ZrO_2 resulted in the following conclusions:[56] (1) fission-fragment fluxes associated with 10^{15} to 10^{16} fissions/cm^3 produce a monoclinic to face-centered cubic (fcc) phase change in ZrO_2, and the uranium, which is in the ZrO_2 in concentrations less than 0.5 at.%, does not act as a nucleation or stabilizing atom in the process; and (2) fast neutrons cannot induce this phase transition at doses up to 6.3×10^{20} neutrons/cm^2.

LiF crystals were irradiated with a neutron flux of 2×10^{17} and annealed at temperatures[57] up to 700°C. Phase-contrast microscopy revealed dislocations in the form of polygonal networks, parallel lines, and closed loops.

A relation has been developed between the energy received by a displaced silicon atom and the distance of this atom from its original site.[58] The bombarding particles considered are electrons. Expressions are derived from data on annealing (in silicon) of the defects produced by 0.7-Mev electrons. (T. G. Knorr)

Theories of Radiation Effects

Using Born-Mayer and Morse potentials for the interactions between lattice ions, Bennemann[59] has found another stable equilibrium configuration for interstitial copper in the fcc copper lattice. Previous reports have shown the stability of the shared interstitial face-centered pair, which are $0.6a$ apart (a = interatomic distance) symmetrically on a line perpendicular to the cube face of and through the location of the original face-centered atom. Bennemann's new configuration is a shared interstitial cube corner pair, which are $0.6a$ apart symmetrically on the [111] direction through the original cube corner.[60]

Baroody[61] has contributed to the calculations of focusing collisions in linear chains of atoms. Uniform spacing is used for the identical atoms that interact during collisions through a repulsive potential. Two energy-dependent parameters are introduced, and the results show ap-

preciably less focusing than followed from the use of earlier approximations. Focusing in (110) chains in copper is expected at 23 ev, which agrees well with the 30 ev obtained from the three-dimensional machine calculation of Gibson et al.[42]

Varley,[62] with some theoretical calculations, has developed an empirical model to explain the results of Makin et al. (see Defects, Metals, above) concerned with the formation of dislocation loops in neutron-irradiated copper. Brinkman's displacement mechanism is the basic assumption, and the theoretical results indicate a somewhat higher efficiency of loop formation than was observed. However, this can be explained in terms of impurities that affect the number of loops formed, either because of the local stresses generated in the displacement spikes or from the fact that they act as subnuclei for the initiation of clusters.

A study has been made of the distribution of multiple thermal points[63] (the small region around a final displaced atom heated to a temperature above the fusion temperature of the metal), which are determined by the distribution of the final displaced atoms. This distribution depends on the mean free path λ of the displaced atoms. The λ was calculated by the pulse method. For copper the actual values are less than those predicted. This confirms the possibility of the appearance of multiple thermal points in spherical layers. An equation was set up for the approximate radius of the layer, and the diffusion of heat from the spherical layer of interstitial atoms was discussed.

Initial results, considering the influence of crystal forces only, have yielded a 0.5-ev activation energy for the migration of a neutral chlorine atom[64] in NaCl. Electrostatic, polarization, and dipole-dipole energy contributions to second order, in terms of the displacements of the ions from their regular positions, were considered. Contributions involving repulsive energy of the defect atom were treated exactly, whereas those of the regular ions were expanded to second order. The defect positions are considered as either at the center of a cube of ions or at the center of a square of ions. Further calculations are in progress. (T. G. Knorr)

Surveys on Radiation-Induced Defects

The ORNL Solid State Division Annual Report[65] is generally interesting. Some of the specifically interesting topics reported are: theoretically determined ranges of 250-ev to 200-kev particles in solids; annealing of neutron-irradiated (at 40°K) tungsten, molybdenum, nickel, lead, tin, sodium, and graphite; stored energy and length changes in B^{10}-doped copper; quenching in copper; and the direct observation of 24-Mev nitrogen-ion tracks in thin platinum films.

Barnes[66] has presented a general description of the effects produced in cladding materials by fast neutrons or fission fragments. Displacement mechanisms are discussed, as well as bubble formation and property changes. The Radiation Effects Information Center has prepared two surveys of interest:[67,68] (1) "Radiation Effects State of the Art, 1960–1961," in which progress is clearly indicated (the inclusion in each section of a list of the current agencies which are studying the listed effects being of particular interest); and (2) "The Effect of Nuclear Radiation in Structural Metals," which includes an extensive bibliography.

The effects of reactor type irradiations on ceramic materials have been studied.[69] Discussions are concerned with damage mechanisms, damage minimization, and recovery of damage. Changes in properties are outlined for ceramics used as fuels, moderators, control elements, and structural members.

(T. G. Knorr)

Effects of Radiation on Mechanical Properties

At Oak Ridge[15] the effects of neutron bombardment on the creep and stress-rupture properties of Inconel, type 304 stainless steel, and niobium–1 wt.% zirconium have been studied in fast-neutron fluxes (>1 Mev) of 0.5×10^{13} to 1×10^{13} neutrons/(cm^2)(sec) and thermal neutron fluxes of 5×10^{13} to 8×10^{13} neutrons (cm^2)(sec). Inconel tubing processed from two different heats showed that the time to rupture under stress at 1500°F in air, as measured by a tube-burst test, was decreased by a factor of 3 to 5 by neutron exposure. Postirradiation measurements indicate that the ductility at rupture is decreased by a factor of 2 to 5 and that the ductility decreases as the time to rupture increases (stress decreases). No conclusions have been reached on the postulate that these effects may be due to natural-boron impurity, although some studies of the effect of

B^{10} concentrations ranging from 1 to 56 ppm are in progress.[65]

Similar in-pile tests[15] on type 304 stainless steel in air at 1300, 1500, and 1600°F indicated a reduction by a factor of 3 in time to rupture at 1500°F (as compared with out-of-pile test data) but no appreciable effect on time to rupture at 1300 and 1600°F. Postirradiation measurements, however, indicate a reduction in ductility at rupture by factors of 2 to 5 at all test temperatures. The ductility at 1300°F appears to be limited to about 1 per cent. The ductility at 1500 and 1600°F is somewhat higher, the strain being as low as 2 per cent in 1500-hr tests.

Short-time tests on irradiated and unirradiated niobium–1 wt.% zirconium alloy specimens in helium at 1800°F indicate that the exposures produced no more than a 10 per cent reduction in rupture strength.

At Hanford[70] the creep-rate dependency of the activation energies for creep of Zircaloy-2 below 280°C has been studied at creep rates of 1×10^{-4}/min to 4×10^{-4}/min prior to study of the effects of irradiation upon creep. The activation energy was found to decrease with increasing strain rate at constant temperature—a result predicted from simple dislocation interaction theory, where the creep activation energy is given by the expression

$$U = U_0 - b\,(\sigma - c\dot{\epsilon})$$

where U_0 = activation energy per dislocation interaction at zero stress
b and c = constants
$\dot{\epsilon}$ = creep rate
σ = applied stress
U = measured activation energy

This simple theory, however, does not predict the observed increasing activation energy with increasing temperature and, therefore, cannot be accepted as a complete explanation of the creep behavior of Zircaloy-2.

In-reactor creep rates of Zircaloy-2 at 500 and 550°F have been measured at 30,000 psi at Hanford.[71] The rates being measured are at the extreme limit of the instrumentation. However, the data do show a substantial difference between in-reactor and ex-reactor creep rates, within the statistical accuracies of the measuring equipment. At 500°F the average creep rate is 10 times the rate measured ex-reactor. At 550°F the rate is at least 17 times that of the ex-reactor rate. Each test is based on test data which may be insufficient to establish the minimum rate.

In-pile tube-burst tests have been made of Zircaloy-2 stressed at 700 and 900°F after an exposure of 5×10^{18} nvt (>1 Mev). With the exception of one specimen at 900°F, the data agree, within the expected scatter band, with out-of-pile control tests. Additional tests are required before conclusions can be drawn.

At Hanford,[72] tensile tests of Zircaloy-2 have been performed after integrated fast-neutron exposures of 0.84×10^{19} and 1.2×10^{20} nvt. Irradiation produces appreciable increases in strength and decreases in ductility, but the directionality of properties in longitudinal and transverse directions persists. An exception is uniform strain, which is strongly direction dependent in the annealed state but is nearly independent of direction in the cold-worked state. For example, the true uniform strains for the longitudinal and transverse directions in the annealed state are 0.047 and 0.007 in./in. (in 2.125 in.), respectively, for an exposure of about 10^{19} nvt. Corresponding values for the 70 per cent cold-worked state are 0.0235 and 0.0244, respectively. It appears, therefore, that cold work is beneficial in reducing the effects of directionality of uniform strain after irradiation, as well as in increasing the uniform strain in the transverse direction.

At Savannah River[73] the relaxation of tensile stresses in specimens of Zircaloy-2 that were irradiated at a temperature below 100°C was compared with the stress relaxation in unirradiated control specimens that were held at the same temperature for the same length of time. Irradiation had no effect on the relaxation of initial stresses of 10,000 and 15,000 psi in annealed specimens. An initial stress of 25,000 psi in annealed specimens relaxed to 19,000 psi with irradiation and to 15,000 psi without irradiation. An initial stress of 15,000 psi in 10 per cent cold-worked specimens relaxed to between 8000 and 10,000 psi with irradiation and to 12,000 psi without irradiation. The irradiations, which were as high as 8×10^{20} fast neutrons/cm^2, decreased the ductility and increased the strength of the specimens.

A series of welded side-wall samples of Zircaloy-2, with and without hot tears, were irradiated at Bettis[74] to an exposure of about

4×10^{21} nvt (fast) (>0.625 ev). The samples were then fatigue tested in bending at 600°F. Taking into account the factors that adversely influence the fatigue behavior of Zircaloy, it is evident that irradiated Zircaloy exhibiting hot tears does not deviate significantly from the scatter band observed for nonirradiated Zircaloy-2 weld channel specimens, with or without hot tears, covering a wide range of channel conditions.

(F. A. Rough and F. R. Shober)

Selected Mechanical Properties of Cladding and Structural Materials

Tensile Properties of APM 257

Mechanical-property data on APM alloy M257, which is a dispersion of 5 per cent Al_2O_3 in a matrix of aluminum, are reported by Atomics International.[75] Tensile data for this alloy are shown in Fig. IV-1, and creep-rupture strengths are given in Fig. IV-2.

Tensile Properties of Chromium

The tensile properties of chromium were determined at Ames Laboratory[76] in an attempt to develop more ductile metals of high corrosion resistance. The influence of annealing temperature on warm-swaged (700°C) chromium is shown in Table IV-2. Annealing above 300°C appears to decrease the ductility of swaged chromium.

Strength of Tungsten and Tantalum Alloys

The creep-rupture strengths of a number of tungsten-base alloys, as reported by Armour Research,[28] are shown below. The stress-rupture tests were conducted at 1600°F at a stress level of 12,000 psi.

Composition, wt.%	Time to failure, hr
90 W–9.7 (Ni-Fe)–0.3 Al_2O_3	17.6
90 W–9.75 (Ni-Fe)–0.25 MgO	19.1
90 W–9.7 (Ni-Fe)–0.3 ThO_2	24.7
90 W–9.6 (Ni-Fe)–0.4 ZrO_2	22.4
90 W–9.95 (Ni-Fe)–0.05 B	24.1
90 W–9.9 (Ni-Fe)–0.1 B	21.4

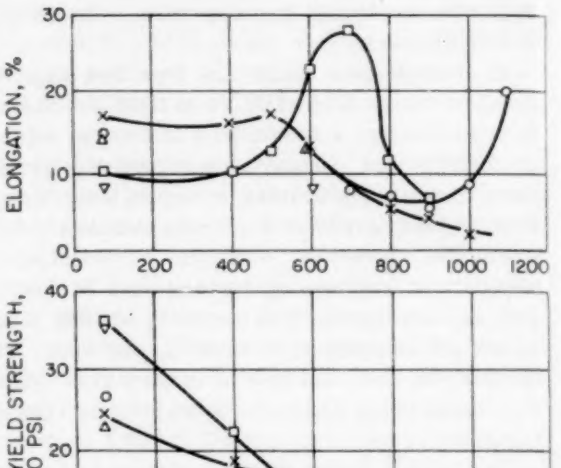

Fig. IV-1 Tensile properties[75] of APM alloy M257. ALCOA data: ×, extruded bar; ∇, sheet. AI data: ○, extruded bar, ¾ in. in diameter; Δ, extruded square tube, 0.100-in. wall; □, sheet.

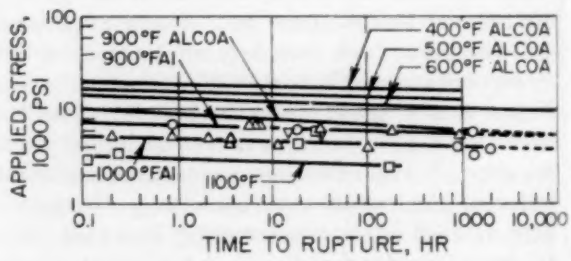

Fig. IV-2 Creep rupture strength of M257 (as extruded).[75] ALCOA's Lot No.: ∇, 458973; ○, 474443; Δ, 482168; □, 800216. AI = Atomics International data.

Table IV-2 ROOM-TEMPERATURE TENSILE PROPERTIES OF SWAGED AND ANNEALED CHROMIUM[76]

Annealing temp., °C	Ultimate tensile strength, psi	Yield strength, psi	Total elongation, %	Reduction of area, %
300	73,700	73,700	26.4	33.2
350	72,600	72,600	2.2	2.9
400	74,100	74,100	1.4	0
500	72,800	72,800	0.4	0
800			0	0

The creep and tensile strengths of a number of tungsten- and tantalum-base alloys being developed by Crucible Steel[77] are shown in Tables IV-3 and IV-4. A recent publication by the Defense Metals Information Center[78] reports on the strength properties of a number of experimental tungsten-base alloys being studied by Thompson Ramo Wooldridge and by Westinghouse. The TRW alloys include tungsten–5 and 15 wt.% molybdenum and tungsten–0.52 wt.% niobium. The latter alloy shows slightly higher strength in the 3000 to 4000°F range than do the tungsten-molybdenum alloys, as illustrated in Table IV-5. The Westinghouse materials are tungsten plus up to 2 wt.% TaC, HfO_2, or ThO_2. Typical high-temperature tensile data for several of these materials are shown in Tables IV-6 and IV-7.

Strength of Vanadium Alloys

A number of vanadium-base alloys are currently being evaluated by Armour.[79] Both tensile strengths and stress-rupture data have been determined. These properties are shown in Tables IV-8 and IV-9, respectively.

Mechanical Properties of Zirconium Alloys

The room-temperature tensile strengths of a zirconium–2 at.% niobium–2 at.% tin alloy under various heat-treatments as reported by Hanford[71] are shown in Table IV-10.

Improvements in the tensile properties of a zirconium–2.5 wt.% niobium alloy by aging were found at Chalk River.[80] Table IV-11 shows[81] the 300°C tensile properties for material that was water quenched from 880°C. The mechanical properties of some other zirconium alloys are shown in Table IV-12.

A summary of the results of creep tests on a number of zirconium-base alloys is reported[82] by the British Nonferrous Metal Research Association. Their results are shown in Table IV-13.

Creep tests on Zircaloy are being conducted at Battelle.[83] A summary of creep data for up to 33,500 hr is presented in Table IV-14. These tests are still in progress.

The properties of several high-strength zirconium-base alloys are reported by Nuclear Metals.[84] Tensile properties are shown in Table IV-15. In addition, the results of aging studies of solution-treated alloys are reported in Table IV-16.

Table IV-3 RESULTS OF CREEP TESTS ON TUNGSTEN AND TANTALUM ALLOYS AT 3000°F AND 7000 PSI IN VACUUM[77]

Nominal composition, wt.%	Duration of tests, hr	Elongation in 0.5 in., %
W	5	4.8
W	5	4.3
W–74.7 Ta	5	1.0
W–11.2 Nb	5	0.55
W–44.4 Ta–11.2 Nb	5	0.83
W–11.6 Mo	5	2.6
W–67.9 Ta–11.7 Mo	5	1.2
Ta–11.7 Mo	5	0.89
W–5.7 Mo–5.7 Nb	5	0.09
W–44.3 Ta–5.7 Mo–5.7 Nb	5	0.45
W–68.0 Ta–5.7 Mo–5.7 Nb	5	0.75
Ta–5.7 Mo–5.7 Nb	5	5.1

Table IV-4 RESULTS OF TENSILE TESTS AT 3000°F ON AS-EXTRUDED TUNGSTEN AND TANTALUM ALLOYS[77]

Nominal composition, wt.%	Ultimate tensile strength, 1000 psi	Elongation in 0.5 in., %	Reduction of area, %
W	14	74	99
W–74.7 Ta	37	3	1
Ta	4	118	99
W–11.2 Nb	50	4	1
W–44.4 Ta–11.2 Nb	54	7	13
W–68.1 Ta–11.2 Nb	6	82	99
Ta–11.4 Nb	6	102	99
W–11.6 Mo	25	47	93
W–44.2 Ta–11.6 Mo	57	5	1
Ta–11.7 Mo	29	29	24
Ta–5.7 Mo–5.7 Nb	18	25	36

The yielding and fracture characteristics of Zircaloy-2 as a function of stress state were investigated, by Knolls workers,[85] at room temperature through the medium of thin-walled cylindrical specimens under internal pressure and axial tension. Stress states from uniaxial longitudinal tension to uniaxial tangential tension were examined. Two tests at elevated temperature were performed at a single stress ratio. It was found that the fracture ductility lessened with increasing biaxiality. A minimum in ductility was found at balanced biaxial tension where the fracture ductility, as expressed by the effective strain, was 29 per cent. The yielding and plastic-flow properties were found to be highly anisotropic. Two methods were used to express the plastic-flow data: a graphical approach and a theoretical analysis based on a

Table IV-5 TENSILE PROPERTIES OF ARC-CAST AND EXTRUDED TUNGSTEN ALLOYS AT 0.020 IN./MIN CROSSHEAD SPEED[78]

Composition, %	Temp., °F	Ultimate tensile strength, psi	Yield strength (0.2% offset), psi	Reduction in area, %	Elongation, %
W–15 Mo	3000	36,000	34,500	78	27.8
	3250	24,450	23,500	80	34.9
	3500	11,190	8,060	95	85
	4000	5,570	4,080	97	125
W–0.52 Nb	3000	38,210	35,075	80	32.6
	3250	22,640	18,660	63.2	46.9
	3500	13,040	7,710	64.7	55.6
	4000	7,250	4,500	90	81.7
W–5 Mo	3000	30,840	29,850	83	28.7
	3250	14,770	10,200	95	66.3
	3500	10,450	5,630	97.9	89.8
	4000	5,400	3,670	95	116

Table IV-6 3000°F TENSILE PROPERTIES OF TUNGSTEN-TaC ALLOYS*[78]

Composition (balance W), %	Yield strength (0.2% offset), psi	Ultimate tensile strength, psi	Elongation, %	Reduction in area, %
0.1 TaC	6,800	9,200	23	43
0.1 TaC	6,900	8,900	27	41
0.65 TaC	14,000	19,000	21	37
0.65 TaC	12,000	16,000	17	36
1.0 TaC	13,500	22,000	21	37
1.0 TaC	7,600	9,600	16	37
0.38 TaC†	16–26,000	22–32,000	7–33	16–42

* Worked 60 per cent at 1700°C and annealed ½ hr at 1600°C.
† Optimum alloy appears to be at about 0.35 per cent TaC.

Table IV-7 HIGH-TEMPERATURE TENSILE DATA FOR THE TUNGSTEN–0.5 PER CENT HfO_2 ALLOYS[78]

Working temp., °C	Yield stress (0.2% offset), psi	Ultimate tensile strength, psi	Elongation, %	Reduction in area, %	Test temp., °F
1700	9,700	13,800	21	44	2700
1700	14,800	20,000	21	38	3000
1600	8,800	14,800	29	44	2700
1600	7,900	13,100	17	20	3000

Table IV-8 VANADIUM-BASE ALLOYS, TENSILE TEST RESULTS[79]

Composition (balance V), wt.%	Ultimate tensile strength, 1000 psi	Yield strength, 1000 psi	Elongation, %	Ultimate tensile strength, 1000 psi	Yield strength, 1000 psi	Elongation, %
	Room temperature			2200°F		
1.0 Ti–60 Nb	151.0	129.7	23	37.8	32.3	114
0.5 H–60 Nb	149.9	130.1	21	37.9	32.2	65
1.0 H–60 Nb	149.6	131.5	19	44.4	40.6	37
2.0 Hf–60 Nb	146.7	136.2	8	34.4	32.2	41
0.5 Zr–60 Nb	148.0	137.2	11	35.7	32.3	65
2.0 Zr–60 Nb				37.4	34.1	37
1 Ti–60 Nb–3.0 Mo	129		4	37.0	34.2	21
1 Ti–60 Nb–5.0 W	145.5	141.5	6	41.4	35.5	12
1 Ti–60 Nb–0.025 B	135.1	131.1	8	35.6	32.2	33
1 Ti–60 Nb–0.05 B	152.0	141.0	8	35.6	32.6	63
1 Ti–60 Nb–0.025 C	144.3	136.5	8	37.8	35.2	69
1 Ti–60 Nb–0.05 C	161.9	152.0	13	35.2	33.4	55
1 Ti–60 Nb–0.025 B–0.025 C	153.7	147.6	10	35.1	31.3	30
1 Ti–60 Nb–0.05 O	141.0	137.0	6	34.9	30.1	20
1 Ti–60 Nb–0.025 N	146.0	140.0	7	31.0	228.3	26
	Room temperature			1200°F		
20 Ti–10 Cr	97.6	87.9	12	78.4	71.3	15
20 Ti–20 Cr	107.6	96.7	6	86.7	81.7	7

Table IV-9 2000°F STRESS-RUPTURE PROPERTIES OF VANADIUM ALLOYS[79]

Alloy composition (balance V), wt.%	Stress, psi	Hours to failure	Elongation, %
1 Ti–60 Nb	10,000	13.4	36
1 Ti–60 Nb–0.025 C	10,000	25	4
1 Ti–60 Nb–0.05 O	10,000	24	7
1 Ti–60 Nb–3 Mo	10,000	9	*
1 Ti–60 Nb–5 W	10,000	13.4	*
1 Ti–60 Nb–0.025 N	10,000	19.0	6
1 Ti–60 Nb–0.025 B	10,000	16.0	21

* Brittle fracture, no elongation.

Table IV-10 ROOM-TEMPERATURE TENSILE DATA FOR ZIRCONIUM–2 AT.% NIOBIUM–2 AT.% TIN[71]

Condition	Hardness, R_C	Ultimate strength, psi	Elongation to fracture, %
Annealed	74	77,200	21
Annealed	74	80,800	25
Annealed + 25% CW*	88	104,000	9.5
Annealed + 50% CW	90	110,000	12
Annealed + 50% CW		108,000	
Water quenched from 950°C	90	110,000	

* CW = cold worked.

theory proposed by R. Hill, either one of which is suitable to express the flow properties of Zircaloy-2 under various states of combined stress.

Miscellaneous

The literature-searching service of the American Society for Metals[86] has published a list of 1704 references to reports and journal articles on refractory and related materials. The period of literature covered is 1958 to 1960.

(J. A. DeMastry)

Selected Metallurgical Aspects of Cladding and Structural Materials

Physical Properties of Refractory Metals

Oak Ridge reports[87] that at least three and probably four intermetallic compounds exist in the niobium-tin system. Only the Nb_3Sn compound had been previously reported. These compounds (as yet unidentified) were produced

Table IV-11 RESULTS OF TENSILE TESTS[81] AT 300°C ON ZIRCONIUM–2.5 WT.% NIOBIUM WATER QUENCHED FROM 880°C

Additional heat-treatment	Test No.	Prop. limit, psi	Yield strength (0.2% offset), psi	Ultimate tensile strength, psi	Elongation, %
A, none	A1	61.9	70.6	81.7	12.5
	B1	66.3	71.3	80.7	12.5
B, 1500 hr at 300°C (air)	A2	65.4	73.4	86.9	13.5
	B2	67.5	75.2	85.6	12.2
C, 88 hr at 400°C (air)	C1	71.4	78.1	87.8	13.0
	D1	76.9	82.6	90.8	12.7
D, 88 hr at 400°C (vacuum)	C2	74.9	81.6	90.8	14.0
+ 1500 hr at 300°C (air)	D2	74.5	81.1	90.3	12.7
E, 6 hr at 500°C (vacuum)	E2	74.4	80.3	87.2	15.1
	F2	57.2	63.6	73.4	14.5
	5	69.6	75.0	83.4	12
	3*	60.3	67.2	75.0	13
F, 24 hr at 500°C (vacuum)	2*	42.2	49.0	60.8	20.5
	6	74.2	80.7	88.6	14.0
G, 24 hr at 500°C (vacuum)	E1	71.2	76.7	85.6	13.5
+ 1500 hr at 300°C (air)	F1	76.5	82.0	89.0	11.5

* These specimens were given a slightly slower quench.

Table IV-12 MECHANICAL PROPERTIES OF SOME ZIRCONIUM ALLOYS[80]

Alloy composition (balance Zr), wt.%	Condition	Temp., °C	Yield strength (0.2% offset), 1000 psi	Ultimate tensile strength, 1000 psi	Elongation in 1 in., %
3 Al	Annealed at	RT	115.4	139.3	17.5
	785°C for 2 hr	100	99.2	123.4	20.0
		200		110.9	19.0
		300	75.0	100.8	20.5
		400	72.6	97.4	19.5
		500	63.3	85.6	22.0
		700	23.2	33.4	44.0
3 Al–0.5 Mo	Annealed at	RT	118.6	139.5	18.5
	785°C for 2 hr	100	112.2	128.2	20.5
		200	92.8	113.5	21.0
		300	83.1	104.3	21.5
		400		99.4	37.5
		500	67.0	82.4	39.0
		700	19.0	27.7	45.0
3 Al–1.5 Mo	Annealed at	RT	118.9	138.3	19.0
	785°C for 2 hr	100	105.9	122.9	21.0
		200	95.2	113.5	24.5
		300	83.2	107.3	25.0
		400	81.3	102.6	25.5
		500	70.2	82.1	28.0
		600	37.3	54.6	35.0
		700	15.3	24.6	70.0
5 Nb	Annealed at	RT	79.2	95.5	30.0
	785°C for 2 hr	100	69.3	83.4	28.5
		200	47.9	66.0	36.5
		300	37.2	61.0	37.5
		400	33.8	56.8	36.0
		500	27.8	37.3	36.0
		700	4.3	8.3	115.0

Table IV-13 SUMMARIZED RESULTS[82] OF CREEP TESTS ON ZIRCONIUM ALLOYS UNDER 2 TSI AT 500°C

Alloy (balance Zr), wt.%	Heat-treatment, air cooled	Total creep in 1000 hr, %	Final or minimum creep rate, 10^{-4} %/hr
Unalloyed	800°C, ½ hr	1.23 (250 hr)	4.2 (250 hr)
0.5 Al	800°C, ½ hr	0.09	0.05
3 Al	800°C, ½ hr	0.94	7.5
4 Al	750°C, ½ hr	0.38	2.5
4 Al	800°C, ½ hr	0.10	0.7
3 Al–8 Nb	750°C, ½ hr	0.29	1.0
3 Al–8 Nb–0.2 Sn	750°C, ½ hr	0.25	1.5
3 Al–8 Nb–0.2 Sn	800°C, ½ hr	0.27	1.0
3 Al–8 Nb–0.5 Sn	750°C, 2 hr	0.20	1.5
3 Al–8 Nb–0.5 Sn	800°C, 1 hr	0.18	0.9
3 Al–8 Nb–2 Sn	750°C, 2 hr	0.22	1.4
3 Al–8 Nb–2 Sn	800°C, 1 hr	0.19	1.2
4 Al–8 Nb–0.2 Sn	750°C, ½ hr	0.34	2.0
4 Al–8 Nb–0.2 Sn	800°C, ½ hr	0.39	2.5
20 Nb (1½ tsi)	600°C, 1 hr	1.53 (725 hr)	

Table IV-14 CURRENT STATUS OF CREEP TESTS ON ZIRCALOY SHEET[83]

Specimen	Temp., °F	Stress, psi	Time in progress,* hr	Deformation, %		Tentative minimum creep rate, %/hr
				On loading	At present	
15 Per Cent Cold-Worked Material						
7-2-1	650	25,000	33,500	0.230	1.795	0.00003
7-4-3	750	12,500	31,000	0.134	2.465	0.00006
Annealed Material						
Zr-A-10	550	22,500	21,500	3.180	4.348	0.000004
Zr-A-13	550	20,000	19,000	1.511	2.852	0.000002
Zr-A-14	550	17,500	19,000	1.250	1.961	<0.000001
Zr-A-15	650	20,000	19,000	2.240	22.78	0.00010
Zr-A-17	650	17,500	19,500	1.778	3.018	0.000065
Zr-A-25	650	15,000	17,500	0.971	1.455	0.000030
Zr-A-28	650	12,500	14,500	0.321	0.473	0.000005
Zr-A-16	750	12,500	19,000	0.447	5.955	0.00025
Zr-A-21	750	10,000	18,000	0.113	2.190	0.00008
Zr-A-26	750	9,000	16,000	0.082	0.687	0.00002
Annealed Material, Temperature and Stress Cycled						
Zr-A-36	550	15,000	8,500	0.765	1.154	0.000005
Zr-A-31	550	12,500	11,500	0.170	0.535	0.000005
Zr-A-34	650	15,000	9,000	0.949	1.279	0.000020
Zr-A-32	650	12,500	11,500	0.265	0.650	0.000015
Zr-A-35	650	9,000	8,500	0.063	0.113	0.000005
Annealed PRTR Zircaloy-2 Pressure Tubing						
11-A-5-1	550	20,000	5,000	0.444	0.631	0.000007
11-A-5-3	550	15,000	3,000	0.187	0.304	0.000005
11-A-5-4	550	12,500	4,000	0.129	0.195	Nil

* Less than actual test time but within 500 hr.

Table IV-15 TENSILE PROPERTIES OF ZIRCONIUM-BASE ALLOYS[84]

Alloy composition (balance Zr), wt.%	Room temperature*			600°C†		
	Yield strength, psi	Ultimate tensile strength, psi	Elongation, %	Yield strength, psi	Ultimate tensile strength, psi	Elongation, %
3 Mo–2 Al	147,500	178,500	10.8	43,600	57,500	33.3
5 Mo–2 Al	145,000	160,000	4.2	48,200	68,300	34.4
7 Mo–2 Al	136,200	147,700	8.7	45,900	76,000	36.2
1 Mo–5 Al	144,000	162,000	12.9	46,000	75,600	29.0
3 Mo–5 Al	191,500	218,500	‡	42,500	65,500	45.0
7 Sn–1.5 Al	129,800	143,800	2.6	51,500	65,500	15.2
7 Sn–2.5 Al	163,000	176,000	3.9	47,400	75,000	16.6

* As extruded.
† Solutionized and aged at 600°C for 1000 hr prior to tests made in air.
‡ Very low elongation.

by annealing niobium wire which contained a mixture of niobium and tin, for 18 hr at 1000°C.

Physical properties of niobium–1 wt.% zirconium alloys from room temperature to 2000°F, as determined by Pratt & Whitney,[88] are shown in Fig. IV-3.

Liquid-phase sintering techniques have been employed by Armour[28] to prepare tungsten-base alloys. Efforts to improve the long-time elevated-temperature strength properties by the addition of finely dispersed oxides to the matrix were unsuccessful because of agglomeration of the oxide particles during sintering. Cold working of the oxide-containing composites did not break up the agglomerates to produce dispersion strengthening at 1600°F.

(J. A. DeMastry)

Physical Properties of Stainless Steel

The physical properties of type 316 stainless steel from room temperature to 1800°F have been summarized by Pratt & Whitney.[88] These are shown graphically in Fig. IV-4.

(J. A. DeMastry)

Physical Metallurgy of Zirconium Alloys

Ultrafine grains of Zircaloy-2 with an average diameter of about 6 μ have been produced by Hanford[89] by annealing in a salt bath for 16 min at 1100°F. They concluded that average grain diameters of 6 μ or smaller can be produced with the following conditions:

1. A highly cold-worked structure, such as that provided by warm extruding twice (10 : 1 extrusion ratio) with an intermediate low-temperature anneal

2. A short annealing time at a low annealing temperature, such as 16 min at 1100°F

3. A rapid heating to the annealing temperature, similar to that afforded by the salt bath

Fisher and Renken[90] have determined the adiabatic elastic moduli of single-crystal alpha zirconium. These values for alpha zirconium at 20°C were derived from measurements of the velocities of ultrasonic waves using the phase-comparison technique of McSkimin. The values computed for a density of 6.505 g/cm^3 are as follows, in units of 10^{12} dynes/cm^2:

$$C_{11} = 1.435 \pm 0.002$$
$$C_{12} = 0.725 \pm 0.002$$
$$C_{13} = 0.654 \pm 0.002$$
$$C_{33} = 1.649 \pm 0.002$$
$$C_{44} = 0.3207 \pm 0.003$$

The temperature dependence of the resistivity of zirconium-oxygen solid solutions has been investigated by German researchers.[91] Measurements were made on specimens, in the form of wires, which had been loaded with oxygen at a pressure of 1.5×10^{-3} mm Hg and at temperatures in the range 1600 to 2030°K. Specimens thus prepared were then investigated between room temperature and 2030°K throughout the stability range of the metallic solid solution (0 to about 30 at.% oxygen). It was found that the resistivity of the oxygen-bearing beta-zirconium phase has a normal temperature dependence and that Matthiessen's rule is obeyed by this phase. However, the more highly oxygenated alpha-zirconium solid solution showed an unexpected temperature dependence of resistivity, and Matthiessen's rule was not obeyed.

Table IV-16 AGING DATA FOR SOLUTION-TREATED* ALLOYS[84]

Aging time† at 600°C, hr	Yield strength, psi	Ultimate tensile strength, psi (RT)	Elongation, %
	Zr–7 Sn–2.5 Al		
0	141,000	158,700	1.9
1	148,000	165,000	0.2
3	145,000	163,000	‡
10	148,000	162,000	‡
30	157,000	167,000	‡
100	159,400	173,000	‡
300	162,000	176,000	‡
1000	164,000	175,000	‡
	Zr–7 Sn–1.5 Al		
0	106,000	131,000	5.5
1	110,500	133,000	5.5
3	113,000	139,000	4.4
10	118,500	137,000	3.1
30	115,500	139,000	0.8
100	119,000	132,000	‡
300	123,500	135,700	‡
1000	124,000	130,000	‡
	Zr–3 Mo–2 Al		
0	107,000	141,500	16.8
1	130,000	143,500	14.6
3	129,000	146,500	16.7
10	127,000	143,300	13.4
30	125,000	142,500	10.2
100	112,500	136,500	4.0
300	110,000	132,500	7.0
1000	94,500	120,500	6.0

* Solution treated 50°C above alpha-to-beta transformation.
† Temperature for 2 hr and water quench.
‡ Not measurable.

It was found that dissolved oxygen reduces the slope of the resistivity-temperature curves and that a negative temperature coefficient arises above a definite critical temperature. This critical temperature is a function of oxygen content; for alpha zirconium containing, for instance, 18 at.% oxygen, it is about 550°K.

The constitution of the zirconium-ZrO_2 system has been established by means of metallographic investigations of resistivity measurements by the same German authors[92] as mentioned above. Wires of reactor-grade zirconium were isothermally and isobarically loaded with oxygen at a pressure of 1.5×10^{-3} mm Hg and at temperatures in the range of 1600 to 2030°K. Under these conditions a uniform oxygen concentration existed throughout the wire cross section at all stages of oxygen loading. According to the present investigation, the phase diagram differs in some particulars from earlier diagrams. These deviations refer to the solubility of oxygen in alpha zirconium, the delineation of the two-phase regions between alpha and beta zirconium, and the solubility of zirconium in ZrO_2. The form of the solubility limit of zirconium in ZrO_2 suggests the existence of a high-temperature form of ZrO_2, stable above 1850°K. This high-temperature form could not be retained by quenching and was therefore not investigated further.

(J. A. DeMastry)

Miscellaneous

A report has been prepared by the Defense Metals Information Center[93] which provides a wide background of data for the nonspecialist and is a general review of the field of high-temperature metals. The general categories of metals suitable for application at temperatures in excess of 800°F are discussed along with the general advantages and limitations of each. Some generalized mechanical- and physical-property data are included.

(J. A. DeMastry)

Diffusion Studies

Two surveys on certain aspects of diffusion have been issued. In a compilation by Knolls,[94] data are included for the self-diffusion of zirconium, niobium, tin, and uranium; for the diffusion of various interstitials and alloying elements in zirconium and in niobium; and for intermediate layer growth in various uranium systems. A comprehensive and well-indexed survey and bibliography on self-diffusion of pure metals in the solid state has been issued by Los Alamos.[95] Included are 367 references to open literature and unclassified reports published from 1950 to 1960. Temperature-dependence equations for self-diffusion coefficients, their method of measurement, the temperature range of study, and a classification of experimental methods are presented in the report. Indexes by metal and by author to the original experimental articles are provided.

A Canadian paper[96] gives the self-diffusion coefficients of crystal-bar zirconium measured between 1100 and 1500°C, using radioactive Zr^{95} as a tracer. This research was conducted at Chalk River and was reviewed here over a year ago while in progress; additional experi-

ments and a slight revision of the Arrhenius equation have been made since then. The final results, which are for the self-diffusion of beta zirconium (1100 to 1500°C), are represented by the equation

$$D = 2.4 \times 10^{-4} \exp(-30{,}100/RT) \text{ cm}^2/\text{sec}$$

This equation gives values that fall within the wide range of results which have been published by others.

A fundamental investigation is being conducted on thermal diffusion at Atomics International.[43] Studies on copper and gold have demonstrated that vacancies migrate in a preferred direction in a temperature gradient. Since the data indicate that the direction is opposite in gold and copper, the existing theory predicts that the ratio of the migration and formation energies is greater than 1 in copper and less than 1 in gold. This relation is consistent with previously determined values of these energies from other types of experiments.

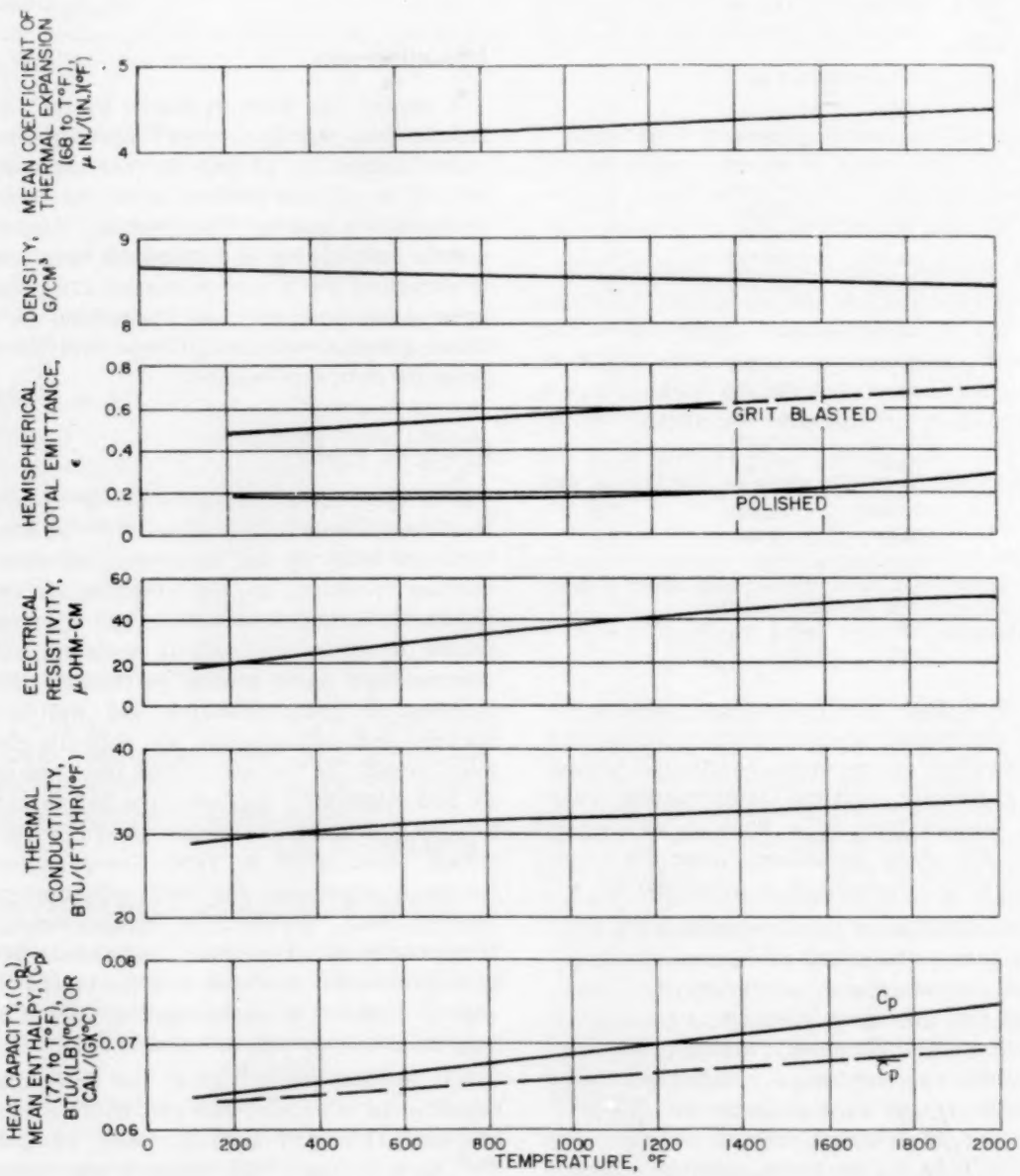

Fig. IV-3 Physical properties of niobium–1 wt.% zirconium alloy.[88]

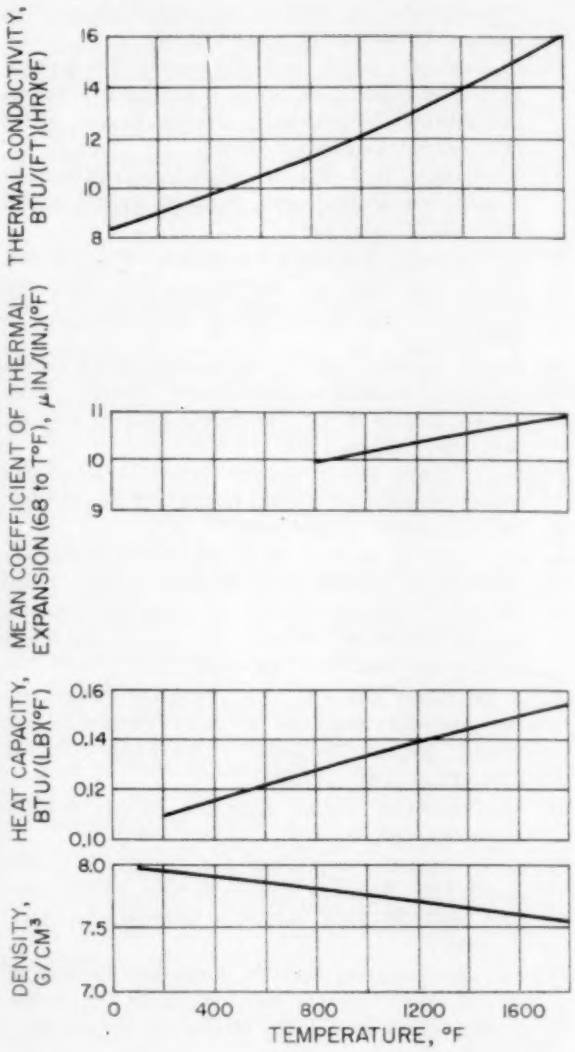

Fig. IV-4 Physical properties of type 316 stainless steel.[88]

An investigation of diffusion barriers for refractory metals, which was reviewed previously, has been continued at Manufacturing Laboratories[97] by conducting screening tests at 1700°C. Comparison of the interdiffusion behavior of a niobium-rhenium couple with that of combinations of rhenium barriers and niobium-base alloys showed no significant change due to alloying of the niobium. On the other hand, the presence of the titanium in a molybdenum–0.5 wt.% titanium alloy apparently resulted in a decrease in the extent of interdiffusion with rhenium, as compared to unalloyed molybdenum. It is also reported that comparison of the extent of interdiffusion in five combinations of barrier metals with the coating metal, chromium, showed that the rhenium-chromium combination exhibited the least interdiffusion. Interdiffusion studies in the three-layer combinations of molybdenum-rhenium-chromium and molybdenum-iridium-chromium indicated that the presence of a barrier can reduce the extent of interdiffusion between molybdenum and the chromium coating by up to 75 per cent.

Diffusion coefficients for the diffusion of niobium in reactor-grade, hafnium-free iodide zirconium were determined at Oak Ridge[87] in the temperature range 900 to 1500°C, in which the body-centered cubic beta phase of zirconium is stable. A radiotracer technique was employed, utilizing Nb^{95}. The temperature dependence of diffusion of niobium in zirconium in this temperature range was determined to be represented by the equation

$$D = 2.06 \times 10^{-4} \exp(-32{,}700/RT) \text{ cm}^2/\text{sec}$$

(D. C. Carmichael)

References

1. J. N. Wanklyn et al., Corrosion of Zirconium and Its Alloys in High Temperature Steam. Part II. The Uptake of Hydrogen During Corrosion, British Report AERE-R-3768, July 1961.
2. Nuclear Metals, Inc., Fundamental and Applied Research and Development in Metallurgy, Research on the Mechanism of Zirconium Alloy Corrosion in High-Temperature Steam. Summary Technical Report to USAEC for the Period July 1, 1960, Through June 30, 1961, USAEC Report NMI-1251, Oct. 6, 1961.
3. B. Griggs et al., Multiple Rate Transitions in the Aqueous Corrosion of Zircaloy, USAEC Report HW-67818(Rev.), Hanford Atomic Products Operation, December 1960.
4. J. C. Griess et al., Effect of Heat Flux on the Corrosion of Aluminum by Water. Part III. Final Report on Tests Relative to the High-Flux Isotope Reactor, USAEC Report ORNL-3230, Oak Ridge National Laboratory, Dec. 20, 1961.
5. H. C. Bowen, Development of Corrosion-Resistant Aluminum Alloys for High-Temperature Water Service, USAEC Report HW-68253, Hanford Atomic Products Operation, March 1961.
6. N. R. Grant, Summary of Corrosion Investigations of High-Temperature Aluminum Alloys, October 1957–December 1959, USAEC Report ANL-6204, Argonne National Laboratory, September 1961.
7. Naval Research Laboratory, NRL Quarterly on Nuclear Science and Technology, Progress Re-

ments and a slight revision of the Arrhenius equation have been made since then. The final results, which are for the self-diffusion of beta zirconium (1100 to 1500°C), are represented by the equation

$$D = 2.4 \times 10^{-4} \exp(-30{,}100/RT) \text{ cm}^2/\text{sec}$$

This equation gives values that fall within the wide range of results which have been published by others.

A fundamental investigation is being conducted on thermal diffusion at Atomics International.[43] Studies on copper and gold have demonstrated that vacancies migrate in a preferred direction in a temperature gradient. Since the data indicate that the direction is opposite in gold and copper, the existing theory predicts that the ratio of the migration and formation energies is greater than 1 in copper and less than 1 in gold. This relation is consistent with previously determined values of these energies from other types of experiments.

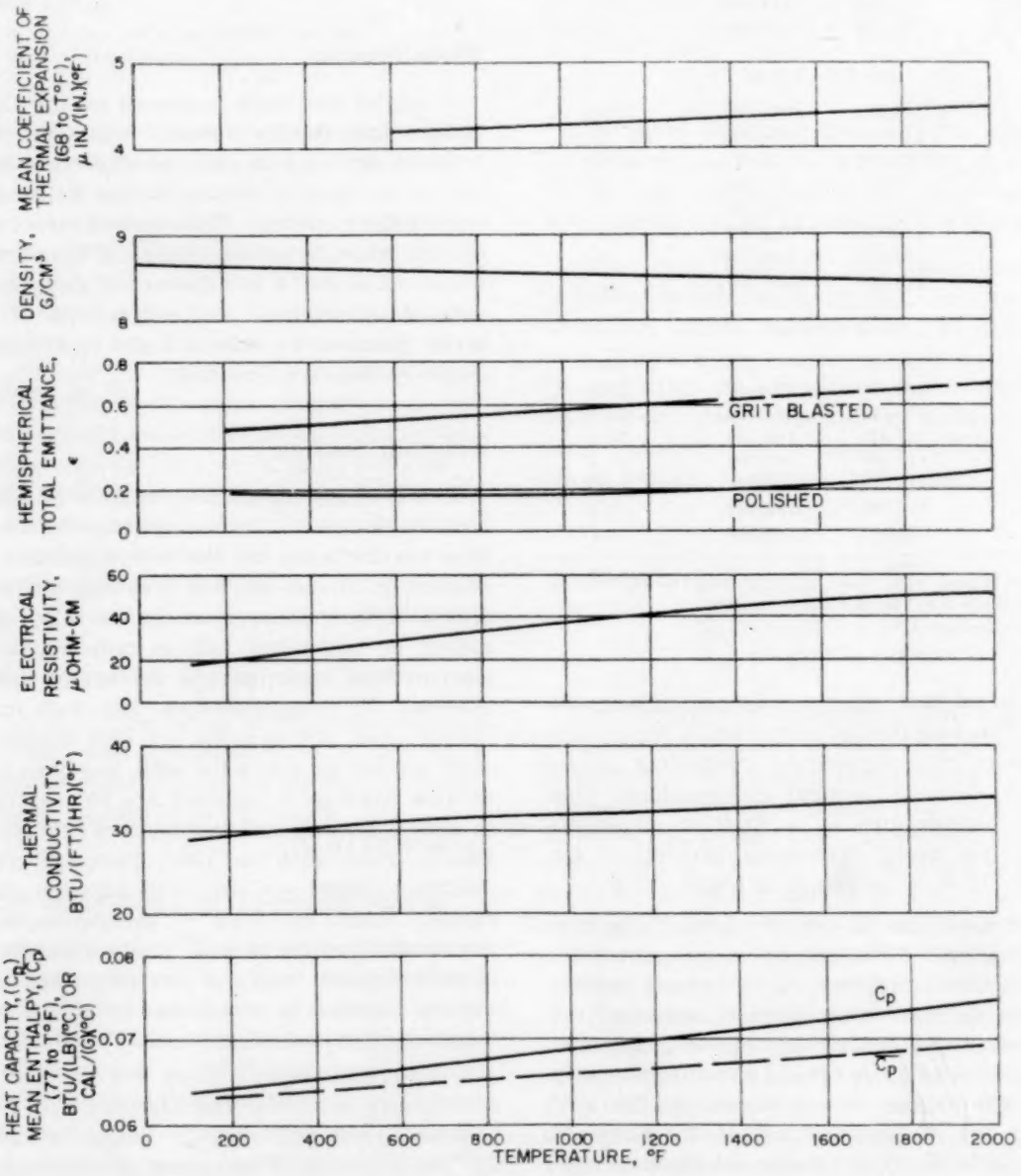

Fig. IV.3 Physical properties of niobium–1 wt.% zirconium alloy.[88]

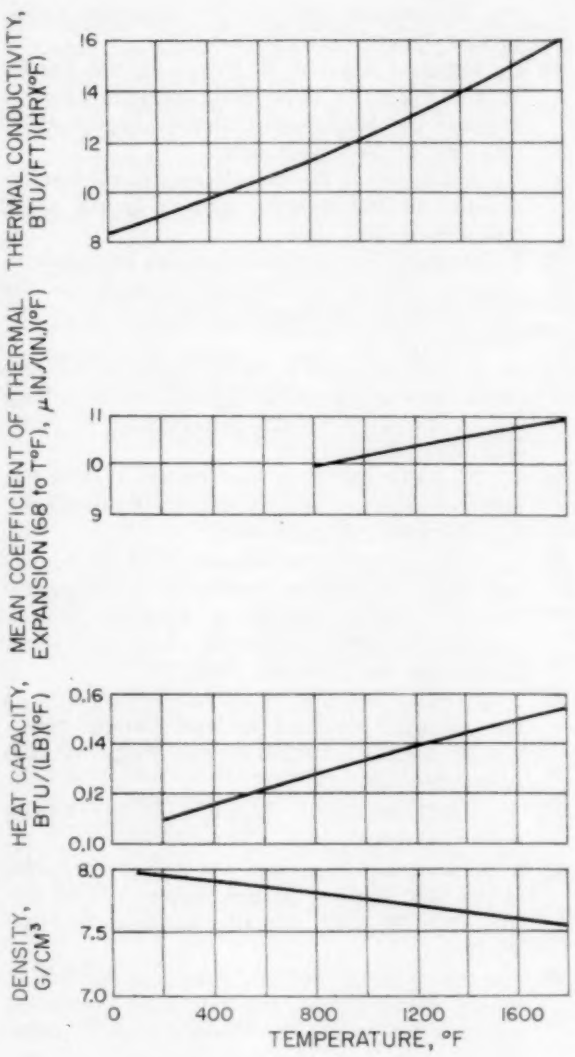

Fig. IV-4 Physical properties of type 316 stainless steel.[88]

An investigation of diffusion barriers for refractory metals, which was reviewed previously, has been continued at Manufacturing Laboratories[97] by conducting screening tests at 1700°C. Comparison of the interdiffusion behavior of a niobium-rhenium couple with that of combinations of rhenium barriers and niobium-base alloys showed no significant change due to alloying of the niobium. On the other hand, the presence of the titanium in a molybdenum–0.5 wt.% titanium alloy apparently resulted in a decrease in the extent of interdiffusion with rhenium, as compared to unalloyed molybdenum. It is also reported that comparison of the extent of interdiffusion in five combinations of barrier metals with the coating metal, chromium, showed that the rhenium-chromium combination exhibited the least interdiffusion. Interdiffusion studies in the three-layer combinations of molybdenum-rhenium-chromium and molybdenum-iridium-chromium indicated that the presence of a barrier can reduce the extent of interdiffusion between molybdenum and the chromium coating by up to 75 per cent.

Diffusion coefficients for the diffusion of niobium in reactor-grade, hafnium-free iodide zirconium were determined at Oak Ridge[87] in the temperature range 900 to 1500°C, in which the body-centered cubic beta phase of zirconium is stable. A radiotracer technique was employed, utilizing Nb^{95}. The temperature dependence of diffusion of niobium in zirconium in this temperature range was determined to be represented by the equation

$$D = 2.06 \times 10^{-4} \exp(-32{,}700/RT) \text{ cm}^2/\text{sec}$$

(D. C. Carmichael)

References

1. J. N. Wanklyn et al., Corrosion of Zirconium and Its Alloys in High Temperature Steam. Part II. The Uptake of Hydrogen During Corrosion, British Report AERE-R-3768, July 1961.
2. Nuclear Metals, Inc., Fundamental and Applied Research and Development in Metallurgy, Research on the Mechanism of Zirconium Alloy Corrosion in High-Temperature Steam. Summary Technical Report to USAEC for the Period July 1, 1960, Through June 30, 1961, USAEC Report NMI-1251, Oct. 6, 1961.
3. B. Griggs et al., Multiple Rate Transitions in the Aqueous Corrosion of Zircaloy, USAEC Report HW-67818(Rev.), Hanford Atomic Products Operation, December 1960.
4. J. C. Griess et al., Effect of Heat Flux on the Corrosion of Aluminum by Water. Part III. Final Report on Tests Relative to the High-Flux Isotope Reactor, USAEC Report ORNL-3230, Oak Ridge National Laboratory, Dec. 20, 1961.
5. H. C. Bowen, Development of Corrosion-Resistant Aluminum Alloys for High-Temperature Water Service, USAEC Report HW-68253, Hanford Atomic Products Operation, March 1961.
6. N. R. Grant, Summary of Corrosion Investigations of High-Temperature Aluminum Alloys, October 1957–December 1959, USAEC Report ANL-6204, Argonne National Laboratory, September 1961.
7. Naval Research Laboratory, NRL Quarterly on Nuclear Science and Technology, Progress Re-

ments and a slight revision of the Arrhenius equation have been made since then. The final results, which are for the self-diffusion of beta zirconium (1100 to 1500°C), are represented by the equation

$$D = 2.4 \times 10^{-4} \exp(-30{,}100/RT) \text{ cm}^2/\text{sec}$$

This equation gives values that fall within the wide range of results which have been published by others.

A fundamental investigation is being conducted on thermal diffusion at Atomics International.[43] Studies on copper and gold have demonstrated that vacancies migrate in a preferred direction in a temperature gradient. Since the data indicate that the direction is opposite in gold and copper, the existing theory predicts that the ratio of the migration and formation energies is greater than 1 in copper and less than 1 in gold. This relation is consistent with previously determined values of these energies from other types of experiments.

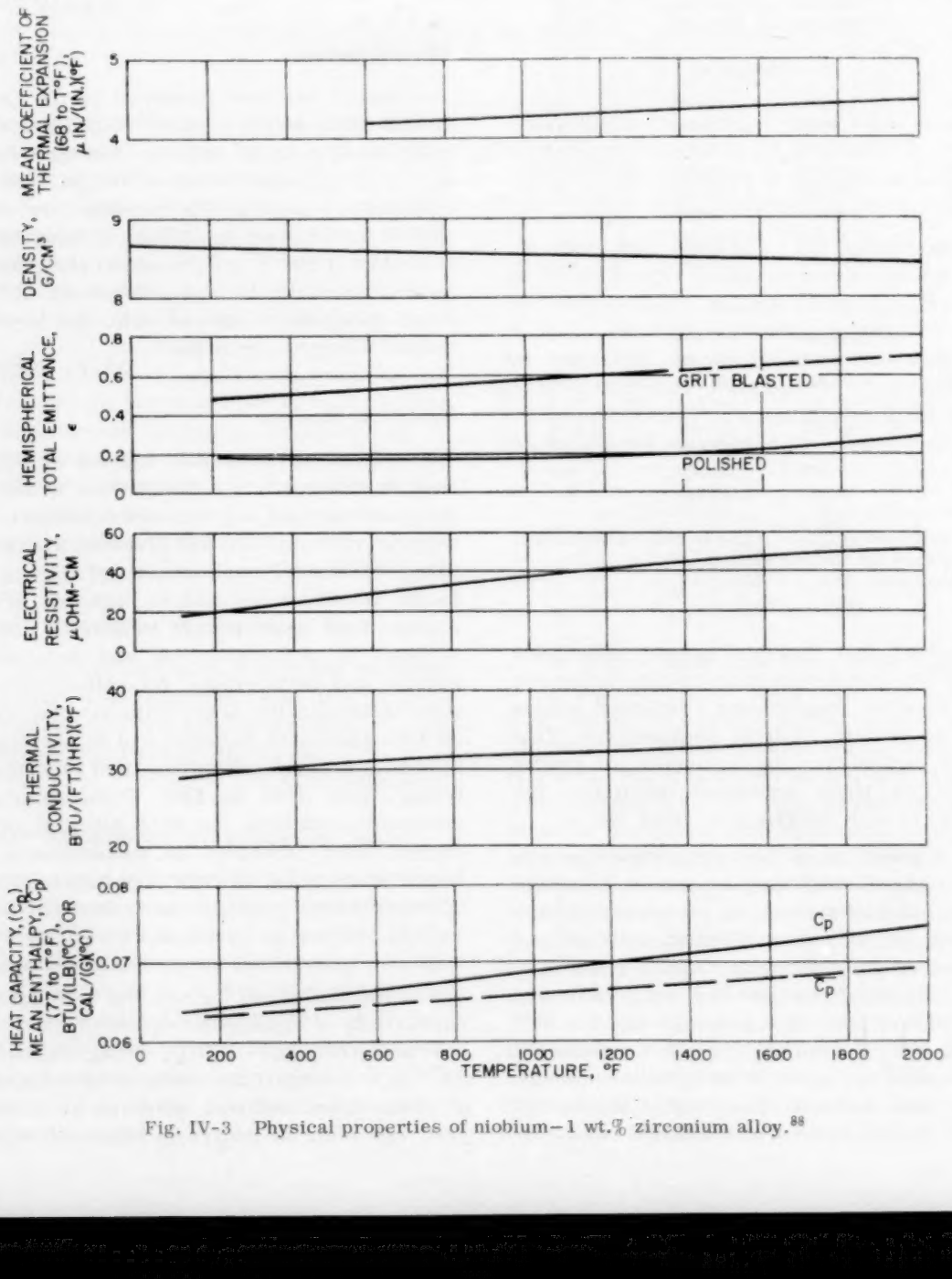

Fig. IV-3 Physical properties of niobium–1 wt.% zirconium alloy.[88]

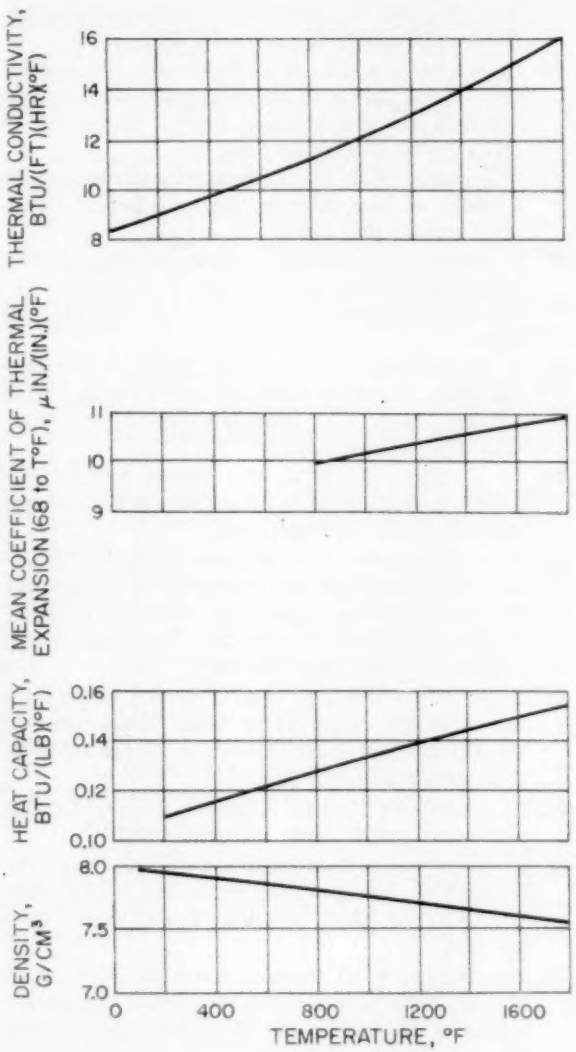

Fig. IV-4 Physical properties of type 316 stainless steel.[88]

An investigation of diffusion barriers for refractory metals, which was reviewed previously, has been continued at Manufacturing Laboratories[97] by conducting screening tests at 1700°C. Comparison of the interdiffusion behavior of a niobium-rhenium couple with that of combinations of rhenium barriers and niobium-base alloys showed no significant change due to alloying of the niobium. On the other hand, the presence of the titanium in a molybdenum–0.5 wt.% titanium alloy apparently resulted in a decrease in the extent of interdiffusion with rhenium, as compared to unalloyed molybdenum. It is also reported that comparison of the extent of interdiffusion in five combinations of barrier metals with the coating metal, chromium, showed that the rhenium-chromium combination exhibited the least interdiffusion. Interdiffusion studies in the three-layer combinations of molybdenum-rhenium-chromium and molybdenum-iridium-chromium indicated that the presence of a barrier can reduce the extent of interdiffusion between molybdenum and the chromium coating by up to 75 per cent.

Diffusion coefficients for the diffusion of niobium in reactor-grade, hafnium-free iodide zirconium were determined at Oak Ridge[87] in the temperature range 900 to 1500°C, in which the body-centered cubic beta phase of zirconium is stable. A radiotracer technique was employed, utilizing Nb^{95}. The temperature dependence of diffusion of niobium in zirconium in this temperature range was determined to be represented by the equation

$$D = 2.06 \times 10^{-4} \exp(-32{,}700/RT) \text{ cm}^2/\text{sec}$$

(D. C. Carmichael)

References

1. J. N. Wanklyn et al., Corrosion of Zirconium and Its Alloys in High Temperature Steam. Part II. The Uptake of Hydrogen During Corrosion, British Report AERE-R-3768, July 1961.
2. Nuclear Metals, Inc., Fundamental and Applied Research and Development in Metallurgy, Research on the Mechanism of Zirconium Alloy Corrosion in High-Temperature Steam. Summary Technical Report to USAEC for the Period July 1, 1960, Through June 30, 1961, USAEC Report NMI-1251, Oct. 6, 1961.
3. B. Griggs et al., Multiple Rate Transitions in the Aqueous Corrosion of Zircaloy, USAEC Report HW-67818(Rev.), Hanford Atomic Products Operation, December 1960.
4. J. C. Griess et al., Effect of Heat Flux on the Corrosion of Aluminum by Water. Part III. Final Report on Tests Relative to the High-Flux Isotope Reactor, USAEC Report ORNL-3230, Oak Ridge National Laboratory, Dec. 20, 1961.
5. H. C. Bowen, Development of Corrosion-Resistant Aluminum Alloys for High-Temperature Water Service, USAEC Report HW-68253, Hanford Atomic Products Operation, March 1961.
6. N. R. Grant, Summary of Corrosion Investigations of High-Temperature Aluminum Alloys, October 1957–December 1959, USAEC Report ANL-6204, Argonne National Laboratory, September 1961.
7. Naval Research Laboratory, NRL Quarterly on Nuclear Science and Technology, Progress Re-

port, July–September, Report NP-11098, Oct. 1, 1961.

8. R. F. S. Robertson, Chalk River Experience in "Crud" Deposition Problem, Canadian Report RLI-5(Rev.)(AECL-1328), Aug. 15, 1961.
9. P. E. Brown (Ed.), Carbon Steel for Water-Cooled Nuclear Reactors, USAEC Report WAPD-257, Westinghouse Electric Corp., Bettis Atomic Power Laboratory, September 1961. (Classified)
10. I. L. Rosenfel'd and V. B. Maksimchuk, Passivity of Corrosion-Resistant Alloys in Solutions of Chlorides, *Zhur. Fiz. Khim.*, 35: 1832–1838 (August 1961).
11. Alco Products, Inc., Evaluation of Kanigen, Electroless Nickel Plating for Steam Side of a Sodium Component Steam Generator, USAEC Report APAE-82, Feb. 15, 1961.
12. L. E. Phillips and F. J. Vawter, Suitability of Inconel for Corrosion Protection on Water Side of Sodium Component Steam Generator, USAEC Report APAE-83, Alco Products, Inc., Mar. 1, 1961.
13. AERE Research Group, Harwell, England, April 1961. (Unpublished)
14. General Electric Co., Flight Propulsion Laboratory Dept., High Temperature Materials Program, Progress Report No. 5, Part A, USAEC Report GEMP-5A, Nov. 15, 1961.
15. Oak Ridge National Laboratory, Aircraft Nuclear Propulsion Program Progress Report for Period of May 1, 1961 to June 30, 1961, USAEC Report ORNL-3226, Dec. 13, 1961. (Classified)
16. D. L. Douglass, General Electric Co., Vallecitos Atomic Laboratory, private communication, January 1960.
17. T. Hurlen et al., Oxidation of Niobium, Technical (Scientific) Note No. 1, Norwegian Report NP-7850, April 1959.
18. E. A. Gulbransen and K. F. Andrew, Oxidation of Niobium Between 375 and 700°C, *J. Electrochem. Soc.*, 105(1): 9 (January 1958).
19. B. F. Brown et al., Protection of Refractory Metals for High Temperature Service, Report NRL-5643, Naval Research Laboratory, May 5, 1961.
20. F. C. Holtz et al., High Temperature Oxidation Protective Coatings for Vanadium-Base Alloys, Report ARF-2227-1, Armour Research Foundation, Illinois Institute of Technology, Sept. 8, 1961.
21. J. J. Rausch and C. R. Simcoe, Low-Temperature Disintegration of Intermetallic Compounds, Report ARF-2981-4, Armour Research Foundation, Illinois Institute of Technology, Aug. 31, 1961.
22. R. A. Jeffreys and J. D. Gadd, Protective Coatings for Columbium, paper presented at Aerospace Materials and Process Engineers Meeting, Dayton, Nov. 14–15, 1961.
23. W. L. Aves et al., Diffusion Coating Process for Columbium-Base Alloys, Progress Report for Feb. 15–May 15, 1961, Vought Astronautics Div., Chance-Vought Corp., August 1961.
24. C. Williams and R. A. F. Hammond, The Resistance to Oxidation of Nickel-Chromium Electrodeposits on Molybdenum, British Report ARDE (MX)-89/60, December 1960.
25. Chromalloy W-2, The Investigation of a Protective Coating on Molybdenum, British Report ARDE (MX)-23/61, May 1961.
26. R. Wachtell, Protective Coatings for Molybdenum, paper presented at Aerospace Materials and Process Engineers Meeting, Dayton, Nov. 14–15, 1961.
27. D. D. Lawthers and L. Sama, High Temperature Oxidation Resistant Coatings for Tantalum Base Alloys, Report SCNC-326, Sylvania Electric Products, Inc., August 1961.
28. F. C. Holtz and R. J. Van Thyne, Armour Research Foundation, Illinois Institute of Technology, June 13, 1961. (Unpublished)
29. H. J. Nolting and R. H. Burgess, Oxidation Resistant High-Temperature Protective Coatings for Tungsten, Second Quarterly Progress Report, Report NP-11069, TAPCO Div., Thompson Ramo Wooldridge, Inc., Nov. 15, 1961.
30. J. M. Baker and S. E. Bolt, Titanium Pump Loop for Aqueous Solutions at High Temperatures, USAEC Report ORNL-3187, Oak Ridge National Laboratory, Dec. 13, 1961.
31. A. Thurlbeck, United Kingdom Atomic Energy Authority, Oct. 6, 1960. (Unpublished)
32. H. E. Johnson, Corrosion and Activity Transfer in the SRE Primary Sodium System, USAEC Report NAA-SR-5363, Atomics International, Oct. 30, 1961.
33. The Metallurgical Society, American Institute of Mining, Metallurgical, and Petroleum Engineers, A Symposium on Metallic Moderator and Cladding Materials, *Nuclear Metallurgy (Volume VII), Special Report Series No. 10*, 1960.
34. Brookhaven National Laboratory, Annual Report, July 1, 1961, USAEC Report BNL-682, November 1961.
35. Los Alamos Scientific Laboratory, Quarterly Status Report on LAMPRE Program for Period Ending August 20, 1961, USAEC Report LAMS-2620, Sept. 29, 1961.
36. C. C. Burwell et al., Corrosion Testing of LAMPRE-I Fuel, *Trans. Am. Nuclear Soc.*, 4(2): (November 1961).
37. Los Alamos Scientific Laboratory, Quarterly Status Report on LAMPRE Program for Period Ending November 20, 1961, USAEC Report LAMS-2647, Dec. 27, 1961.
38. M. T. Simnad (Ed.), Proceedings of the 10th Annual AEC Corrosion Symposium, Held at San Diego, California, May 9 Through 11, 1961.
39. Argonne National Laboratory, Reactor Development Program Progress Report for October 1961, USAEC Report ANL-6454, Nov. 15, 1961.

40. Argonne National Laboratory, Reactor Development Program Progress Report for November 1961, USAEC Report ANL-6473, Dec. 15, 1961.
41. P. G. Lucasson and R. M. Walker, Research Directed Toward the Study of the Radiation Damage Thresholds of the Elements, Scientific Report No. 4, Report 61-GC-166, General Electric Co., Research Laboratory, April 1961.
42. J. B. Gibson et al., Dynamics of Radiation Damage, *Phys. Rev.*, 120: 1229 (1960).
43. Atomics International, Annual Technical Progress Report, AEC Unclassified Programs, USAEC Report NAA-SR-6370, Aug. 15, 1961.
44. R. L. Hines, Radiation Effect of Positive Ion Bombardment. Progress Report, June 15 to Sept. 15, 1961, USAEC Report TID-14041, Northwestern University.
45. Sh. Sh. Ibragimov and A. N. Voreb'ev, Radiation-Induced Hardening of Molybdenum, *At. Energ.*, 11: 65–66 (July 1961).
46. W. R. Thomas and J. L. Whitton, The Behavior of Dislocations in Neutron Irradiated Aluminum, *Acta Met.*, 9: 1075–1076 (December 1961).
47. M. J. Makin et al., The Formation of Dislocation Loops in Copper During Neutron Irradiation, British Report AERE-R-3770, July 1961.
48. M. J. Makin et al., Dislocation Loops and Hardening in Neutron Irradiated Copper, *Phil. Mag.*, [8] 6(63): 465–468 (March 1961); see also British Report AERE-R-3523.
49. A. L. Bement, Some Effects of Neutron Radiation on the Mechanical Properties and Structural Characteristics of High-Purity Iron, USAEC Report HW-66425, Hanford Atomic Products Operation, Sept. 1, 1960.
50. A. N. Ivanov and N. F. Pravdyuk, Influence of Neutron Irradiation on the Electrical Resistance of Certain Metals, Russian Translation SCL-T-371, by Sandia Corp., 1960.
51. Sh. Sh. Ibragimov et al., Investigation of the Influence of Fast Neutrons on the Characteristic Temperature of Iron and Steel, *Fiz. Metal. Metalloved. Akad. Nauk S.S.S.R.*, 10(2): 166–167, 316–317 (1960).
52. R. M. Walker, Electron Induced Radiation Damage in Pure Metals, Report 60-GC-150, General Electric Co., Research Laboratory, Nov. 29, 1960.
53. D. W. Pashley and A. E. B. Presland, Ion Damage to Metal Films Inside an Electron Microscope, *Phil. Mag.*, [8] 6(68): 1003–1012 (August 1961).
54. P. B. Price, Direct Observations of Ion Damage in Cadmium, *Phys. Rev. Letters*, 6(11): 615–617 (June 1961).
55. D. G. Martin, The Influence of Impurity Atoms on the Annealing Kinetics of Neutron Irradiated Copper, British Report AERE-R-3843, October 1961.
56. Oak Ridge National Laboratory, Nov. 7, 1961. (Unpublished)
57. E. Kubo and Y. Katano, Observations of Dislocation Network in Neutron-Irradiated LiF Crystal, *J. Phys. Soc. Japan*, 16: 347–348 (February 1961).
58. B. Ya. Yurkov, The Range-Energy Relationship for Atoms in Crystalline Silicon Knocked Out into Interstitial Sites by Electron Bombardment, *Fiz. Tverd. Tela* [U.S.S.R. Sbornik (Suppl.)] II: 63–69 (1959).
59. K. H. Bennemann, Stable Atomic Configurations for an Interstitial in Copper, *Phys. Rev.*, 124(3): 669–670 (Nov. 1, 1961).
60. K. H. Bennemann, Theoretical untersuchungen uber die Lage des Zwischengitteratoms in Kupfer, *Z. Physik.*, 165: 445–463 (Nov. 21, 1961).
61. E. M. Baroody, Focusing Collisions in a Linear Chain of Atoms, *Phys. Rev.*, 124(3): 745–747 (Nov. 1, 1961).
62. J. H. O. Varley, The Agglomeration into Clusters of Interstitial Atoms and Vacancies Generated by Fast Neutron Irradiation, British Report AERE-R-3786, July 1961.
63. A. Corciovei and D. Grecu, The Creation of Multiple Thermal Points by Radiation, *Compt. rend.*, 252: 3964–3966 (June 19, 1961).
64. R. O. Hatcher and G. J. Dienes, Relaxation and Activation Energies for an Interstitial Neutral Defect in an Alkali Halide Lattice, *Phys. Rev.*, 124(3): 726–735 (Nov. 1, 1961).
65. Oak Ridge National Laboratory, Solid State Division Annual Progress Report for Period Ending August 31, 1961, USAEC Report ORNL-3213, Dec. 29, 1961.
66. R. S. Barnes, Radiation Effects in Cladding Materials, in *Fuel Element Fabrication with Special Emphasis on Cladding Materials*, Vol. 2, pp. 93–104, Academic Press, London and New York, 1961.
67. Battelle Memorial Institute, Radiation Effects Information Center, Radiation Effects State of the Art, 1960–1961, Report REIC-22, June 30, 1961.
68. F. R. Shober, The Effect of Nuclear Radiation on Structural Metals, Report REIC-20, Battelle Memorial Institute, Radiation Effects Information Center, Sept. 15, 1961.
69. J. Howie, Radiation Damage in Ceramics, *Nuclear Eng.*, 6: 299–303 (July 1961).
70. Hanford Atomic Products Operation, Fuels Development Operation Quarterly Progress Report, July, August, September 1961, USAEC Report HW-71422, Oct. 13, 1961. (Classified)
71. Hanford Atomic Products Operation, Fuels Development Operation Quarterly Progress Report, April, May, June 1960, USAEC Report HW-67904, July 15, 1960. (Classified)
72. F. W. Albaugh, Reactor and Fuels Research and Development Operation Monthly Report, October 1961, USAEC Report HW-71535A, Hanford Atomic Products Operation, Nov. 15, 1961. (Classified)

73. J. W. Joseph, Jr., Stress Relaxation in Zircaloy-2 During Irradiation at Less Than 100°C, USAEC Report DP-623, Savannah River Laboratory, October 1961.
74. Westinghouse Electric Corp., Bettis Atomic Power Laboratory, Technical Progress Report, Core Materials and Quality Engineering, USAEC Report WAPD-MRK-11, Oct. 6, 1961. (Classified)
75. E. G. Kendall et al., Fabrication Development of APM Alloys for Fuel Elements, USAEC Report NAA-SR-6213, Atomics International, Dec. 15, 1961.
76. Ames Laboratory, 1961. (Unpublished)
77. E. J. Dulis et al., Research on Workable Refractory Alloys of Tungsten, Tantalum, Molybdenum, and Columbium, Report WADD-TR-61-134, Crucible Steel Co. of America, April 1961.
78. V. D. Barth, Review of Recent Developments in the Technology of Tungsten, Report DMIC-Memo-139, Battelle Memorial Institute, Defense Metals Information Center, Nov. 24, 1961.
79. B. R. Rajala and F. C. Holtz, Improved Vanadium-Base Alloys, Report ARF-2210-4, Armour Research Foundation, Illinois Institute of Technology, Aug. 25, 1961.
80. H. R. Longfield, Atomic Energy of Canada, Ltd., 1960. (Unpublished)
81. L. G. Bell and W. Evans, Heat-Treatment and Mechanical Properties of Zirconium–2.5 Wt.% Niobium Alloy, Canadian Report AECL-1395.
82. S. Harper, Creep Properties of Zirconium Alloys, British Report NP-10710, September 1961.
83. R. W. Dayton and C. R. Tipton, Jr., Progress Relating to Civilian Applications During September 1961, USAEC Report BMI-1546, Battelle Memorial Institute, Oct. 1, 1961. (Classified)
84. G. A. Henrikson, High Strength Zirconium-Base Alloys, USAEC Report NMI-1244, Nuclear Metals, Inc., Feb. 22, 1961.
85. R. L. Mehen, Effect of Combined Stress on Yield and Fracture Behavior of Zircaloy-2, *Trans. ASME, J. Basic Eng.*, 83(4): 499–512 (December 1961).
86. American Society for Metals, Refractory Materials. A Literature Search, USAEC Report TID-3560, November 1961.
87. Oak Ridge National Laboratory, Oct. 9, 1961. (Unpublished)
88. Pratt & Whitney Aircraft Div., Final Design and Development Report of the PWAR-11C Reactor Experiment, USAEC Report PWAC-333, June 30, 1961. (Classified)
89. R. L. Knecht, Annealing Warm-Extruded Zircaloy-2 to an Ultrafine Grain Size, USAEC Report HW-68835, Hanford Atomic Products Operation, March 1961.
90. E. S. Fisher and C. J. Renken, Adiabatic Elastic Moduli of Single Crystal Alpha Zirconium, *J. Nuclear Materials*, 4(3): 311–315 (1961).
91. E. Gebhardt et al., Investigation of the Zirconium-Oxygen System, Part 1—The Electrical Resistivity of Oxygen-Containing Zirconium (in German), *J. Nuclear Materials*, 4(3): 241–254 (1961).
92. E. Gebhardt et al., Investigation of the Zirconium-Oxygen System—Part 2 (in German), *J. Nuclear Materials*, 4(3): 255–268 (1961).
93. J. E. Campbell et al., Introduction to Metals for Elevated-Temperature Use, Report DMIC-160, Battelle Memorial Institute, Defense Metals Information Center, Oct. 27, 1961.
94. L. S. DeLuca, A Compilation of Diffusion Data from Unclassified Sources for Zirconium, Uranium, and Niobium Systems, USAEC Report KAPL-M-LSD-2, Knolls Atomic Power Laboratory, July 7, 1961.
95. R. L. Andelin and L. E. Godfrey, Bibliography on Self-Diffusion of Pure Metals in the Solid State, USAEC Report LAMS-2562, Los Alamos Scientific Laboratory, May 1961.
96. G. Kidson and J. McGurn, Self-Diffusion in Body-Centered Cubic Zirconium, *Can. J. Phys.*, 39: 1146–1157 (August 1961).
97. Manufacturing Laboratories, Inc., Investigation of Diffusion Barriers for Refractory Metals, Report NP-10666, July 25, 1961.

Section

V

Reactor Materials

Special Fabrication Techniques

Melting, Casting, Working, Heat-Treatment

Melting and Casting

The effect of electron-beam melting on the purification of small charges of hafnium metal is reported by the Bureau of Mines.[1] Significant levels of iron, aluminum, and titanium were removed by subjecting buttons of metal to electron beams of different power levels. Hardness decreases were also reported. Concerned with the same subject of metal purification, Darling discusses the factors important in reducing the oxygen content of chromium, copper, molybdenum, and niobium.[2] In summary, it is shown that the oxides can be quantitatively reduced in nonvolatile metals (at process temperature) by vacuum processes. Important in this regard is that the reduction tendency is considerably greater than the tendency of the metals to form carbides.

Atomics International has been active in the investigation of melting and casting processes for reactor fuels. This is evident in reports on research to find suitable coatings for graphite crucibles used for thorium-base alloys containing 1 to 13 wt.% uranium[3] and on the successful development of techniques for the casting of thin plates of uranium-molybdenum alloys.[4]

From results based on carbon-pickup coatings for crucibles, it was concluded that ThO_2 was ineffective; BeO coatings deserved further study; and wash coatings of Y_2O_3 and ZrO_2 and flame-sprayed coatings of ZrO_2 gave best results. Good coatings limited carbon pickup in the melt to about 500 ppm, whereas carbon contents as high as 7700 ppm were noted in thorium alloys melted in ThO_2-coated crucibles. Typical of Atomic International's success in casting thin plates (12 by 3 by 0.04 in.) were castings of both the uranium–3.8 wt.% molybdenum–0.15 wt.% aluminum and uranium–10 wt.% molybdenum alloys. A significant factor in this success was the use of horizontal graphite molds heated to within a few hundred degrees of the alloy melting point.

Hot and Cold Working

On the basis of studies over an extended period of time, Nuclear Metals has summarized[5] its development of fabrication techniques for yttrium. The primary extrusion of cast ingots; the secondary extrusion of semifinished shapes; and the swaging, drawing, and rolling to finished shape and dimensions are covered. Success in producing yttrium in the form of rod, wire, tube, and sheet is cited. Extrusion in copper sheaths at 1350°F is suggested, whereas lower temperatures (<1000°F) can be used for final shape or sizing operations without sheaths. Another uncommon metal, rhenium, is the subject of a recent interesting report.[6] Both sintered powder compacts and electron-beam-melted material were studied. One compact was successfully rolled to a 6- by 6- by 0.005-in. sheet, and two electron-beam-melted ingots were rolled to 0.085-in. sheet (one at room temperature, one at 300 to 500°F). Warm rolling was effective in reducing edge cracking.

The feasibility of a powder-rolling process for molybdenum and tungsten sheet was investigated by Los Alamos Scientific Laboratory.[7] Strip, 45 to 60 mils thick and 85 per cent dense, was produced using hydrogen-reduced powder. Strip 20 mils thick, suitable for stamping of flat shapes, was obtained after hot rolling at or near 1500°C.

An international review of the technology of the family of aluminum products known as SAP (sintered aluminum products) and APM (alu-

minum powder metals) is available from two recent publications.[8,9] Kendall (Atomics International) and Mann (France) both report on the properties, fabrication, and uses of these materials in fuel-cladding applications.

Another review, dated somewhat in the past but recently brought to this reviewer's attention, is a comprehensive survey of the state of the art for extrusion and forging.[10] It confines itself mainly to the refractory metals tungsten, molybdenum, niobium, and tantalum. The following needs cited are significant:

1. Improved die materials
2. Improved lubricants
3. Fundamental knowledge of properties of extruded materials
4. Means of obtaining higher ram speeds
5. Improved protection of materials at high temperature

More specific in interest has been Crucible Steel's investigation of F-48, Cb-74, D-41, and D-31 alloys.[11] In terms of hot strength, ductility, and forgeability (closed die forging), Cb-74 was best.

Experimental work on the extrusion of materials by use of a fluid under hydrostatic pressure has been carried on at Nuclear Metals.[12] Reporting on a year's work, Randall et al. suggest that the use of a liquid to transmit the pressure may be valuable for two reasons: (1) friction between billet and container will be eliminated, and (2) friction between the die and the material will be reduced. Results lead to the conclusions that:

1. For the experimental conditions employed, aluminum and copper require the same pressure at room temperature to extrude a billet with a pressurized fluid as with a well-lubricated billet by conventional means.
2. The extrusion of brittle materials requires a restraining pressure at the exit end of the die.
3. Greater single-step reductions are possible with the hydrostatic extrusion of beryllium and yttrium than are possible with drawing.

Heat-Treatment

The economies possible in the direct heat-treatment of gamma-extruded uranium rods to obtain the desired structure, as opposed to the present process of gamma extrusion followed by alpha rolling or extrusion, are obvious. This advantage is responsible for current work by Mallinckrodt.[13] Preliminary results are encouraging in that, after annealing the as-extruded cores for 4 hr at 950°F and subjecting them to a standard beta heat-treatment and oil quenching at 130°F, structures comparable to those obtained by the present process were produced.

Mallinckrodt has also presented a detailed description[14] of its process for the control of hydrogen in ingot uranium (vacuum outgassing in the alpha temperature range). The choice of an alpha temperature range was based on the inability of uranium to support its own weight at 1850°F, although, in the gamma range, diffusion coefficients 5 to 20 times those in the alpha range were indicated. Hydrogen diffusion coefficients showed no dependence on initial hydrogen or carbon contents, cold work, grain size, or preferred orientations, provided that a uniform distribution was present initially. Further, outgassing at 950°F had no effect on structure. The outgassing after beta heat-treatment is feasible at either 950 or 1200°F, depending on whether a recrystallized structure is desired. This postbeta treatment offers a finished core with essentially zero hydrogen at the surface.

The recovery and recrystallization behavior of zirconium and zirconium alloys are the subject of two "newsy" reports by Hanford.[15,16] Not only do Gray and his colleagues consider past work in a comprehensive manner, but they have extended the knowledge in this field with pointed experimental inquiries into a variety of real and practical considerations. The variables chosen were cold work, annealing time, temperature, and furnace atmosphere.

(E. L. Foster)

Cladding

Cladding by Rolling and Swaging

In the Hanford studies[17] of roll cladding of plutonium-bearing fuels, small coupons of plutonium metal have been clad with Zircaloy-2 by rolling at 750 to 800°C in a mild-steel jacket to a total reduction in thickness of 90 to 95 per cent. Zircaloy self-bonds were good, but core-to-cladding bonds were only marginal. Hanford workers are also investigating Zircaloy cladding of PuO_2.

A final report[18] was issued by Nuclear Metals concerning the fabrication of fuel assemblies from a single composite plate. Various con-

figurations referred to as spirals, box spirals, ribbon candy, and honeycomb assemblies have been fabricated from aluminum-clad aluminum-uranium fuel plates. As described in the last Review under the heading "Aluminum-Uranium Alloys," coolant-channel spacing in these assemblies is maintained by dimpling the composite in nonfueled areas. Complete process specifications are given[18] for each type of assembly.

Smith and Porembka at Battelle are investigating cold roll bonding of type 410 stainless steel to Zircaloy-2 pressure tubes.[19] They have found that a 40 per cent reduction of these composites will produce bonding. Mating surfaces are machined to 500 μin., rms, and then scratch brushed just prior to rolling.

Aeroprojects is investigating the application of ultrasonic welding to a modification of the roll-bonding process.[20] The report deals primarily with development of equipment, but there are a few examples of bonded materials.

(H. D. Hanes)

Pressure Bonding

A report has been issued[21] on the final phase of a 2½-year study of techniques for the fabrication of stainless-steel-clad uranium dioxide fuel elements by the gas-pressure-bonding process. The work demonstrated that fuel rods can be fabricated by gas-pressure bonding, using cold-pressed oxide fuel. Good dimensional control was achieved for fuel rods and for compartmented flat-plate fuel-element assemblies. Effort was then diverted to applying the techniques developed to the fabrication of rods using pelletized fuel, for irradiation in the Vallecitos Boiling-Water Reactor (VBWR).

As discussed in the last issue of this Review, the investigation of the fabrication of low-cost ceramic fuel elements is being continued[19,22] by evaluating the gas-pressure-bonding process combined with vibratory-packing techniques and UO_2 sheet-rolling techniques. Four flat-plate fuel assemblies, each containing two rolled UO_2 platelet cores fabricated by Gladding, McBean & Co., have been pressure bonded. A slight tendency toward cracking of the cores during bonding has been reduced by altering the rate of pressure application during initial heating.

Fuel rods containing uranium dioxide compacted by vibration, and also by swaging, have been assembled by Hanford and are being gas-pressure bonded at Battelle. Cladding materials included in this test are Inconel X, type 304L stainless steel, type 406 stainless steel, Zircaloy-2, and Zircaloy-4.

A paper[23] has been published by Paprocki and Hodge on a study of the cladding of solid and powdered delta-phase zirconium hydride with stainless steel. In this work the best results were obtained by gas-pressure bonding at 1700°F for 3 or 4 hr followed by 1 to 2 hr at 1900°F, using a pressure of 10,000 psi. Although intermediate layers of other metals were also studied, it was found that the best bonds were obtained by direct cladding.

The investigation of the gas-pressure bonding of beryllium-clad UO_2 fuel elements, which was reviewed in some detail in the last issue of this Review, is being continued at Battelle.[19,22,24] It has been shown that a coating of BeO, sprayed as a slurry, is a satisfactory barrier material to prevent reaction during bonding between the beryllium cladding and the stainless-steel spacers. Emphasis is currently being placed on the self-bonding of beryllium by studying the effects of grit-blasted and shaper-finished surfaces of various roughnesses. Specimens with surfaces blasted with chilled iron grit prior to bonding have yielded encouraging results.

(E. S. Hodge and D. C. Carmichael)

Diffusion Bonding

A eutectic diffusion-bonding process, using external die pressure, has been developed at Atomics International[8] for end closure of aluminum-clad fuel elements with ceramic fuel. These fuel elements consist of UO_2 pellets contained in aluminum-alloy fuel tubes, which are extruded aluminum-powder-metallurgy products, dispersion strengthened with Al_2O_3. Prior to bonding, the tubes are cleaned and the end plugs are cleaned and electroplated with 0.1-mil-thick silver, which was determined to be the most desirable eutectic-forming metal. In this bonding process, which is performed in an inert-atmosphere glove box, the surfaces of the plug and tubing are brought into contact, using a pressure of 5000 psi exerted by a pneumatically loaded collet die that applies uniform radial pressure. Induction heating is used to heat the die and the components to be bonded to the eutectic melting temperature of silver and aluminum (1050°F). As characteristic of this type of bonding, the localized eutectic melting at the interfaces forms the bond, and continued

heating causes the eutectic-composition metal to diffuse into the bodies being joined. It is reported that the end closures obtained in this work have remained leaktight after thermal cycling or after internal pressurizing and have not failed in burst tests.

In a translation[25] from an Italian paper, methods of joining stainless steel and Zircaloy-2 tubing are discussed, and studies conducted on solid-phase diffusion bonding are described. Although multiple intermediate layers of other metals were investigated, it was found that the joints obtained directly between the stainless steel and Zircaloy by solid-state diffusion below 1050°C possessed the best properties, including resistance to corrosion. In a German article[26] the metallic bonding between uranium and aluminum for reactor fuel elements is discussed. A diffusion-bonding technique, using zinc and tin intermediate layers, was developed for forming a bond between aluminum and uranium which is reportedly suitable for fuel elements for a low-temperature, water-cooled reactor. For coolant temperatures between 230 and 500°C, a diffusion-bonding technique using nickel was applied. (D. C. Carmichael)

Coextrusion

The coextrusion process is being used by the Germans[27] for the manufacture of fuel plates for the Argonaut reactor. The enriched U_3O_8 fuel material is clad directly with the aluminum cladding to a finish profiled bond. Manufacturing techniques, materials questions, and technical data are extensively described. (C. B. Boyer)

Canning

A recent patent[28] describes a device for consolidating an alkali-metal thermal bond between a fuel element and its jacket. It consists of a heater and electromagnet surrounding the fuel element so that, while it is heated, a rotating magnetic field will agitate the alkali metal and work out void spaces.

Argonne has developed a process[29] for sodium bonding of EBR-II fuel and blanket elements. The required amount of sodium in the form of extruded rod is placed inside the type 304 stainless-steel-cladding tube which has been welded closed at one end. Heat is applied to melt down the sodium rod. The tube is placed in a vacuum furnace at 150°C with an inert-gas pressure of $\frac{1}{3}$ atm. After 10 min the argon gas pressure is raised to 1 atm and the furnace temperature is raised to 550°C for another 10-min period, after which the assembly is cooled to room temperature. This thermal treatment ensures, first, that dissolved gases in the sodium will be removed and, second, that the proper wetting action between the sodium and cladding will occur in the desired areas.

Extruded fuel rods are then placed in the tube on top of the frozen sodium at the bottom. The assembly is next heated to a temperature above the melting point of the sodium. At the same time, a 60-cycle vibration is imparted to the assembly by an electromechanical vibrator. This procedure results in the settling of the fuel rod to the bottom of the cladding tube. The top end of the assembly is then welded closed. After a check for leaks is made, the element is subjected to a bonding operation. This process consists of holding the element at 550°C for 4 hr with simultaneous application of vertical 60-cycle vibration as before. The element is cooled by a blast of air, deliberately tailored to freeze the annular sodium progressively from top to bottom. This procedure is effective in eliminating freezing voids, which would appear as unbonded areas in subsequent nondestructive examination.

A method for applying aluminum-silicon coatings to uranium rods is described in a recent patent.[30] The process consists of preheating the rods to the coating temperature and placing them between two rotating rollers. The coating metal or alloy in a liquid form is then poured between one of the rollers and the uranium. The desired thickness of coating is achieved by rotating the rollers continuously, thus building up the coating thickness. (E. G. Smith, Jr.)

Electroplating

Electrodeposited chromium cermets containing zirconium boride were found to protect molybdenum, tantalum, and tungsten in flame tests at 3860°F for 20 to > 40 min and in air at 2000°F for 60 min. The coatings, 3 to 4 mils thick, were produced by electrodeposition in chromium-plating baths containing dispersions of ~45-μ ZrO_2 particles. Small particles were not so effective. Zirconium oxide cermets were not so protective as zirconium boride cermets. The cermet coatings were superior to coatings applied by electrophoresis, vapor-phase deposition, or exothermic reactions.[31] Electrodepos-

ited cermets are now being evaluated as oxidation-resistant coatings for graphite in the same laboratory. Abstracts for a relatively comprehensive list of pertinent literature references were compiled by Value Engineering Company.[32]

The National Bureau of Standards is turning attention[33] to chromium silicide and chromium boride coatings for oxidation protection of niobium and tantalum, after nearly a year's work on anodized coatings which proved ineffective. Electroplating and vapor-phase deposition will be combined to produce the chromium silicide and boride coatings.

Uranium-metal ingots produced in Poland were pressed from uranium precipitated at the cathode in a divided cell containing fused salt and excess uranium oxide.[34] The cathode and anode compartments were separated by an aluminum oxide diaphragm to prevent contamination of the uranium with uranium oxide.

The quality of highly protective, 2.5-mil nickel plate is influenced by surface and subsurface defects in thorium and uranium, according to Battelle electrochemists.[24] Abrasive polishing before plating is recommended. Electropolishing after abrasive polishing is desirable for uranium but is unnecessary for thorium. By nickel plating in two layers, with intermediate heating at 500°F to outgas hydrogen, blistering was avoided when specimens with 3-mil nickel plate were heated.[19] The first layer of nickel was 1 mil thick. The second, after hydrogen outgassing, was 2 mils thick. (W. H. Safranek)

Nonelectrolytic Chemical-Plating Techniques

Work on the chemical vapor deposition of tungsten by hydrogen reduction of WF_6 is being carried out by several organizations.[35–37] It was pointed out that the presence of HF may accelerate the process and permit the formation of more uniform coatings. Replating can be conducted with epitaxial growth of a second layer. The bases of greatest interest are graphite and a tungsten–beryllium oxide composite.

Chemical vapor deposition of iron is being used to prepare alpha-iron single crystals (whiskers) by hydrogen reduction[38] of molten $FeCl_2$ at 730°C. Structures 1 to 2 mm in diameter and up to 80 mm long can be produced.

Treatment of a carbon body with nickel carbonyl to render it less porous was described.[39] Nickel is deposited in the pores of the body by decomposition of the carbonyl. The temperature of the body is raised to just above the melting point of the nickel-carbon eutectic, which is formed by solution of carbon from the body in the deposited nickel. The molten eutectic wets the carbon surfaces and penetrates pores and voids in the carbon body. On subsequent cooling to room temperature, carbon is precipitated. The nickel remaining is removed by contacting it with CO at 60°C to form the volatile carbonyl, which is fugitive. Iron carbonyl also can be so used.

Coating of uranium with nickel by pyrolysis of nickel carbonyl, followed by a diffusion heat-treatment at 500 to 600°C, is feasible.[40] Interest in pyrolytic graphite as a useful high-temperature material is widespread.[41–43] Current investigations are providing more complete information regarding the extent to which various control parameters influence the quality of the product. Boron nitride[43] can be deposited by controlled pyrolysis of various inorganic and organic compounds. The nature of the decomposition products of a number of metal formates was explored.[44] Some of these products may be of interest for reactor-core-materials applications.

Diffusion type high-temperature-oxidation resistant coatings for refractory metals are receiving wide attention. These usually are applied by pack methods involving mass transfer of the coating material through the vapor phase; complex silicide or oxide coatings on tungsten,[45,46] niobium,[47–49] tantalum,[49,50] molybdenum,[49] chromium,[49] nickel,[49] and vanadium[51] are currently under investigation. An alkali metal fluoride activator is used in most of these processes.

(E. M. Sherwood)

Welding and Brazing

Several foreign patents covering improved joining techniques have been issued. The technique of introducing ultrasonic energy into a molten weld pool using filler wire as the coupling member was patented in 1961 in England.[52] Presumably the vibrations break up oxide films, reduce weld-metal grain size, and result in improved mechanical properties. A very similar technique was described in a Soviet welding magazine[53] in 1960. Neither publication gives data to demonstrate the effectiveness of

this approach, but the concept appears to be worthy of investigation.

A British patent[54] on a procedure for making dissimilar-metal joints outlines the following steps:

1. Zirconium is buttered in the joint area with niobium or titanium.
2. The buttered edge is then welded to stainless or mild steel with vanadium.

Variations of this technique have been studied for a number of years, but this reviewer is not aware of any service applications. Apparently joints of this type have poor corrosion resistance or dimensional stability.

The combined use of welding and metal spraying to effect closures on fuel elements is described in a French patent.[55] Metal spraying is used to deposit a "creep-resistant metal" around end caps and fuel-element extremities.

Use of a "readily deformable" material to transmit the pressure during pressure welding is said[56] to improve results. Beryllium was joined to itself at 750 to 850°C, using mild steel to transmit the pressure. If the readily deformable material flows sufficiently, it should be possible to obtain joint forces similar to those obtained by gas pressure.

Studies at Westinghouse[57] of brazing fabrication procedures for the Carolinas-Virginia Tube Reactor program have been completed. The zirconium-beryllium binary alloy and two ternary alloys containing iron or copper were investigated for suitability as brazes. The investigation covered corrosion resistance in 680°F water and mechanical properties after brazing. The zirconium-beryllium alloy was found to have the best combination of useful properties. Preparation of this alloy involves hydriding, crushing in argon, and vacuum degassing. Powder alloy produced this way has a minimum content of hydrogen, oxygen, and nitrogen. Time and temperature during the brazing cycle are critical. Best results were obtained with a 5-min braze cycle at 990 to 1035°C, followed by a diffusion treatment of 1 hr at 800°C.

Tentative conclusions have been reported[1] from the Bureau of Mines welding study of niobium and tantalum. These are as follows:

1. Tantalum welds are embrittled by oxygen in excess of 900 ppm when carbon and nitrogen are below 100 ppm.
2. Tantalum welds are embrittled by carbon in excess of 1250 ppm when oxygen and nitrogen are at a low level.
3. Any combination in which the combined concentrations of two of the three interstitial elements (carbon, nitrogen, and oxygen) exceed 700 ppm embrittles welds in tantalum or niobium.
4. The embrittling effects of oxygen, nitrogen, and carbon are not additive.
5. Welds that will undergo a 180° bend can be made in the niobium–1 wt.% zirconium and niobium–10 wt.% hafnium–1 wt.% zirconium alloys. Strength of welds in these alloys is equal to or is better than base-metal strength. Welds in the niobium–10 wt.% hafnium–10 wt.% tungsten and niobium–15 wt.% tungsten–5 wt.% molybdenum–1 wt.% zirconium alloys are brittle.

Studies of friction welding or bonding of reactor components have been started at Battelle (references 19, 22, 24, and 58). This process was developed in the Soviet Union. Recently commercial equipment has been marketed in the United States for friction welding round bar or rod sections. The Battelle studies are directed at solving end-closure problems with materials of poor weldability. Aluminum powder metallurgy (SAP) welding is currently being studied. Closure bonds covering 50 to 70 per cent of the joint area have been obtained.

Canadian experience with the zirconium–5 wt.% beryllium brazing alloy[59] has shown inferior corrosion resistance for large exposed areas of braze alloy. Samples were prepared by brazing in vacuum or argon and were exposed to 360°C water. After about 56 days, the following weight gains were recorded:

Base metal	22 mg/dm^2
Braze, in as-brazed condition	125 mg/dm^2
Braze, in pickled condition	95 mg/dm^2

(R. E. Monroe)

Explosive Forming

A program is being conducted to determine the optimum strain-rate conditions, transfer media, and forming temperature necessary to achieve maximum formability with selected refractory materials.[60,61] Three basic materials, arc-cast molybdenum–½ wt.% titanium, tungsten, and either niobium alloy Nb-7

CT-2WZ, are being tested, using both a unidirectional trough die and a multidirectional cup die.

The effect of draw-ring pressure on forming was investigated. With excessive draw-ring pressure, failure of the metal specimen occurred almost completely around the periphery of the draw radius. With no draw-ring pressure, except for the mass of the ring itself, reasonably good results were obtained. Tests conducted with both 0.010- and 0.040-in.-thick material at draw-ring pressures of from zero to 1000 lb showed very little difference in results.

In high-temperature (1000°F) explosive forming, the problem of thermal detonation of the explosive becomes acute. This was solved by inserting the charge in a phenolic glass fiber container machined to the shape of the charge and filling the remaining volume with aluminum oxide. An alumina transfer medium appears to be optimum for high-temperature forming. Because of the impedance of the alumina, only weak reflections occur at the explosive-alumina interface. This attenuates the initial pressure experienced by the specimen and smooths out the pressure profile.

An attempt was made to determine the maximum achievable draw with a nominal amount of elongation. It was concluded that optimum metal flow, and hence maximum draw, requires low draw-ring pressure and proper preform size. Die design is also an important factor. The draw plate should be so designed as to minimize the distance between the inner edge of the ring and the die draw radius.

Strain-rate measurements were obtained during this testing by moving a high-coercive-force permanent magnet concentrically through a shielded inductance coil. The d-c voltage thus generated is directly proportional to linear velocity. It is monitored by an oscilloscope and recorded photographically. The movement of the core through the coil is calibrated in terms of volts per unit velocity. Thus the oscilloscope trace can be replotted in terms of forming velocity.

A study has been conducted to determine the formability and metallurgical characteristics of various aluminum alloys, steels, and titanium resulting from the application of an explosive load.[62] Tests were conducted on these materials in the annealed, ¼-hard, ½-hard, and fully hardened conditions. Three forming dies of different configurations and representing increasing difficulty of forming were used during this testing. The first die, a flanged cup die, was used to demonstrate the deep drawability of the materials and to permit the determination of the optimum flange width-to-diameter ratio for each material. A bulged cylinder die was next used to determine the ability of the material to flow under biaxial tensile loading. The third die, a large hemispherical one, was employed to demonstrate the effects of size on the ability to explosively form a hemispherical shape. These tests were conducted underwater with a vacuum between the part and the die. Three types of explosives were used: (1) 60 per cent gelatin dynamite, (2) Primacord, and (3) EL-506A sheet explosive.

The data obtained from this testing indicate that both austenitic and precipitation-hardening stainless steels may be explosively formed into intricate shapes. There are also indications that welds in these materials, when properly rolled, will, in most cases, withstand as much deformation as the parent material. During explosive forming, an appreciable amount of work hardening occurs, making intermediate anneals necessary to obtain maximum forming. The yield strength of austenitic alloys will be increased considerably by the cold working resulting from explosive forming, and ductility will be lowered somewhat.

Both the heat-treatable and work-hardening aluminum alloys lend themselves very well to explosive forming. Heat-treatable aluminum alloys may be satisfactorily formed in the annealed condition. However, in the fully heat-treated and aged condition, the formed material shows large amounts of springback. Fatigue properties of the 5086-H34 aluminum alloy do not appear to be altered by the cold working resulting from explosive forming. Titanium alloys were found to lend themselves to explosive forming only at 800 to 1200°F, depending on their alloy content.

With regard to die material, the results obtained during this testing showed that, for short runs with relatively low explosive pressures, kirksite (a zinc-base alloy) may be used. Overall ductile iron has been found to be the best die material of those tested. It is strong and has the ability to withstand explosive shock. Concrete dies with epoxy faces were suitable for extremely large workpieces, although it appears that they could be used only for "one-shot" operations.

A Dynapak machine with a Bridgeman anvil apparatus, modified for impact application and capable of producing pressures of 500,000 psi, has been used to compact UO_2 powder to a bulk density of 10.86 g/cm^3 (>99 per cent of theoretical density).[63] The uranium dioxide was compacted in a stainless-steel capsule at 1000 to 1200°C. Temperature variations in this range and O/U ratio variations from 2.01 to 2.26 appear to have little effect on the compacted density at impact pressures of 500,000 psi. With lower impact pressures, indications are that higher compacted UO_2 densities can be obtained by increasing the temperature or the O/U ratio.

High-energy impacted UO_2 specimens have been annealed at temperatures of 1300 to 1700°C for 12 hr, resulting in a density decrease of approximately 2 per cent. It is suspected that this decrease is due to an expansion of the specimen on annealing, caused either by the release of residual stresses or the expansion of gases trapped in the UO_2 during compaction.

Additions of 0.5 and 0.1 wt. % TiO_2 to micronized UO_2 were found to inhibit slightly the densification of the UO_2. However, no reaction between the TiO_2 and UO_2, such as the formation of a eutectic, was evidenced.

Electrodeposited UO_2 crystals, ThO_2, Al_2O_3, and a 50 mole % $ThO_2-Al_2O_3$ powder mixture have been high-energy impacted at 1100 to 1200°C and 500,000 psi in unsealed stainless-steel capsules. The densities obtained were 99.2, 95.9, 84.9, and 90.0 per cent of theoretical density, respectively. Uranium monocarbide has also been high-energy impacted under similar conditions, except that the stainless-steel capsule was evacuated. A density of 97.4 per cent of theoretical was obtained; however, extensive reaction occurred between the plastically deformed UC and the type 304L stainless steel.

The Dynapak machine has also been used to form steel jackets for plate type fuel elements of cold-worked 0.010- to 0.020-in.-thick AISI 406 steel, and a 7.6 wt.% aluminum, 5.1 wt.% chromium, balance iron alloy.[64] A comparison is under way to determine whether high-energy-rate forming has an advantage over slow-press forming. Indications are that less springback and wrinkling occur during the high-energy-rate forming.

A paper[65] concerning the potential and application of explosive energy for the compacting of metal powders has been presented by Paprocki et al. The techniques used for explosive compaction are briefly described as being either direct or indirect and utilizing either high or low explosives. Direct compaction is described as a technique in which dies, in the usual sense, are not generally used. Direct compacting procedures with high explosives are usually required to achieve high green strengths and compacted densities with the very refractory materials. Indirect compacting techniques utilizing low explosives are most suitable for the more ductile and less refractory materials.

The components used to prepare an assembly for compacting a tungsten rod are shown in Fig. V-1. They consist of a mild-steel tube, the end plugs, the tungsten powder, and the sheet explosive. The assembly is completed by simply pouring the powder into the tube, inserting the end plugs, and sealing the assembly in an electron-beam welder to ensure evacuation to a very low pressure. The assembly is then wrapped in Du Pont EL506-A plastic sheet explosive and the charge is detonated under several feet of water in a pit.

Shapes other than rods can be made by introducing modifications into the process. Tubing can be produced by using concentric mild-steel tubes, filling the annulus between the tubes with the powder to be compacted and the center tube with the same or a different powder. After compaction, the mild steel is removed by leaching. Tubes and rods possessing nonuniform cross sections, and flutes, fins, or ribs can also be produced.

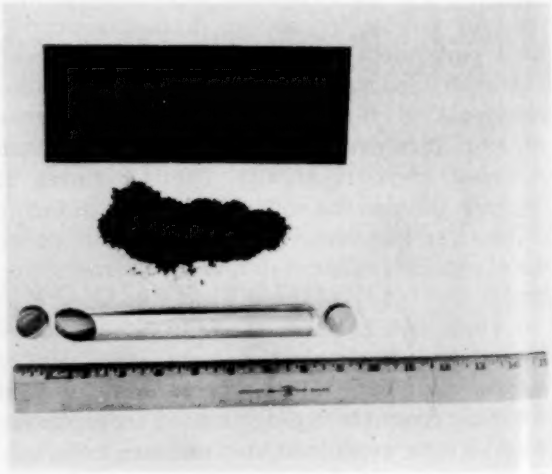

Fig. V-1 Components used to prepare a tungsten rod specimen by the direct approach.[65]

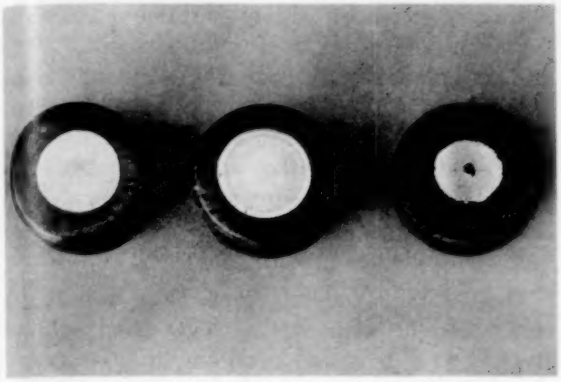

Fig. V-2 Effect of charge density on the structure of explosively compacted tungsten rods.[65]

The charge density (grams of explosive per square inch of surface area) required to compact a specimen of a given size of a given material is dependent on the strength of the material, its density, and degree of confinement. Figure V-2 shows the cross sections of three different tungsten bars. When proper charge density is used, a uniformly dense body such as that shown on the left is produced. The center specimen has a small area in the center of the bar which is slightly denser than the rest of the cross section, indicating that the charge density was somewhat high. The specimen on the right has a hole or "spike" at the center, with radial cracks extending outward. This defect is indicative of an excessive charge density. It is probably the result of a combination of the stresses from the tensile tails which follow the explosively generated compressive waves and the tensile stresses generated as a result of overrecovery of elastic strain induced in the specimen early in the compacting cycle.

Experiments have been conducted using the direct approach with various metal and nonmetal powders and dispersions. A representative example of the data obtained during this testing is given in Table V-1. The powders listed in this table were compacted under water at ambient temperature, and the final densities given are as-compacted densities. Figures V-3 and V-4 show the as-compacted tungsten and beryllia structures.

There are indications that it may be possible, by improving present techniques, to explosively compact most materials in such a manner that sintering, at least in the usual sense of the word, may not be necessary. The effects of explosive compaction both below and above ambient temperature should be of great interest for certain applications.

Battelle has recently constructed a new explosive metalworking facility at its West Jefferson site. Two explosion-forming pits, one 6 ft in diameter and the other 13 ft in diameter, are located in the floor of a prefabricated steel building, which also contains an explosive-handling area, laboratory and office space, and a detonation-control room. The pit design is based primarily on the design developed by

Table V-1 DATA ON EXPLOSIVE COMPACTION OF METAL POWDERS[65]

Metal powder	Particle size	Initial density,* % of theoretical	Ratio of powder to explosive, g/g	Final density,† % of theoretical
Tungsten	100 mesh	44.5	1.833	97.0
Haynes Stellite 25	−325 mesh	45.5	0.754	94.6
Haynes Stellite 31	−180 mesh	36.8	0.550	96.4
Zircaloy-2	150 mesh	27.2	0.378	97.0
Beryllium	−200 mesh	31.7	0.155	96.0
70 vol.% 347 S.S.−30 vol.% UO_2	−325 mesh S.S. and 100 mesh UO_2	53.0	14.800	94.4
97 vol.% Ta−3 vol.% ThO_2	−325 mesh	50.4	2.110	97.0
80 vol.% $MoSi_2$−20 vol.% ZrB_2	−325 mesh	46.0	0.741	95.3
20 vol.% ZrB_2−80 vol.% $MoSi_2$	−325 mesh	56.8	0.844	95.6
Beryllia	−325 mesh	68.3	0.679	96.0
70 vol.% W−30 vol.% UO_2	100 mesh	30.3	1.168	96.8
Reactor-grade graphite	−325 mesh	31.8	0.272	93.5
$MoSi_2$	−325 mesh	36.8	0.750	98.1

* Calculated density.

† Density determined by pycnometer methods.

Fig. V-3 Explosively compacted tungsten. The measured density is 97 per cent of the theoretical density.[65]

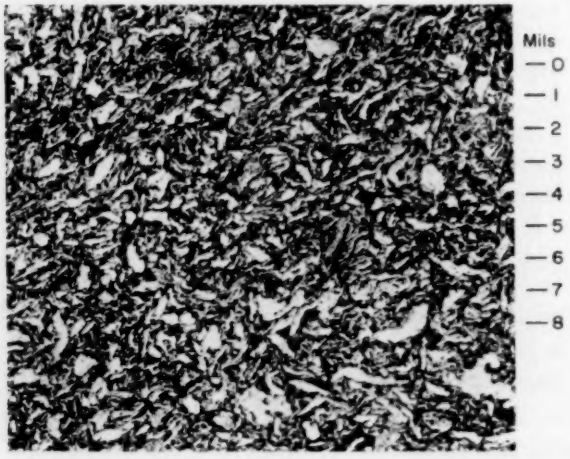

Fig. V-4 Explosively compacted BeO. The measured density is 96.0 per cent of the theoretical density.[65]

Lockheed for Wright Field. Additions have been incorporated into the basic pit design to prevent the transmission of ground shock waves to the building and building foundation.

(C. C. Simons)

Ceramic Technology

McClelland and associates[66,67] have described Atomics International's equipment and capabilities for hot-pressing ceramic oxides. Temperatures up to 2000°C and pressures as high as 6000 psi on a 4-in.-diameter piece are employed. The power supply is rated at 100 kw at 3000 cps and heats a graphite susceptor. The die material also is graphite; National Carbon ATJ grade is preferred. The authors report that they can press to tolerances of a few mils with good surface finish. A theoretical discussion of hot pressing is presented, and end-point densities of BeO and Al_2O_3 under various pressing conditions are given.

Los Alamos investigators have reported a technique for slip-casting MgO from aqueous slips.[68] The principal problem in casting MgO is its tendency to hydrate. Hydration not only destroys the desirable qualities of a casting slip but also introduces problems in subsequent ceramic processing. Stoddard and associates have found that maintaining the slip temperature at about 1°C retards hydration of the MgO, even during prolonged ball milling. Dried castings made from cold aqueous slips had densities in the range of 70 to 75 per cent of the theoretical density. These could then be fired at 1600°C to densities of 93 to 96 per cent of the theoretical density. The fired pieces had no open porosity, and their transverse strength was in the range of 20,000 psi.

Investigators at Aeroprojects, Inc., West Chester, Pa., are studying applications of ultrasonic energy to ceramic forming processes.[69-72] In compaction experiments using Norton Company 38-900 grade Al_2O_3, it was shown that activating the top ram with ultrasonic energy resulted in high as-pressed pellet densities at comparatively low forming pressures. For example, pellets having densities up to 82.6 per cent of the theoretical density were formed at 2600 psi by activating the ram with from 25 to 100 watts of 10-kc ultrasonic energy. Energy was applied for only 3.5 sec during actual compaction. Under normal conditions, densities in the range of 50 per cent of the theoretical density are observed. Extrusion experiments in which the extrusion die was activated ultrasonically were made. For a given mix, activation permitted extrusion at a higher rate and with less pressure. Activation of slip-casting molds during casting resulted in higher densities and lower water contents in the cast pieces.

Oak Ridge scientists,[73] in studying the densification rate of ThO_2 as temperature is increased, found that the rate reached a maximum at about 1000°C. The rate then decreased with increasing temperatures, reaching a minimum

at about 1200°C. A further increase in temperature resulted in yet another increase in densification rate. Similar rate studies on the fluorite-structure materials CaF_2 and CeO_2 showed similar minima at about the same fraction of the absolute melting temperature as for ThO_2. These data suggest that minima in the plot of densification rate versus temperature may be characteristic for fluorite-structure materials. The authors postulate a change in the mechanism of material transport to account for their observations.

(A. K. Smalley)

Ceramic Coatings

A report by Sandia[74] suggests that less titanium be used in ceramic-to-metal bonding. A common procedure is to use a titanium-cored silver-copper eutectic braze wire containing 12 wt.% titanium. It was found that bonding can take place after only a small amount of titanium has entered the molten braze solution. At this point the braze is soft. The presence of more titanium in the braze causes the brittleness considered typical of such seals.

A glassy phosphate coating melting at about 800°C was found by Ames Laboratory[75] to have better adherence to yttrium than those previously investigated, and to provide some oxidation resistance. The coating had the following composition in wt.%: 70 P_2O_5, 12 Al_2O_3, 14 Na_2O, and 4 Fe_3O_4.

General Electric[76] has been investigating coatings for molybdenum. Of primary concern was oxidation resistance at 2000 to 2600°F, but thermal-shock and impact resistance were also considered. Four commercial coatings were evaluated, and the infiltration of flame-sprayed oxide coatings with refractory glasses was investigated. For the test procedure used, the commercial coatings were classified in the following order, listing the best first: GE system 300, Chromalloy W-2, Climax Al-Cr-Si, and Linde LM-S. Mullite or alumina was flame sprayed on molybdenum coated with niobium or tantalum. The coated metals were then impregnated with a refractory glass. It was concluded that serious tensile stresses existing in the flame-sprayed coatings caused cracking during the subsequent glass infiltration. No coatings were found which met all the requirements for propulsion and missile components.

(B. W. King)

Nondestructive Testing

Ultrasonic Techniques

In the evaluation of ultrasonic test devices for inspection of adhesive bonds, Martin Company[77] has continued attempts not only to determine void (unbonded) areas but also to investigate the quality of the bonds. The instruments evaluated were able to detect unbonded areas, porosity, and bond-thickness variations, but they were not effective in the detection of substandard bonds due to poor surface preparation or undercure of the adhesive. In some cases bond degradation in service due to fatigue, heat exposure, or corrosion could be determined roughly. All the instruments evaluated were resonance types except one, which was a pulse-echo type.

The bond problem is one of general concern in the reactor field, and, fortunately, ultrasonic techniques have proven invaluable in inspecting for defective bonds. Among the interesting problems that have been solved ultrasonically are the inspection of Zircaloy-clad NPR fuel elements for end-cap bond integrity at Hanford[78] and the remote-control inspection for unbond in irradiated fuel elements at Bettis.[79]

The Canadians[80] have developed a test to detect outside-diameter and inside-diameter cracks (either longitudinal or transverse) in Zircaloy tubing, the dimensions of which are one-fifteenth of the wall thickness deep and one wall thickness long, using Lamb-wave techniques in an immersion system. The tubing dimensions are 1.0-in. OD by 0.026-in. wall, 0.6-in. OD by 0.025-in. wall, and 0.6-in. OD by 0.017-in. wall. They have found that $\frac{1}{4}$- by 1-in. rectangular ceramic or lithium sulfate crystals have given best results. Masking these transducers to $\frac{1}{8}$ by $\frac{5}{16}$ in. does not reduce the sensitivity, but it does reduce the noise level. Such masking limits the forward tube travel. Peaking coils increased the sensitivity of the system when the Sperry Reflectoscope Model UR-50-E-600 was used. The pulse repetition rates ranged from 400 to 600 cps, and the tubing revolved at speeds of 200 to 500 rpm. Helices of $\frac{1}{8}$ to $\frac{3}{16}$ in. are required to detect very small defects.

With their automatic flaw alarm, the Canadians claim that a "good shop operator without prior ultrasonic testing experience can learn to set

up the equipment and carry out production testing in about 2 months." However, skilled technical backup is required to evaluate the rejected tubing.

Oak Ridge[81] uses a split-beam technique to eliminate the necessity of inspecting tubing twice in opposite circumferential directions to detect poorly oriented defects such as laps, folds, or other nonradial discontinuities. In this system the transducer is centered squarely over the tubing, and separate portions of the sound beam enter the tubing and are simultaneously propagated in opposite circumferential directions. As the tube is rotated, radial cracks are detected with equal response by both portions of the split beam, but nonradial cracks are detected by unequal response as they approach toward or recede from the beam origin. Oak Ridge credits the Fresnel effect, which produces maxima and minima of ultrasonic intensity across the sound-beam diameter, as being a major factor in the accomplishment of this technique improvement.

(D. Ensminger)

NDT Techniques Other Than Ultrasonic

Since excellent image sharpness is now available with the use of gadolinium screens in direct-exposure neutron radiography, some interesting applications have been studied.[82] In one such application, the high absorption of adhesives in such structures as aluminum-skinned, adhesive-bonded honeycomb permit an excellent view of areas which are thin or void of the adhesive. A second interesting application is in the determination of the uniformity of the distribution of boron carbide within a zirconium-clad, sintered boron carbide poison element. This is a relatively simple problem for neutron radiography because of the high neutron absorption of the boron. By X-ray techniques, however, it is a difficult task since the X-ray absorption by all materials present in the sample is so similar.

Oak Ridge[83] has under development an eddy-current device that will be used for thickness measurements. This device is based on the phase shift only in the measurement of thickness and utilizes a through-transmission technique. This most interesting approach theoretically eliminates the dependence on coil-to-specimen or coil-to-coil spacing that is normally encountered in eddy-current testing. From a practical sense, this spacing dependence will not be completely eliminated. However, it is believed that it can be reduced to a very low level.

(C. L. Seale)

References

1. Bureau of Mines, Albany Metallurgy Research Center, Quarterly Metallurgical Progress Report No. 12, July 1, 1961–September 30, 1961, USAEC Report USBM-U-863.
2. A. S. Darling, Low Pressure Metallurgy. The Reduction of Oxides by Carbon, *Metallurgia*, 64: 71–75 (August 1961).
3. N. H. Katz et al., Vacuum Induction Melting and Casting of Thorium and Thorium-Uranium Alloys, USAEC Report NAA-SR-5833, Atomics International, Oct. 30, 1961.
4. N. H. Katz and M. H. Binstock, Casting of Long and Thin Plates of Uranium-Molybdenum Alloys, USAEC Report NAA-SR-6227, Atomics International, Nov. 1, 1961.
5. A. L. Geary and P. Loewenstein, Fundamental and Applied Research and Development in Metallurgy. Yttrium Fabrication, USAEC Report NMI-1247, Nuclear Metals, Inc., July 25, 1961.
6. A. H. Springmeyer and J. H. Port, The Development of Fabrication Techniques for Producing High Purity Rhenium Strip, Report NP-10602, Chase Brass and Copper Co., Inc., July 25, 1961.
7. W. H. Lenz and C. E. Peterson, The Powder Rolling of Molybdenum and Tungsten, USAEC Report LAMS-2612, Los Alamos Scientific Laboratory, June 1961.
8. E. G. Kendall et al., Fabrication Development of APM Alloys for Fuel Elements, USAEC Report NAA-SR-6213, Atomics International, Dec. 15, 1961.
9. K. E. Mann and M. B. Boudouresques, Sinter Aluminum as Cladding Material for Fuel Elements, French Report CEA-1993, 1961.
10. National Research Council, State-of-the-Art Report by Panel on Forging and Extrusion of the Committee on the Development of Manufacturing Process for Aircraft, Report MAB-139-M(F3), Oct. 15, 1960.
11. R. O. Carson, The Development of Optimum Manufacturing Methods for Columbium Alloy Forgings, Report ASD-TR-7-782(V), Crucible Steel Co. of America, August 1961.
12. R. N. Randall et al., Fundamental and Applied Research and Development in Metallurgy, Extrusion by Hydrostatic Pressure. Final Report for the Period July 1, 1960 Through June 30, 1961, USAEC Report NMI-1250, Nuclear Metals, Inc., July 13, 1961.

13. Mallinckrodt Chemical Works, Process Development Quarterly Progress Report, July–September 1961, USAEC Report MCW-1469, Nov. 1, 1961.
14. J. A. Fellows, Alpha Phase Vacuum Outgassing of Dingot Uranium, USAEC Report MCW-1467, Mallinckrodt Chemical Works, Aug. 21, 1961.
15. S. H. Bush et al., Recovery and Recrystallization of Zirconium and Its Alloys. Part 1. Specimen Compositions, Cold Working, Heat Treatment, and Survey of Literature, USAEC Report HW-69678, Hanford Atomic Products Operation, May 1961.
16. D. L. Gray, Recovery and Recrystallization of Zirconium and Its Alloys. Part 2. Annealing of Cold-Worked Zirconium, USAEC Report HW-69679, Hanford Atomic Products Operation, March 1961.
17. Hanford Atomic Products Operation, Plutonium Metallurgy Operation Quarterly Progress Report, January–March 1961, USAEC Report HW-68486, Apr. 15, 1961. (Classified)
18. R. G. Jenkins et al., Wound and Folded Single-Sheet Fuel Elements, USAEC Report NMI-1246, Nuclear Metals, Inc., Aug. 25, 1961.
19. R. W. Dayton and C. R. Tipton, Jr., Progress Relating to Civilian Applications During November 1961, USAEC Report BMI-1557, Battelle Memorial Institute, Dec. 1, 1961. (Classified)
20. Aeroprojects, Inc., Applications of Ultrasonic Energy, Task 5: Development of Ultrasonic Roll-Bond Cladding for Plate Type Fuel Elements, USAEC Report NYO-9589, June 1961.
21. S. J. Paprocki (Ed.), Progress on the Use of Gas-Pressure Bonding for Fabricating Low-Cost Ceramic, Cermet, and Dispersion Fuels, USAEC Report BMI-1555, Battelle Memorial Institute, Nov. 24, 1961.
22. R. W. Dayton and C. R. Tipton, Jr., Progress Relating to Civilian Applications During October 1961, USAEC Report BMI-1549, Battelle Memorial Institute, Nov. 1, 1961. (Classified)
23. The Metallurgical Society, American Institute of Mining, Metallurgical, and Petroleum Engineers, A Symposium on Metallic Moderator and Cladding Materials, *Nuclear Metallurgy (Volume VII), IMD Special Report Series No. 10*, 1960.
24. R. W. Dayton and C. R. Tipton, Jr., Progress Relating to Civilian Applications During September 1961, USAEC Report BMI-1546, Battelle Memorial Institute, Oct. 1, 1961. (Classified)
25. A. Bassi et al., The Possibility of Producing a Metallurgical Bond Between Stainless Steel and Zircaloy-2, USAEC Translation AEC-tr-4811 [translated from *Met. ital.*, 51: 509–514 (1959)].
26. G. Schneider, Metallic Bonding Between Uranium and Aluminum for Reactor Fuel Elements, *Metall.*, 15: 675–679 (July 1961).
27. K. Ennerst et al., Manufacture of Fuel Plates for Research Reactors by the Coextrusion Technique (in German), *Atomwirtschaft*, 6: 325–332 (June 1961).
28. Harry O. Monson and R. A. Jaross, Method and Apparatus for Effecting Thermal Bonds, U. S. Patent 3,005,079 (to USAEC), Oct. 17, 1961.
29. E. S. Sowa and E. L. Kimont, Development of a Process for Sodium Bonding of EBR-II Fuel and Blanket Elements, USAEC Report ANL-6384, Argonne National Laboratory, July 1961.
30. J. W. Robinson and L. D. Eubank, Method of Applying Metallic Coatings, U. S. Patent 2,994,951 (to USAEC), Aug. 8, 1961.
31. J. Huminik, Jr., Investigation of Oxidation and Erosion Resistant Coatings on Molybdenum, Tantalum, and Tungsten, Report NP-10576, Value Engineering Co., Inc., Mar. 6, 1961.
32. C. H. Wright et al., Electrodeposition of Erosion and Oxidation Resistant Coatings for Graphite, Quarterly Progress Report, Value Engineering Co., Inc., June 15, 1961.
33. V. A. Lamb and J. L. Sligh, National Bureau of Standards, July 1, 1960. (Unpublished)
34. V. Rafalskii and E. Taubman, Production of Metal Uranium Ingot from Uranium Oxides by Electrolysis of Molten Media, Polish Report PAN-204/IV, 1960.
35. A. Brenner and J. H. Connor, Deposition of Tungsten from the Vapor Phase, Report NBS-7389, National Bureau of Standards, Dec. 1, 1961.
36. High Temperature Materials, Inc., Design, Development, and Fabrication of Vapor-Deposited Tungsten Components, Monthly Progress Report for Oct. 15–Nov. 15, 1961.
37. F. W. Hoertel, Vapor Deposition of Tungsten and the Effects of Process Variables, Report No. 1, U. S. Department of Interior, Bureau of Mines, November 1961.
38. C. M. Wayman, Observations on the Growth of α-Iron Single Crystals by Hydrogen Reduction, *J. Appl. Phys.*, 32(10): 1844–1845 (October 1961).
39. D. H. Gurinsky, Method for Treating Graphite Product, U. S. Patent 2,995,471 (to USAEC), Aug. 8, 1961.
40. Method of Metal Coating, French Patent 1,203,765, Aug. 3, 1959.
41. W. Meier et al., Pyrolytic Carbon Deposition on Graphite, *Schweiz. Arch. angew. Wiss. u. Tech.*, 26: 29–38 (1960).
42. General Electric Co., Flight Propulsion Laboratory Dept., Fabrication of Pyrolytic Graphite Rocket Nozzle Components, Progress Report for August and September 1961, Oct. 3, 1961.
43. R. Francis and E. P. Flint, Pyrolytic Refractory Materials for Solid Fuel Rocket Motor Applications, Final Report, Arthur D. Little, Inc., Aug. 10, 1961.
44. V. Zapletal et al., Thermal Dissociation of Some Metal Formates, *Chem. listy*, 50: 1406–1409 (1956).

45. H. J. Nolting and R. H. Burgess, Oxidation Resistant High-Temperature Protective Coatings for Tungsten, First Quarterly Progress Report, May 1–July 31, 1961, Report NP-10672, Thompson Ramo Wooldridge, Inc., Aug. 15, 1961.
46. H. J. Nolting and R. H. Burgess, Oxidation Resistant High-Temperature Protective Coatings for Tungsten, Second Quarterly Progress Report, Aug. 1–Oct. 31, 1961, Report NP-11069, Thompson Ramo Wooldridge, Inc., Nov. 15, 1961.
47. W. L. Aves et al., Diffusion Coating Process for Columbium-Base Alloys, Progress Report for Feb. 15–May 15, 1961, Vought Astronautics Div., Chance Vought Corp., May 1961.
48. P. M. Arzhanyi et al., An Investigation of the Structure and Phase Composition of a Silicon Diffusion Coating for Niobium, *Issledovaniya Zharoproch. Splavam, Akad. Nauk S.S.S.R., Inst. Met. im. A. A. Baĭkova*, 6: 201–205 (1960).
49. V. A. Lamb and J. L. Sligh, National Bureau of Standards, Jan. 3, 1961. (Unpublished)
50. M. G. Bowman and N. H. Krikorian, Method of Forming Tantalum Silicide on Tantalum Surfaces, U. S. Patent 3,002,852 (to USAEC), Oct. 3, 1961.
51. J. L. Bliton et al., High-Temperature Oxidation Protective Coatings for Vanadium-Base Alloys, Second Bimonthly Progress Report for Aug. 12–Oct. 11, 1961, Armour Research Foundation, Illinois Institute of Technology, Nov. 6, 1961.
52. N. F. Eaton, Improvements in or Relating to Welding, British Patent 875,035, Aug. 16, 1961.
53. A. A. Erokhin and L. L. Silvin, Ways of Introducing Ultrasonic Vibrations into a Welding Bath, *Savrochne Proizvodstvo*, (5): 4–7 (May 1960).
54. A. Garlick, Improvements in or Relating to the Welding of Zirconium, British Patent 874,271, Aug. 2, 1961.
55. Improvement in the Closing of the Extremities of Fuel Element Cans with Welded Caps, French Patent 1,238,811, July 11, 1960.
56. J. Williams and W. Munroe, Improvements in or Relating to Pressure Welding of Metals, British Patent 877,580, Sept. 13, 1961.
57. P. P. King, Brazing Zircaloy Fuel Assembly Components for the Carolinas-Virginia Tube Reactor, USAEC Report CVNA-85, Westinghouse Electric Corp., Atomic Power Dept., 1960.
58. S. W. Porembka, Progress on USAEC/AECL Cooperative Program During December 1961, Jan. 5, 1962.
59. H. R. Longfield, Atomic Energy of Canada, Ltd., July 29, 1960. (Unpublished)
60. Chromalloy Corp., Propellex Chemical Division, A Study of Explosive Forming Selected Refractory Metals. Progress Report No. 2, July 1 Through Aug. 31, 1961, Report NP-10736, Sept. 15, 1961.
61. Chromalloy Corp., Propellex Chemical Division, A Study of Explosive Forming Selected Refractory Metals. Progress Report No. 3, Sept. 1 Through Oct. 31, 1961, Report NP-11124, Nov. 15, 1961.
62. D. S. Adams et al., High Energy Forming of Metallic Sheet Materials, Report WAL-624.5/1, Ryan Aeronautical Co., February 1961.
63. Hanford Atomic Products Operation, Fuels Development Operation Quarterly Progress Report, April, May, June 1961, USAEC Report HW-70557, July 15, 1961. (Classified)
64. Hanford Atomic Products Operation, Fuels Development Operation Quarterly Progress Report, July, August, September 1960, USAEC Report HW-69085, Oct. 15, 1960. (Classified)
65. S. J. Paprocki et al., Explosive Compaction of Powder Materials, Report SP-62-29, Creative Manufacturing Seminars, 1961-62, American Society of Tool and Manufacturing Engineers, Detroit, Michigan.
66. J. D. McClelland and W. M. Smith, Research Hot Pressing, USAEC Report NAA-SR-6441, Atomics International, Oct. 30, 1961.
67. J. D. McClelland and E. H. Zehms, Effect of Pressure and Temperatures on the End Point Density of Aluminum, USAEC Report NAA-SR-6436, Atomics International, Sept. 30, 1961.
68. S. D. Stodderd et al., Preparation of Pure Impervious Magnesia by Aqueous Slip Casting, USAEC Report LAMS-2639, Los Alamos Scientific Laboratory, Oct. 27, 1961.
69. W. B. Tarpley and H. Kartluke, Application of Ultrasonic Vibration to Cold Pressing of Ceramic Pellets, USAEC Report NYO-10005, Aeroprojects, Inc., November 1961.
70. Aeroprojects, Inc., Applications of Ultrasonic Energy, Progress Report No. 19, USAEC Report NYO-2573, March 1960.
71. Aeroprojects, Inc., Applications of Ultrasonic Energy, Progress Report No. 20, USAEC Report NYO-2574, April 1960.
72. Aeroprojects, Inc. (Unpublished)
73. Oak Ridge National Laboratory, Oct. 9, 1961. (Unpublished)
74. F. W. Clinard, Metallurgical Phenomena Associated with Active Metal Bonding, USAEC Report SCTM-215-61(11), Sandia Corp., September 1961.
75. Ames Laboratory. (Unpublished)
76. J. W. Graham and W. B. Hall, Protective Coatings for Molybdenum Alloys, Summary Report, Report R60FPD307 (AD-259028), General Electric Co., Flight Propulsion Laboratory Dept., Mar. 31, 1960.
77. J. P. Reese and V. H. Boruff, Evaluation of Ultrasonic Test Devices for Inspection of Adhesive Bonds (Summary Report), Report ER-10911-9, Martin Co., August 1961.
78. Hanford Atomic Products Operation, Fuels Development Operation Quarterly Progress Report, July, August, September 1961, USAEC Report HW-71422, Oct. 13, 1961. (Classified)
79. Westinghouse Electric Corp., Bettis Atomic Power Laboratory, Core Materials and Quality Engineering Technical Progress Report for the Period June 26, 1961 to September 25, 1961,

USAEC Report WAPD-MRK-11, Oct. 6, 1961. (Classified)

80. W. A. Sawyer, Ultrasonic Testing of Thin Wall Zircaloy Tubing, Canadian Report R61CAP9(Rev.) (AECL-1360), August 1961.
81. R. W. McClung, Development of Nondestructive Tests for the EGCR Fuel Assembly, *Nondestructive Testing*, 19(5): 352–358 (September–October 1961).
82. Argonne National Laboratory, Reactor Development Program, Progress Report, October 1961, USAEC Report ANL-6454, Nov. 15, 1961.
83. C. V. Dodd and W. D. Brown, Oak Ridge National Laboratory, 1961. (Unpublished)

LEGAL NOTICE

This document was prepared under the sponsorship of the U. S. Atomic Energy Commission. Neither the United States, nor the Commission, nor any person acting on behalf of the Commission:

A. Makes any warranty or representation, expressed or implied, with respect to the accuracy, completeness, or usefulness of the information contained in this report, or that the use of any information, apparatus, method, or process disclosed in this report may not infringe privately owned rights; or

B. Assumes any liabilities with respect to the use of, or for damages resulting from the use of any information, apparatus, method, or process disclosed in this report.

As used in the above, "person acting on behalf of the Commission" includes any employee or contractor of the Commission, or employee of such contractor, to the extent that such employee or contractor of the Commission, or employee of such contractor prepares, disseminates, or provides access to, any information pursuant to his employment or contract with the Commission, or his employment with such contractor.

NUCLEAR SCIENCE ABSTRACTS

The U. S. Atomic Energy Commission, Division of Technical Information, publishes *Nuclear Science Abstracts (NSA)*, a semimonthly journal containing abstracts of the literature of nuclear science and engineering.

NSA covers (1) research reports of the U. S. Atomic Energy Commission and its contractors; (2) research reports of government agencies, universities, and industrial research organizations on a world-wide basis; and (3) translations, patents, books, and articles appearing in technical and scientific journals.

Complete indexes covering subject, author, source, and report number are included in each issue. These are cumulated quarterly, semiannually, and annually providing a detailed and convenient key to the literature.

Availability of *NSA*

SALE *NSA* is available on subscription from the Superintendent of Documents, U. S. Government Printing Office, Washington 25, D. C., at $22.00 per year for the semimonthly abstract issues and $15.00 per year for the four cumulated-index issues. Subscriptions are postpaid within the United States, Canada, Mexico, and all Central and South American countries, except Argentina, Brazil, British and French Guiana, Surinam, and British Honduras. Subscribers in these Central and South American countries, and in all other countries throughout the world, should remit $27.50 per year for subscriptions to semimonthly abstract issues and $17.50 per year for the four cumulated-index issues.

EXCHANGE *NSA* is also available on an exchange basis to universities, research institutions, industrial firms, and publishers of scientific information. Inquiries should be directed to the Division of Technical Information Extension, U. S. Atomic Energy Commission, P. O. Box 62, Oak Ridge, Tennessee.